

Two new species of freshwater stingrays of the genus *Paratrygon* (Chondrichthyes: Potamotrygonidae) from the Orinoco basin, with comments on the taxonomy of *Paratrygon aiereba*

Correspondence:
Thiago Silva Loboda
loboda_bio@yahoo.com.br

 Thiago Silva Loboda^{1,4},  Carlos A. Lasso²,  Ricardo de Souza Rosa³ and  Marcelo Rodrigues de Carvalho⁵

Submitted August 19, 2020

Accepted January 25, 2021

by Toby Daly-Engel

Epub June 11, 2021

The genus *Paratrygon*, currently recognized as the sole monotypic genus of the family Potamotrygonidae, has a considerably greater diversity than previously indicated, including molecular studies, which supported *P. aiereba* (hitherto the only recognized species in the genus) as a possible species complex. Here we describe two new species of the genus that are both endemic to and sympatric in the Orinoco basin. *Paratrygon aiereba*, type species of the genus, is now restricted to the Amazon basin. Both new species are identified and defined through morphological characters such as coloration, dermal denticle morphology, arrangement of thorns, distribution and morphology of ventral lateral line canals, morphology of skeletal elements, and morphometrics. An extensive comparison of these characters between the new species herein described and *P. aiereba* is presented. Finally, a taxonomic reappraisal of *P. aiereba* is provided through a revision of preserved material and its original description, plus new evidence about its type-locality, collectors, and a reconsideration of the destination of its type-specimen.

Keywords: Amazon basin, Batoidea, Freshwater Stingrays, Morphology, Myliobatiformes.

Online version ISSN 1982-0224

Print version ISSN 1679-6225

Neotrop. Ichthyol.

vol. 19, no. 2, Maringá 2021

¹ Centro de Ciências Biológicas e da Natureza (CCBN), Universidade Federal do Acre, Rodovia BR-364, km 04, Distrito Industrial, 69920-900 Rio Branco, AC, Brazil. loboda_bio@yahoo.com.br (corresponding author).

² Instituto de Investigación de Recursos Biológicos Alexander von Humboldt (IAVH), Cl. 28a #15-09 Bogotá, DC, Colombia. classo@humboldt.org.co.

³ Departamento de Sistemática e Ecologia (CCEN), Universidade Federal da Paraíba, Cidade Universitária, 58051-900 João Pessoa, PB, Brazil. rsrosa@dse.ufpb.br.

⁴ Departamento de Zoologia, Instituto de Biociências (IBUSP), Universidade de São Paulo, Rua do Matão, Trav. 14, n.101, 05508-900 São Paulo, SP, Brazil.

⁵ Formerly of 4.

O gênero *Paratrygon*, reconhecido atualmente como o único gênero monotípico da família Potamotrygonidae, possui uma considerável alta diversidade do que previamente indicado, incluindo estudos moleculares, que corroboravam *P. aiereba* (a única espécie reconhecida para o gênero até então) como um possível complexo de espécies. Aqui descrevemos duas novas espécies do gênero para a bacia do Orinoco, ambas endêmicas e simpátricas para esta bacia. *Paratrygon aiereba*, espécie tipo do gênero, agora está restrita para a bacia Amazônica. Ambas novas espécies são identificadas e definidas através de caracteres morfológicos tais como coloração, morfologia dos dentículos dérmicos, arranjo dos espinhos pontiagudos, distribuição e morfologia dos canais ventrais da linha lateral, morfologia dos elementos do esqueleto e morfometria. Uma comparação extensiva destes caracteres entre as novas espécies aqui descritas e *P. aiereba* é apresentada. Finalmente uma reavaliação taxonômica de *P. aiereba* é fornecida através da revisão de espécimes preservados e de sua descrição original, além de novas evidências sobre sua possível localidade-tipo, coletores, e uma reconsideração do destino de seu espécime-tipo.

Palavras-chave: Arraias dulcícolas, Bacia Amazônica, Batoidea, Morfologia, Myliobatiformes.

INTRODUCTION

The family Potamotrygonidae Garman, 1877 is composed of two subfamilies, five genera and 38 valid species (Carvalho *et al.*, 2016; Silva, Loboda, 2019), with the neotropical freshwater stingrays (subfamily Potamotrygoninae) being represented by four genera and 36 species: *Paratrygon* Duméril, 1865, currently monotypic, *Potamotrygon* Garman, 1877, the most diverse genus with 31 species, and *Plesiotrygon* Rosa, Castello & Thorson, 1987 and *Heliotrygon* Carvalho & Lovejoy, 2011 with two species each. This subfamily is considered monophyletic by many authors, and the following synapomorphies are the most cited as corroboration: a long pre-pelvic process present in the anterior medial portion of the pelvic girdle, a reduced rectal gland, and low concentration of urea in the blood (Garman, 1913; Thorson *et al.*, 1978; Rosa, 1985a; Lovejoy, 1996; Carvalho *et al.*, 2004). The distribution of potamotrygonins is restricted to South American rivers that flow into the Caribbean Sea and Atlantic Ocean, with the exception of rivers located between the Parnaíba and La Plata basins and the rivers of Patagonia (Compagno, Cook, 1995; Rosa *et al.*, 2010).

In the last ten years, a series of taxonomic revisions and species descriptions based on morphological characters considerably increased our understanding of the diversity of the subfamily. These works resulted in the description of 13 new species of *Potamotrygon*, one new species of *Plesiotrygon*, and one new genus, *Heliotrygon* with two new species (Carvalho, Lovejoy, 2011; Carvalho, Ragno, 2011; Silva, Carvalho, 2011; Carvalho *et al.*, 2011; Loboda, Carvalho, 2013; Fontenelle *et al.*, 2014; Carvalho, 2016a,b; Fontenelle, Carvalho, 2017; Silva, Loboda, 2019). Besides these taxa, a new subfamily was included alongside potamotrygonins in the family Potamotrygonidae: the subfamily Styracuninae

Carvalho, Loboda & Silva, 2016 for two marine/estuarine species previously known as “amphi-American” species of *Himantura* Müller & Henle, 1837, *Styracura schmardae* (Werner, 1904) and *S. pacifica* (Beebe & Tee-Van, 1941) (Carvalho *et al.*, 2016). However, regarding the genus *Paratrygon*, morphological revisions in this sense have not been done since Rosa (1985a), who revised the entire family Potamotrygonidae.

Duméril (1865) created the subgenus *Paratrygon* exclusively for the species *Trygon aiereba* Müller & Henle (1841). Günther (1870) raised *Paratrygon* to genus level (Günther, 1870; Rosa, 1991). After Garman (1877), who described the genera *Disceus* and *Potamotrygon*, and until the revisions made by Rosa (1985a,b; 1991) and Rosa *et al.* (1987), the main taxonomic discussions related to the family always involved these three genera plus the nominal genus *Elipesurus* Schomburgk (1843) (Miranda Ribeiro, 1907; Garman, 1913; Fowler, 1951; Castex, 1964; Bailey, 1969). Rosa (1985b; 1991) addressed the taxonomic history of *Paratrygon* and recognized it as the senior synonym of *Disceus*, and considered *Elipesurus* as a *nomem dubium* (Rosa 1985b; 1991; Carvalho *et al.*, 2003).

The taxonomic history of the species *Paratrygon aiereba* (Walbaum, 1792) was also examined by Rosa (1991), who analyzed the type-specimens of *Trygon stroglyopterus* Jardine, 1843 and *Disceus thayeri* Garman, 1913. Rosa (1991) concluded that *P. aiereba* is the senior synonym of *T. stroglyopterus* and *D. thayeri*, and suggested that the type-specimen of *P. aiereba* (previously regarded as deposited in the Bavarian State Collection of Zoology in Munich) was lost, very probably during the World War II.

Paratrygon aiereba is distributed in two major river basins of South America: the Amazon and Orinoco (Rosa, 1985a; Carvalho *et al.*, 2003; Rosa *et al.*, 2010). However, as in other potamotrygonin species with vast geographic distributions (*e.g.*, *Potamotrygon motoro* (Müller & Henle, 1841), *P. orbignyi* (Castelnau, 1855) and *P. scobina* Garman, 1913), some populations of *Paratrygon aiereba* show consistent variation in certain morphological characters, especially coloration. This variation may be indicative of genetic isolation and that *P. aiereba* is, in fact, a species complex (Carvalho *et al.*, 2003; Rosa *et al.*, 2010). These findings have been further corroborated by molecular data. Frederico *et al.* (2012) showed through an analysis of Mitochondrially encoded ATP synthase membrane subunit 6 (ATPase 6) and Cytochrome c oxidase subunit I (COI) that there exists genetic divergence between *P. aiereba* populations from the Xingu, Tapajós, Araguaia, Negro and Solimões-Amazonas rivers. Also, molecular studies conducted by Garcia *et al.* (2016) with populations of *P. aiereba* from the rivers of the Amazon and Orinoco basins in Colombia and Venezuela showed some divergence in three mitochondrial genes: ATPase 6, COI and also Cytochrome *b* (*Cytb*).

Despite that *P. aiereba* was one of the first described species of potamotrygonids, there is no extensive literature on this species. The two most relevant works about its morphology are Garman (1913, who described this species as *Disceus thayeri*) and Rosa (1985a). Other authors who addressed the morphology of this species were Lovejoy (1996) and Shibuya *et al.* (2010) on the ventral canals of the lateral line system, and Lovejoy (1996), Carvalho *et al.* (2004) and Carvalho, Lovejoy (2011) on skeletal components and musculature. Taniuchi, Ishihara (1990) and Moreira *et al.* (2018) described the external and internal morphology of the clasper. Lasso *et al.* (1996; 2013; 2016) and Sánchez-Duarte *et al.* (2016) provided data on reproduction, feeding habits and development in Orinoco and Amazon basins (Venezuela and Orinoco), and Araújo (2011) about *P. aiereba* in the Amazon (Negro River) basin.

Since Rosa (1985a), phylogenies based on morphological characters showing the interrelationships among the genera of Potamotrygoninae have been proposed. In his analysis Rosa (1985a) found *Plesiotrygon* to be the sister group of the clade *Potamotrygon* + *Paratrygon*. Lovejoy (1996) and Carvalho *et al.* (2004) found *Paratrygon* as sister group of *Potamotrygon* + *Plesiotrygon*, and when the genus *Heliotrygon* was described, Carvalho, Lovejoy (2011) showed *Paratrygon* + *Heliotrygon* as the sister group of *Potamotrygon* + *Plesiotrygon*, and made an extensive description of the synapomorphies for each clade. It is important to emphasize that all these works described morphological characters of *Paratrygon* in order to make a comparison with other potamotrygonins. A comprehensive taxonomic and morphological review exclusive to *Paratrygon aiereba* had not been made until Loboda (2016).

The necessity to review the taxonomic history and type-specimens related to *P. aiereba*, *Trygon stroglypterus* and *Disceus thayeri* is fundamental to understand this species complex. The main issue is to morphologically delimit *P. aiereba*. Even after Rosa (1991), who thoroughly addressed this discussion, it is evident that these nominal species were synonymized based on diagnostic characters of the genus *Paratrygon*. These characters have never been interpreted as possibly representing morphological differences between distinct and isolated populations of *Paratrygon*, and Rosa (1991) did not extensively examine characters with systematic potential, such as color patterns or thorn rows on the tail. Even the type-localities of these nominal species could help clarify if they represent distinct populations of *P. aiereba*. Lastly, Loboda (2016) made a taxonomic and morphological review exclusively of the hitherto monotypic genus *Paratrygon*, including the type-species *P. aiereba* and its synonyms. Here we present part of these results in relation to the genus *Paratrygon* in the Orinoco basin, and review the identity of *P. aiereba*.

MATERIAL AND METHODS

A total of 75 specimens of the genus *Paratrygon* were measured and had their external morphological characters (described below) analyzed, including the type-specimens of *Trygon stroglypterus* (ZMB 4632) and *Disceus thayeri* (MCZ 297-S, MCZ 563-S, and MCZ 606-S). Some specimens were selected for analysis of internal morphology through dissections, X-ray radiography, and clearing-and-staining (following Dingerkus, Uhler, 1977). Non-type specimens were designated in addition to the type specimens due to presenting some damaged marks or/and missing some disc or/and body parts. Serial numbers of the uncatalogued non-type specimens were previously requested, however, until the completion of this work, they were not sent to us. Specimens examined were from the following collections: American Museum of Natural History, New York (AMNH), Instituto de Investigación de Recursos Biológicos Alexander von Humboldt, Villa de Leyva (IAvH-P), Instituto de Ciencias Naturales, Universidad Nacional de Colombia, Bogota (ICN), Instituto de Investigaciones de la Amazonia Peruana, Iquitos (IIAP), Instituto Nacional de Pesquisas da Amazônia, Manaus (INPA), Museum of Comparative Zoology, Harvard University, Cambridge (MCZ), Muséum national d'Histoire naturelle, Paris (MNHN), Museu Paraense Emilio Goeldi, Belém (MPEG), Museo de Historia

Natural, Universidad Nacional Mayor de San Marcos, Lima (MUSM), Museu de Zoologia, Universidade Federal da Paraíba (UFPB), Universidade de São Paulo, São Paulo (MZUSP), Naturhistorisches Museum, Wien (NMW), National Museum of Natural History, Smithsonian Institution, Washington D.C. (USNM), Museum für Naturkunde, Berlin (ZMB), Zoologische Staatssammlung München, München (ZSM).

Twenty-eight measurements were taken (in mm) on all specimens following Bigelow, Schroeder (1953), Rosa (1985a), Taniuchi, Ishihara (1990) and Loboda, Carvalho (2013). Measurements were expressed in the tables as percentages of disc width (% DW). Means and Standard Deviations (SD) were related to percentages of disc width, and ranges were expressed in millimeters and percentages (except disc width). Means and SD also include type and not-type specimens, and the number (N) of analyzed specimens was included in a separate column. Specimens with deformities in disc, tail, pelvic fins and other parts of the body had the measurements regarding these parts excluded.

The following external morphological characters were analyzed: dorsal and ventral coloration of disc, tail, pelvic fins and claspers; morphology and distribution of dermal denticles on the disc and tail (following Deynat, Séret, 1996 and Silva, Loboda, 2019); distribution and morphology of dorsal and lateral thorn rows of the tail; morphology of spiracular process (and occurrence of dermal denticles on this structure); morphology of caudal stings; morphology and distribution of teeth in both dental plates (following Stehmann, 1978 and Rosa, 1985a [indicated in the diagnoses as number of upper rows/number of lower rows]); and arrangement of clasper grooves and pseudosiphon (following Taniuchi, Ishihara, 1990 and Moreira *et al.*, 2018).

Counts of vertebrae, fin radials and teeth were made from radiographs (either with the aid of a negatoscope or digitally with the program OsiriX), or on the specimens themselves (mainly for tooth counts with the aid of magnifying glasses or stereoscopic microscopes Leica EZ4 and M80). The majority of radiographs were made in the Radiology Section of the Hospital Veterinário da Faculdade de Medicina Veterinária e Zootecnia (HOVET-USP), São Paulo. Counts of vertebrae and fin rays followed Compagno (1999).

Analysis of internal morphological components included distribution and morphology of the ventral canals of lateral line and the skeleton: neurocranium, jaws and hyoid archs, synarcual cartilage, branchial basket, pectoral and pelvic girdles, and clasper. Nomenclature of ventral canals of lateral line followed Garman (1888) and Lovejoy (1996). Nomenclature for main components of the skeleton followed Garman (1913), Compagno (1977; 1999), Rosa (1985a), Nishida (1990), Lovejoy (1996); Carvalho *et al.* (2004) and Carvalho, Lovejoy (2011).

Abbreviations. *ACVF* = anterior cerebral vein foramen, *ADF* = anterodorsal fenestra, *ang* = angular component of hyomandibular canal, *ANT* = antorbital cartilage, *AOC* = antorbital cartilage condyle, *AS* = articular surface, *AT1* = accessory terminal 1, *AVC* = anterior ventral condyle, *AVF* = anteroventral fenestra, *AX* = axial cartilage, *bp* = basal plate, *B1* = basal 1, *B2* = basal 2, β = beta cartilage, *CB* = coracoid bar, *ccp* = central coronal plate, *cr* = crown, *DLC* = dorsolateral crest, *DLP* = dorsolateral process, *DM* = dorsal marginal cartilage, *DMC* = dorsomedial crest, *DS* = dorsal socket, *DT1*

= dorsal terminal 1, *DT2* = dorsal terminal 2, *ELF* = endolymphatic foramina, *ESAF* = efferent spiracular artery foramen, *FCF* = frontoparietal component of fontanelle, *FM* = foramen magnum, *FPC* = foramen of preorbital canal, *FPF* = frontoparietal component of fontanelle, *FSP* = first segment of propterygium, *HF* = hyomandibular facet, *HMD* = hyomandibular canal, *HYO* = hyomandibula, *ICAF* = internal carotid artery foramina, *IOC* = infraorbital canal, *IP* = iliac process, *IS* = internasal septum, *ISP* = ischial process, *IVF* = interorbital vein foramen, *JFC* = junction of the four canals, *JMR* = junction of medial radials, *jug* = jugular component of hyomandibular canal, *L* = Hyomandibular–Meckelian ligament, *LbX* = lateralis branch of vagus nerve foramen, *LC* = lateral commissure, *lcr* = lateral coronal ridge, *LEF* = lateral external face, *LP* = lateral process, *LPP* = lateral prepelvic process, *LS* = lateral stay, *MC* = Meckel's cartilage, *MNC* = mandibular canal, *MSC* = mesocondyle, *MSP* = mesopterygium, *MTC* = metacondyle, *MTP* = metapterygium, *NAS* = nasal canal, *NC* = nasal capsule, *nil* = nasointernal loop, *NSC* = nasal cartilage, *OC* = occipital condyle, *OF* = obturator foramen, *OFS* = orbital fissure, *OP* = optic pedicel, *orb* = orbitonasal component of supraorbital canal, *PB* = puboischiadic bar, *PC* = procondyle, *PCF* = precebral component of fontanelle, *PDF* = postdorsal fenestra, *PLF* = perilymphatic foramina, *pnc* = prenasal component of nasal canal, *pnl* = prenasal loop, *POP* = postorbital process, *PPP* = prepelvic process, *PPT* = propterygium, *PQ* = palatoquadrate, *PRO* = propterygium, *PRP* = preorbital process, *PSM* = posterior segments of metapterygium, *pst* = posterior subpleural tubules, *PVC* = posterior ventral condyle, *PVF* = postventral fenestra, *RPJ* = rostral projection, *SAS* = small articulation surface, *sbr* = subrostral component of supraorbital canal, *SCP* = scapular process, *SF* = small foramen, *SNC* = spinal nerve canal, *SNF* = spinal nerve foramen, *SOC* = supraorbital crest, *SP* = supraorbital process, *spc* = subpleural component of hyomandibular canal, *spl* = subpleural loop, *SPO* = supraorbital canal, *spt* = subpleural tubule, *sub* = suborbital component of supraorbital canal, *VLP* = ventrolateral process, *VM* = ventral marginal cartilage, *vS* = vesicles of Savi, *II* = optic nerve foramen, *III* = oculomotor nerve foramen, *VII* = hyomandibular ramus of facial nerve foramen, *IX* = glossopharyngeal nerve foramen, *X* = vagus nerve foramen.

RESULTS

Paratrygon orinocensis, new species

urn:lsid:zoobank.org:act:86CC950D-66B1-44C2-B7D1-DC8BF88A089B

(Figs. 1–17, Tabs. 1–2)

Disceus thayeri. —Fernández-Yépez, 1949:1–2 (brief morphological description; occurrence in Orinoco basin).

Paratrygon aiereba. —Lasso *et al.*, 1996:39–47, 49, figs. 3–5, 9, 11, 12, (morphometry, weight, sexual maturity, pregnancy, size of litter, feeding habits, occurrence in Caño Guaritico, Apure River subbasin, Venezuela). —Barbarino, Lasso, 2005:93–107, figs. 1,

4–10 (occurrence in Apure River, biological data, habitat, feeding habits, pregnancy, size of litter, morphometry, weight, sexual maturity, fishing data, commercialization). —Barbarino, Lasso, 2009:24–31, figs. 1–3 (commercialization, fishing data, habitat, morphometry, weight, reproduction data, sexual maturity). —Lasso *et al.*, 2009:128 (occurrence in delta of Orinoco River). —Lasso *et al.*, 2011:87–88, 469, 493, fig. 61 (brief morphological description; feeding habits, biology, distribution, fishing data, species list of Orinoco River delta). —Lasso, Sánchez-Duarte, 2012: 23, 42, 132–134, 308, 314, 318 (list of endangered species of fish in Colombia, brief morphological description, distribution, ecology, conservation). —Muñoz-Osorio, Mejía-Falla, 2013:189–191 (occurrence in Bitá River, brief morphological description, size of litter, conservation). —Lasso *et al.*, 2013:137–150, figs. 4–6, 9, 12–13 (brief morphological description, conservation, distribution, biological data, fishing data). —García-Villamil *et al.*, 2013:290–293, figs. 5–6 (molecular systematics, phylogenetic discussion). —Sánchez-Duarte *et al.*, 2016: 319, 321–322 (specimen trade); —García *et al.*, 2016:4481–4482 (molecular systematics, phylogenetic discussion).

Paratrygon sp. —García *et al.*, 2016:4484–4489, fig. 2, p. 4484, fig. 3, p. 4485, fig. 4, p. 4485, fig. 5, p. 4486 (molecular systematics, phylogenetic discussion).

Paratrygon sp.1. —Loboda, 2016: vol.1. vii–viii, 33, 60–61, 75, 87, 97–113, 117, 119–123, 126–127, 142, 156, 190–192, 229–236, vol.2. xv–xvi, 76–90, figs. 105–126, (morphometry, morphological description, taxonomic revision, diagnosis, previous misidentifications, distribution).

Holotype. IAvH-P 11939, female, 286 mm DW, Colombia, Vichada, Puerto Carreño, río Orinoco, locality of Piedra casa Bojonawi, 06°06'07.5"N 67°29'11.9"W, 1 Dec 2013, C. Lasso & M. A. Morales-Betancourt.

Paratypes. (10 specimens). IAvH-P 12449, male, 573 mm DW, Colombia, Vichada, Puerto Carreño, río Orinoco, locality of playa Reserva Natural Bojonawi, 06°06'07.2"N 67°29'11.9"W, 6 May 2014, C. Lasso & M. A. Morales-Betancourt. IAvH-P 12448, male, 421 mm DW, same data as anterior. IAvH-P 11940, male, 345 mm DW, Colombia, Vichada, Puerto Carreño, río Orinoco, locality of Piedra casa Bojonawi, 06°06'07.5"N 67°29'11.9"W, 28 Jun 2013, C. Lasso & M. A. Morales-Betancourt. IAvH-P 12439, female, 270 mm DW, Colombia, Vichada, Puerto Carreño, río Bitá (tributary of río Orinoco), 06°09'10.7"N 67°35'45.1"W, 1 Jan 2014, C. Lasso & M. A. Morales-Betancourt. MZUSP 117220, male, 299 mm DW, Venezuela, Apure, Muñoz, Río Apure (tributary of río Orinoco), Guaritico stream, 07°53'32.5"N 68°52'49.8"W, 23 Feb 2011, F. P. L. Marques & L. Sanchez. USNM 233944, 5, 3 females and 2 males, 245–420 mm DW, Venezuela, Delta Amacuro, Guayana, río Orinoco, locality of Cabrian, between Puerto Ordaz and Los barrancos de Fajardo, 08°34'12"N 62°15'48"W, 11 Nov 1979, E. C. Marsh.

Non-types. (11 specimens). IAvH-P 11943, female, 372 mm DW, Colombia, Vichada, Puerto Carreño, río Orinoco, below Natural Park of Bojonawi, 06°05'51"N 67°29'04.4"W, 11 Oct 2013, C. Lasso. IAvH-P 11942, female, 297 mm DW, same data as anterior. IAvH-P 12440, female, 249 mm DW, Colombia, Vichada, Puerto Carreño, río Bitá (tributary of Río Orinoco), 06°09'10.7"N 67°35'45.1"W, 1 Jan 2014,

C. Lasso. IAvH-P 11941, female, 248 mm DW, Colombia, Vichada, Puerto Carreño, río Orinoco, locality of Natural Reserve Bojonawi, 06°06'07.5"N 67°29'11.9"W, 12 Jun 2013, C. Lasso & M. A. Morales-Betancourt. IAvH-P 12443, female, 245 mm DW, Colombia, Vichada, Puerto Carreño, locality of Playa Caricari, 06°05'46.3"N 67°29'04.7"W, 28 Feb 2014, C. Lasso & M. A. Morales-Betancourt. IAvH-P 11938, male, 242 mm DW, same data as IAvH-P 11943. IAvH-P 12444, female, 241 mm DW, same data as IAvH-P 11943. IAvH-P 12445, female, 236 mm DW, Colombia, Vichada, Puerto Carreño, locality of Playa Caricari, 06°05'46.3"N 67°29'04.7"W, 5 Mar 2014, C. Lasso & M. A. Morales-Betancourt. IAvH-P 12442, 2, 1 female and 1 male, 174–178 mm DW, Colombia, Vichada, Puerto Carreño, río Orinoco, below Natural Reserve Bojonawi, 06°05'51"N 67°29'04.4"W, 11 Oct 2013, C. Lasso & M. A. Morales-Betancourt. IAvH-P uncatalogued, 382 mm DW, Colombia. ICN uncatalogued, 4, 2 females and 2 males, 209–355 mm DW, Colombia.

Diagnosis. *Paratrygon orinocensis* is distinguished from congeners by a combination of characters. *Paratrygon orinocensis* without lateral rows of thorns on tail (*vs. P. aiereba* and *Paratrygon parvaspina* with lateral rows of thorns on tail). Dermal denticles on the central region of the disc of *P. orinocensis* have wide and high crowns, presenting a central coronal plate very similar morphologically to its lateral coronal ridges, which in adults can be more than 12 (*vs. P. aiereba* and *P. parvaspina* that have small dermal denticles on the central disc, with high and narrow crowns presenting higher and pointed central coronal plates surrounded by minor, pointed or rounded lateral coronal ridges, which in turn vary between three and six). *Paratrygon orinocensis* has 22–35/20–29 teeth (*vs. P. aiereba* with 16–26/14–20, and *P. parvaspina* with 31/19–22); central teeth of *P. orinocensis* with more developed and high cusps than *P. aiereba* and *P. parvaspina*. In *P. orinocensis* the spiracles are small and triangular, with mean length 5.6% DW [4.5–7.9% DW] (*vs. quadrangular* and larger spiracles in *P. aiereba*, with mean length 6% DW [4.4–11.6% DW], and very small and quadrangular spiracles in *P. parvaspina* with mean length 5.2% DW [4.9–5.8% DW]). *Paratrygon orinocensis* has a short and straight spiracular process with developed and numerous dermal denticles (*vs. larger* and knob shaped spiracular process that almost covers the spiracle aperture and with some small dermal denticles in *P. aiereba*, and an extremely short and reduced spiracular process in *P. parvaspina* that is more perceptible in adult specimens, with few dermal denticles). *Paratrygon orinocensis* has a minute rostral projection (*vs. P. aiereba* that has a relatively large rostral projection, and *P. parvaspina* that has a large and circular rostral projection).

Description. For general aspect of *Paratrygon orinocensis* see Figs. 1–3, for morphological characters examined see Figs. 8–17. Measurements and counts are shown in Tabs. 1–2, and S1–S2. *Paratrygon orinocensis* presents a more rounded than subcircular disc, with mean disc length 107.7% DW [104.4–112.8%]. Anterior margin of disc with a prominent concavity at its medial portion, being clearly visible and pronounced (Figs. 1–3, S1). Disc also relatively short in comparison with total length, with mean of distance between anterior margin of disc and cloaca 85.6% DW [81.5–91.7% DW].

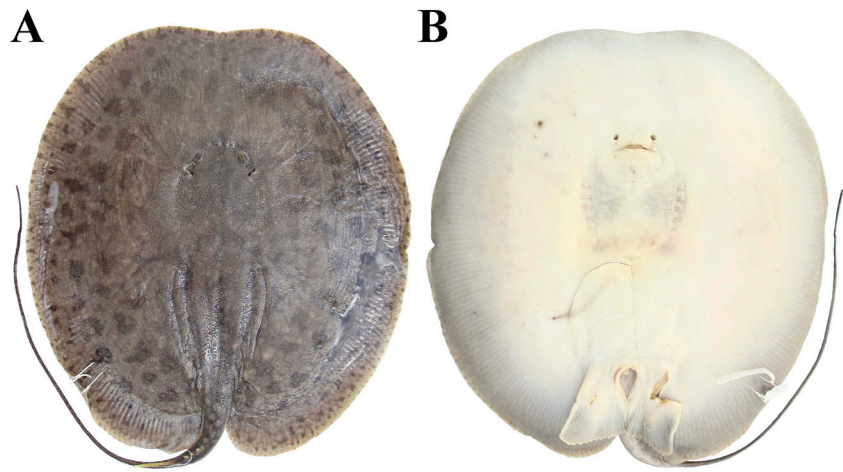


FIGURE 1 | Holotype of *Paratrygon orinocensis*, IAvH-P 11939, adult female, 286 mm DW, from Orinoco river. **A.** dorsal and **B.** ventral views.

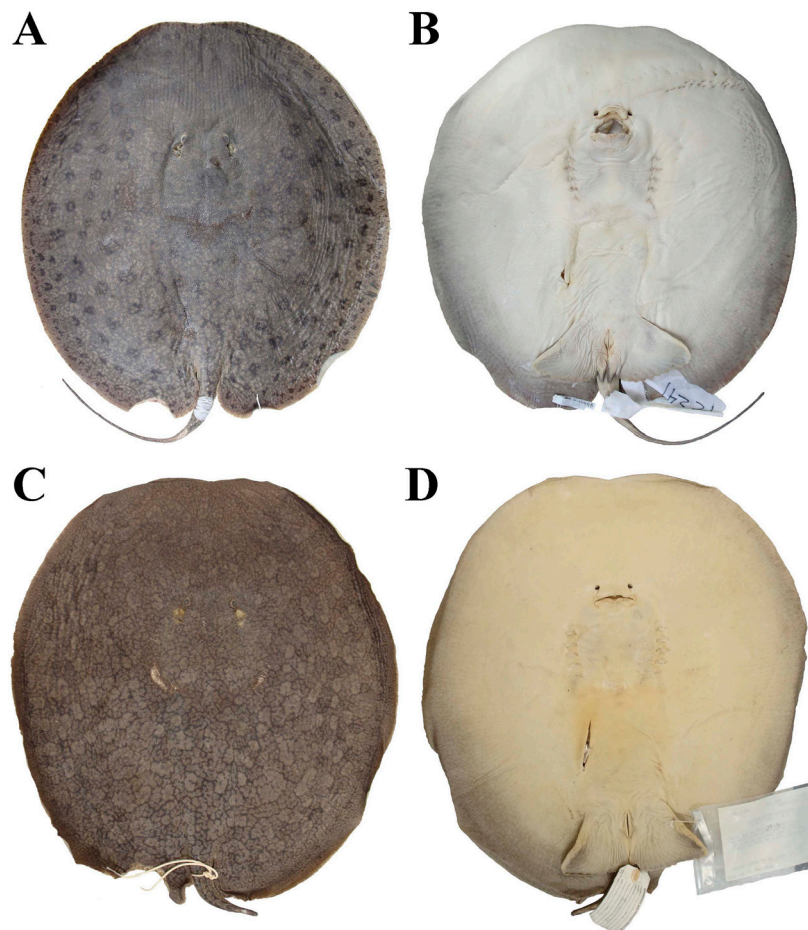


FIGURE 2 | Paratypes of *Paratrygon orinocensis*. IAvH-P 12448, subadult male, 421 mm DW, from Orinoco river. **A.** dorsal and **B.** ventral views. USNM 233944a, adult female, 420 mm DW, from Orinoco river. **C.** dorsal and **D.** ventral views.

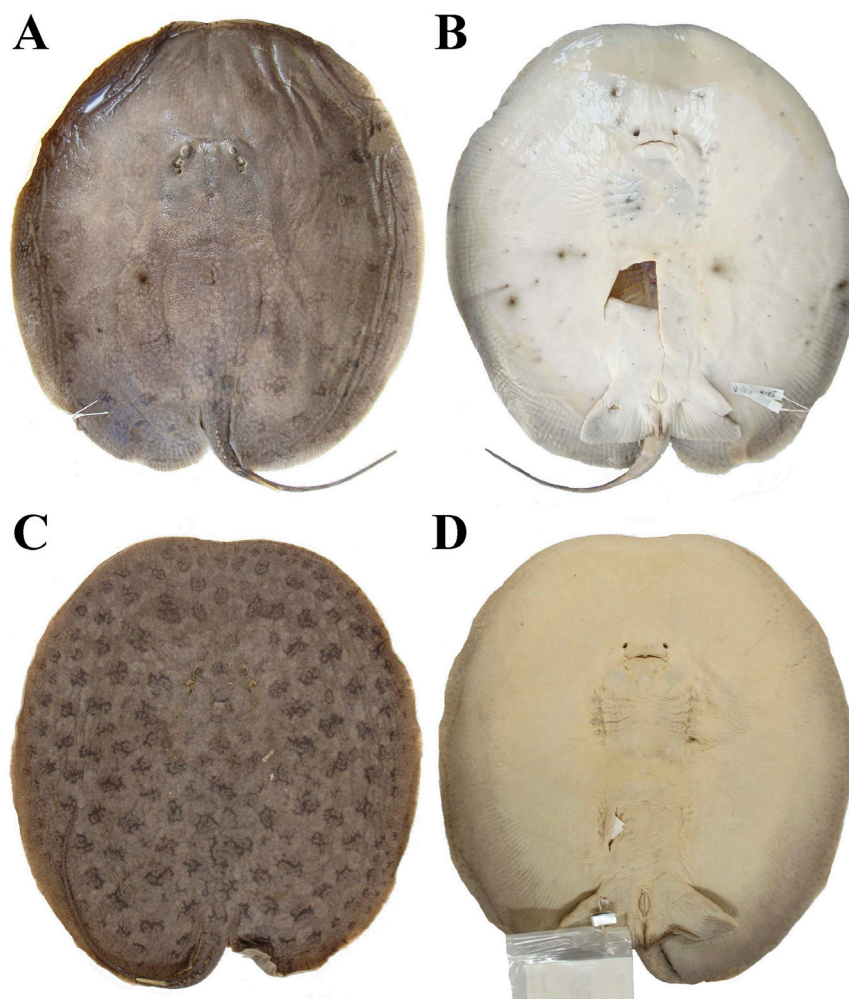


FIGURE 3 | Paratypes of *Paratrygon orinocensis*. IAvH-P 11940, juvenile male, 345 mm DW, from Orinoco river. **A.** dorsal and **B.** ventral views. USNM 233944b, juvenile male, 335 mm DW, from Orinoco river. **C.** dorsal and **D.** ventral views.

TABLE 1 | Measurements of specimens of *Paratrygon orinocensis* including the holotype (IAvH-P 11939). Mean, Standard Deviation (SD) and ranges are expressed in millimeters (mm) and proportions of disc width (%DW); (N) corresponds to the number of specimens analyzed.

<i>Paratrygon orinocensis</i>	Holotype IAvH-P 11939		Mean		SD		Range				N
	mm	%DW	mm	%DW	mm	%DW	mm		%DW		
Total length	584	204.2	551.2	191.0	124.5	43.3	287	866	115.7	283.7	26
Disc length	305	106.6	322.9	107.7	94.3	2.2	190	634	104.4	112.8	26
Disc width	286	100.0	299.8	100.0	86.0	0.0	174	573	100.0	100.0	26
Interorbital distance	28	9.8	29.2	9.9	7.4	1.0	21	56	8.6	12.9	26
Interrespiracular distance	43	15.0	46.6	15.8	11.3	1.6	36	86	13.8	20.7	26
Eye length	6	2.1	5.5	1.9	1.0	0.4	4	7	1.2	2.8	26
Spiracle length	16	5.6	16.6	5.6	4.4	0.7	12	30	4.5	7.9	26
Preorbital length	86	30.1	90.2	29.9	28.4	1.5	49	181	26.3	32.1	25
Prenasal length	77	26.9	82.6	27.5	23.4	1.2	44	150	24.7	30.3	26



TABLE 1 | (Continued)

<i>Paratrygon orinocensis</i>	Holotype IAvH-P 11939		Mean		SD		Range				N
Preoral length	86	30.1	92.7	30.9	26.9	1.4	50	172	28.1	34.0	26
Internasal length	24	8.4	24.9	8.3	7.7	0.5	15	52	7.4	9.4	26
Mouth width	30	10.5	29.8	10.0	8.2	0.6	18	56	8.8	10.8	26
Distance between first gill slits	56	19.6	60.0	20.1	16.3	0.8	37	113	18.8	21.7	26
Distance between fifth gill slits	49	17.1	52.0	17.3	15.6	0.9	30	105	15.1	19.1	26
Branchial basket length	30	10.5	32.4	10.9	8.3	0.7	21	56	9.8	12.9	26
Length of anterior margin of pelvic fin	53	18.5	50.7	16.9	15.8	1.4	31	108	12.9	18.8	26
Pelvic fins width	104	36.4	117.1	38.7	39.2	3.1	56	256	32.2	44.7	26
External length of clasper	-	-	12.1	3.4	12.3	1.7	5	50	2.6	8.7	11
Internal length of clasper	-	-	30.6	8.9	23.0	2.7	13	99	7.1	17.3	11
Distance between cloaca and tail tip	330	115.4	281.5	100.7	94.3	42.2	65	418	26.2	189.3	26
Tail width	20	7.0	18.8	6.5	3.5	0.9	13	27	4.2	9.0	26
Distance between snout tip and cloaca	233	81.5	253.2	85.6	70.6	2.3	151	474	81.5	91.7	25
Distance between pectoral axil and posterior margin of pelvic fin	14	4.9	10.6	3.8	2.8	1.0	5	17	2.0	5.6	25
Distance between cloaca and caudal sting	72	25.2	68.8	23.5	17.6	3.8	45	132	17.2	36.0	26
Caudal sting length	34	11.9	35.0	12.0	11.6	2.1	20	77	6.7	15.3	22
Caudal sting width	2	0.7	2.7	1.0	0.9	0.3	2	5	0.6	1.7	23
Dorsal pseudosiphon length	-	-	4.3	1.1	2.6	0.3	2	8	0.6	1.4	3
Ventral pseudosiphon length	-	-	20.0	4.5	15.6	2.0	7	42	2.9	7.3	3

Head small, with relatively short interorbital and interspiracular distances (means, respectively, 9.9% DW and 15.8% DW). Eyes small (mean diameter 1.9% DW) and slightly pedunculated. Spiracles positioned laterally in relation to eyes (Figs. 4A–C, 5), greater than eyes (mean length 5.6% DW), and oval-triangular in shape (Fig. 5). Spiracular process short, straight and covering part of posterior portion of spiracular aperture, presenting developed dermal denticles (Fig. 5). Preorbital, prenasal and preoral distances with means, respectively, 29.9% DW, 27.5% DW, and 30.9% DW. Internasal distance with mean of 8.3% DW, and mouth width with mean of 10% DW. Teeth triangular, large, cuspidate, arranged in quincunx in both jaws, presenting few differences in size between teeth from central and lateral rows, but central teeth slightly greater. Adult specimens possess pointed and high cusps, with teeth of central rows and in the lower jaw more developed (Fig. 6). Tooth rows in adults 22–35/20–29, with exposed teeth in symphysis 2–4/3–4 (Tab. 2).

Branchial basket rectangular, with mean distance between first pair of gill slits (anterior portion of branchial basket) 20.1% DW, and mean distance between fifth pair of gill slits (posterior portion) 17.3% DW. Branchial basket with mean distance between first and fifth gill slits 10.9% DW. Pelvic fins triangular and dorsally covered by the disc (Figs. 1B, 2B, D, 3B, D; S1B, D), with mean length of anterior margin 16.9% DW. Distances between distal portions of pelvic fins, and between the axils of pectoral and pelvic fins, with means respectively of 38.7 and 3.8% DW.

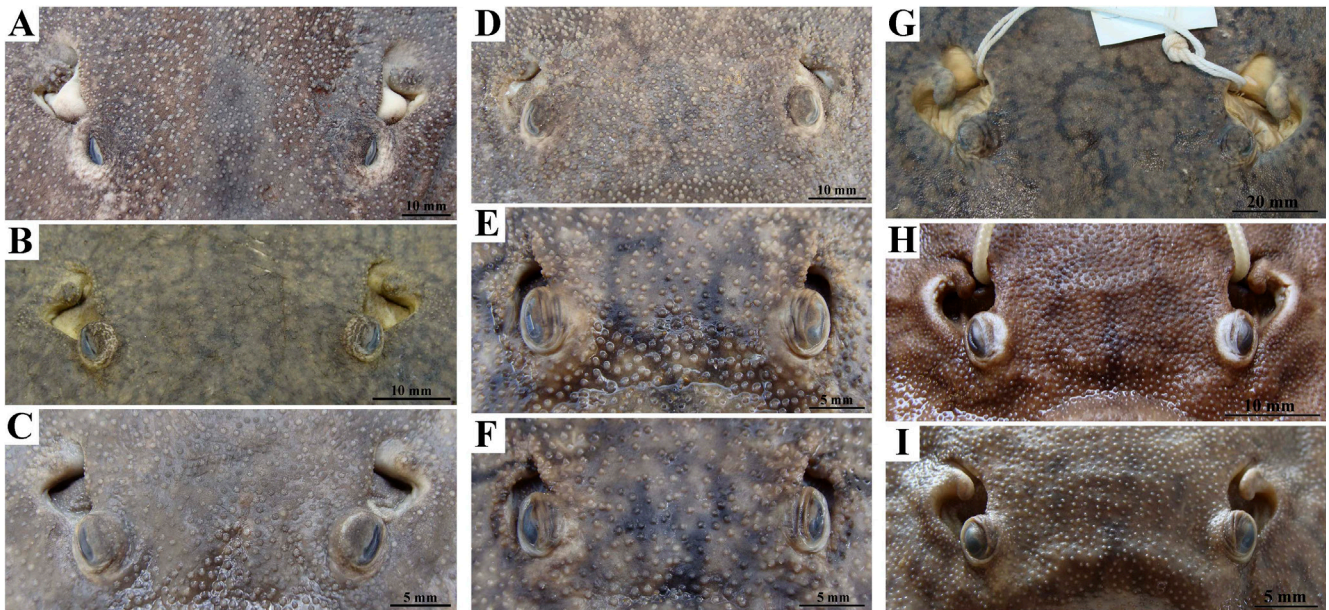


FIGURE 4 | Frontal view of eyes and spiracles of the three species of genus *Paratrygon*. *Paratrygon orinocensis*: A. IAvH-P 12449 (paratype), adult male, 573 mm DW, from Orinoco river. B. USNM 233944a (paratype). C. IAvH-P 11939 (holotype). *Paratrygon parvaspina*: D. IAvH-P 12447 (holotype), adult female, 450 mm DW, from Bitá river. E. IAvH-P 12441 (paratype), juvenile female, 225 mm DW, from Tomo river. F. IAvH-P 12446 (paratype), juvenile male, 212 mm DW, from Tomo river. *Paratrygon aiereba*: G. MPEG uncatálogued, adult male, 578 mm DW, from Marajó island. H. MZUSP 14774, juvenile female, 256 mm DW, from Jutáí river. I. MUSM uncatálogued, juvenile male, 220 mm DW.

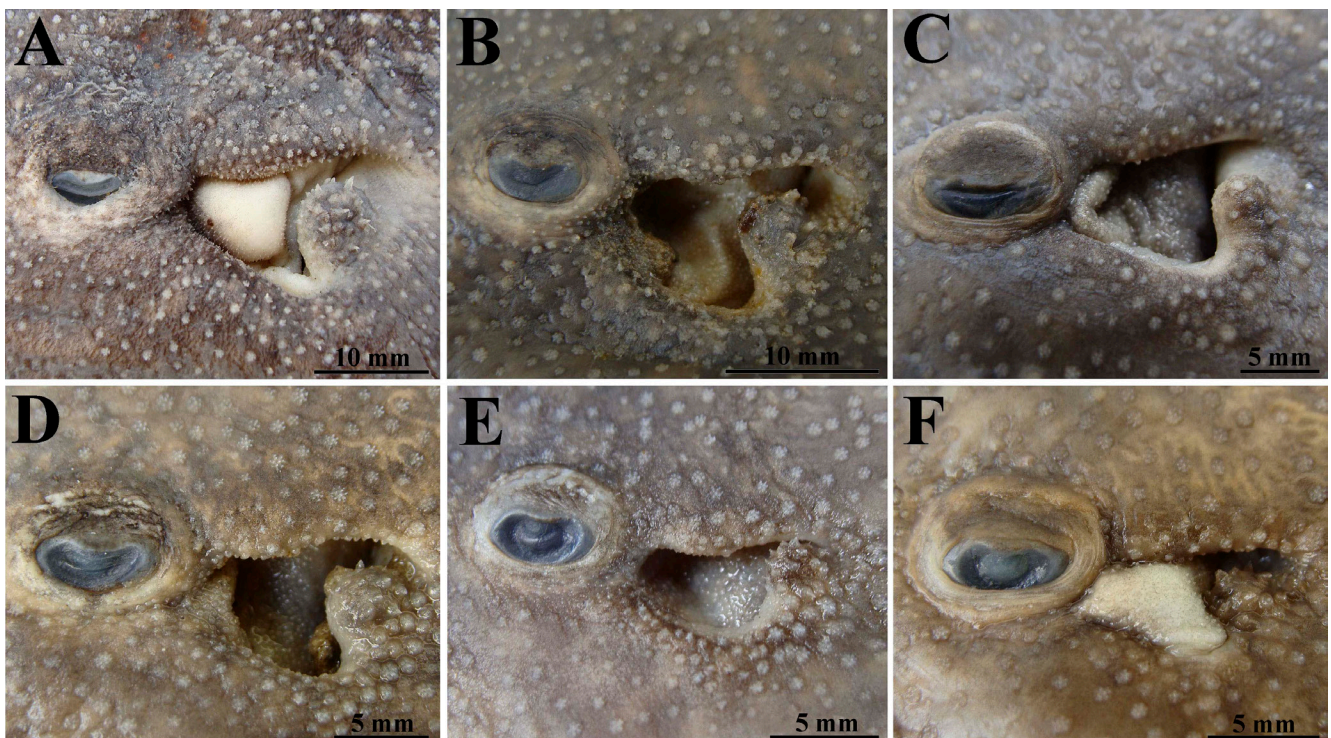


FIGURE 5 | Lateral view of spiracles and spiracles process of *Paratrygon orinocensis*. A. IAvH-P 12449 (paratype). B. IAvH-P 12448 (paratype). C. IAvH-P 11939 (holotype). D. IAvH-P 11942, juvenile female, 297 mm DW, from Orinoco river. E. IAvH-P 11938, juvenile male, 242 mm DW, from Orinoco river. F. IAvH-P 11941, juvenile female, 248 mm DW, from Orinoco river.

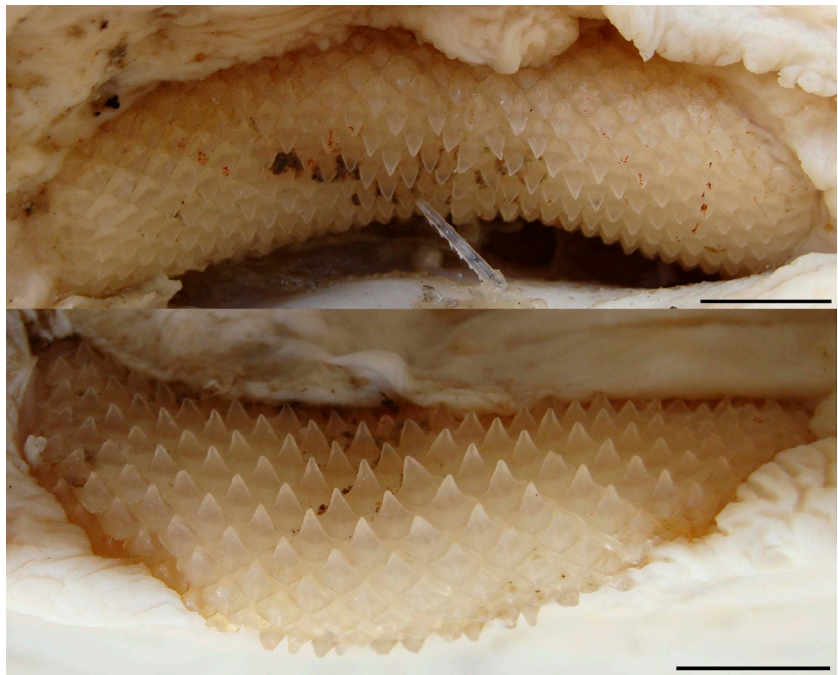


FIGURE 6 | Upper (above) and lower (below) teeth of *Paratrygon orinocensis*, IAvH-P 12449 (paratype). Scale bars = 5 mm.

TABLE 2 | Meristic data taken from four specimens of *Paratrygon orinocensis* radiographed; “M” corresponds to the mode.

Paratrygon orinocensis	IAvH-P 12449	IAvH-P 12448	USNM 233944	MZUSP 117220	M	Range
Precaudal vertebrae	-	-	42	45	-	42 - 45
Caudal vertebrae	-	-	-	-	-	-
Total vertebrae	-	-	-	-	-	-
Diplospodylic vertebrae	-	-	-	-	-	-
Propterygial radials	-	-	49	49	49	49
Mesopterygial radials	-	-	25	24	-	24 - 25
Metapterygial radials	-	-	42	43	-	42 - 43
Total radials	-	-	116	116	116	116
Pelvic radials	-	-	22	20	-	20 - 22
Tooth rows of upper jaw	35	23	-	22	-	22 - 35
Tooth rows of lower jaw	29	21	-	20	-	20 - 29
Symphysis of upper jaw	4	4	-	2	4	2 - 4
Symphysis of lower jaw	4	3	-	4	4	3 - 4

Clasper short, robust and cylindrical with rounded tips in adult and subadult specimens. Claspers present significant increase in size from neonates to adults: ranges of external and internal lengths in neonates and juveniles, respectively, 2.1 to 3%, and 7.1 to 8.7% DW, in subadult specimen, respectively, 3.6 and 9.5% DW, and in

adult specimen analyzed 8.7 and 17.3% DW. Pseudosiphon and ventral pseudosiphon also grow from juveniles to adults: ranges of lengths of pseudosiphon and ventral pseudosiphon, respectively, 0.6 to 1.2% and 2.9 to 3.3% DW in neonates and juveniles, and 1.4% and 7.3% DW in adult specimen (see S2 for more details).

Tail very long compared to the *P. aiereba* and *P. parvaspina*, with a short base, and a pre-caudal sting portion narrow; post-caudal sting portion extremely long and filiform (Figs. 1–3; S1). Mean of distance from cloaca to caudal sting insertion (pre-caudal sting portion of tail) 23.5% DW (Tab. 1). Mean tail width 6.5% DW, presenting a proportional decrease in size from juveniles to adults: range in neonates from 7.2 to 9% DW, in juveniles from 5.1 to 7.3% DW, in subadult analyzed 6.4% DW, and in adults from 4.2 to 5.7% DW. Mean distance from cloaca to tail tip 100.7% DW, also with a proportional decrease from juveniles to adults: range in neonates 164.1 to 189.3% DW, in juveniles 26.2 to 150% DW, in subadult analyzed 66.3% DW, and in adults 27.1 to 59% DW (Tabs. 1–2; S2). Dorsal and ventral tail folds present but poorly developed, more easily recognizable in the portion immediately after caudal sting; some specimens with a medial ventral groove in the tail from its base to the origin of ventral fold.

Squamation. Dermal denticles present on entire dorsal region of disc and tail. Denticles greater in central region of disc, more concentrated and more visible than denticles on disc margins. Denticles on tail between tail base and caudal sting insertion are bigger than denticles located from caudal sting insertion to the tip of tail.

Dermal denticles on central disc region with diameters from 1–2 mm (Fig. 7). These denticles present a wide and high crown (*cr*), with a central coronal plate (*ccp*) morphologically similar to the lateral coronal ridges (*lcr*) that surround it (Fig. 7). Dermal denticles on central region of disc generally with four to six lateral coronal ridges in juvenile specimens; subadults and adults present two rows of *lcr* surrounding the central coronal plate, with more than a dozen ridges in total. Dermal denticles on anterior margin of disc with similar morphology to central disc, however with fewer *lcr*: just one row of *lcr* surrounding *ccp*, and number of lateral ridges between three to six (Fig. 8). Two morphological types of dermal denticles on tail base (Fig. 9A): one very similar to denticles on anterior margin of disc and central disc but with fewer *lcr* (Figs. 9C–D), and another type similar to the thorns on tail (but much smaller), with just a very high and developed *ccp* in its crown (Fig. 9B).

One to two dorsal rows of developed thorns with broad base present on tail of adult specimens; dorsal rows originate just after base of tail and extend almost to base of caudal sting (Figs. 10A–B). Subadults and larger juvenile specimens generally with just one dorsal row of thorns, with few specimens presenting duplicate rows near the caudal sting base; thorns in these specimens also high and with broad base, slightly larger near caudal sting region (Figs. 10C–E). Majority of juvenile specimens with just a part of the single dorsal row with small thorns, with a slightly larger thorns near the caudal sting (Figs. 10F–G). Neonates with a single poorly developed row of minute thorns at tail base (Fig. 10H).

Caudal sting with mean length 12% DW [6.7 and 15.3% DW]; caudal sting mean width 1% DW [0.6 and 1.7% DW] (Tab. 1). Subadult and larger juvenile specimens with one or two well developed caudal stings, with lateral serrations distributed along

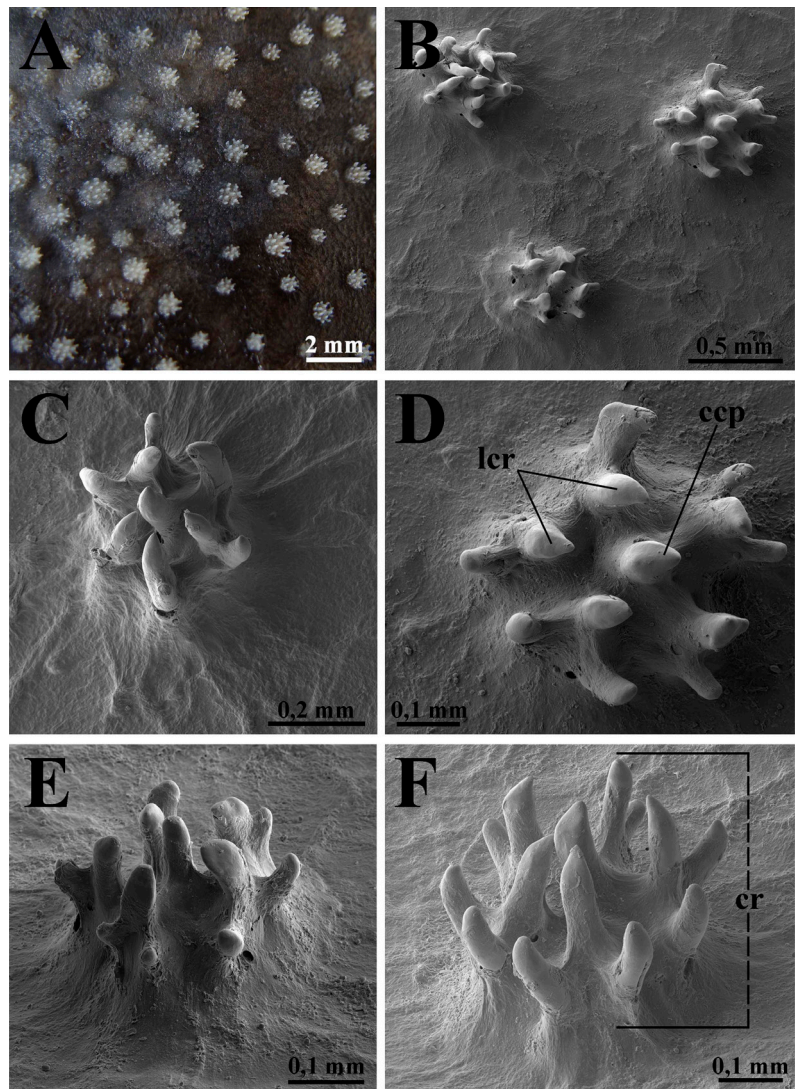


FIGURE 7 | Dermal denticles in the central disc of *Paratrygon orinocensis*. **A.** dorsal view of dermal denticles of IAvH-P 12448. **B.** dorsal view of three dermal denticles of MZUSP 117220 (paratype), juvenile male, 299 mm DW, from Apure river, made by Scanning Electron Microscopy (SEM image). **C.** dorsal view of one central dermal denticle of MZUSP 117220 (SEM image). **D.** morphology detail of a central dermal denticle of MZUSP 117220 (SEM image) in dorsal view. **E.** lateral-dorsal view of one central dermal denticle of MZUSP 117220 (SEM image). **F.** lateral-dorsal view of one central dermal denticle showing the crown (MZUSP 117220, SEM image). ccp = central coronal plate, cr = crown, lcr = lateral coronal ridge.

their entire length or just on their terminal half; lateral serrations more developed in the terminal portion of the sting (Figs. 11A–C). Caudal stings without a dorsal medial groove. Younger juveniles and neonates with caudal stings similar to subadults, however with reduced number of serrations and only on terminal half of sting (Figs. 11D–F).

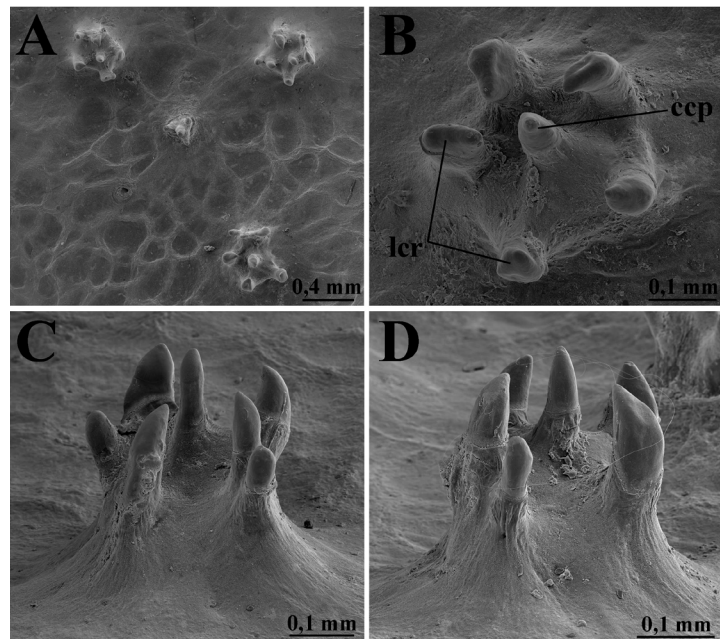


FIGURE 8 | Dermal denticles in anterior margin of the disc of *Paratrygon orinocensis*, MZUSP 117220 (SEM images). **A.** dorsal view of four dermal denticles. **B.** morphology detail of one denticle in dorsal view. **C.** and **D.** lateral views of anterior margin dermal denticles. ccp = central coronal plate, lcr = lateral coronal ridge.

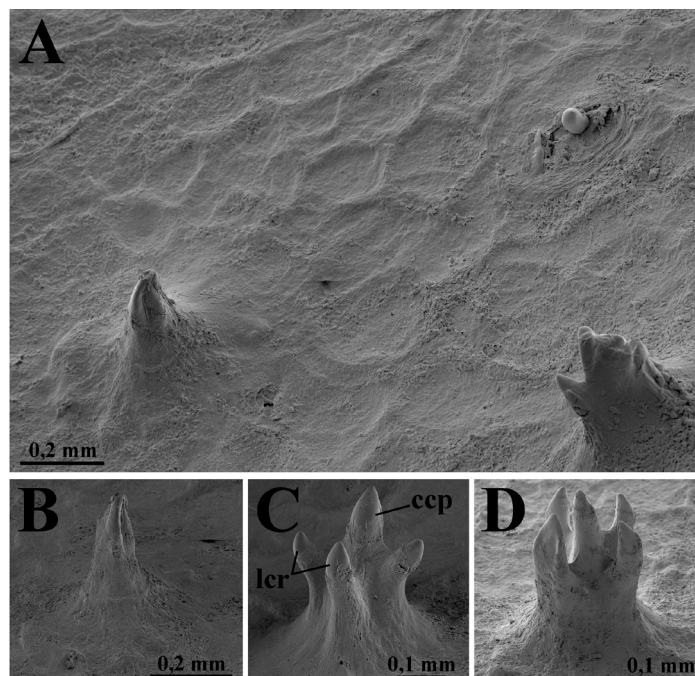


FIGURE 9 | Posterior margin and tail's basis dermal denticles of *Paratrygon orinocensis*, MZUSP 117220 (SEM images). **A.** dorsal-lateral views of three dermal denticles showing the two morphological types: one more similar with the central disc dermal denticles (left down corner), and other more similar with thorns of tail's dorsal row (right down corner); left above a bud of a denticle. **B.** morphology detail of one pointed dermal denticle in lateral view. **C.** and **D.** lateral views of two dermal denticles. ccp = central coronal plate, lcr = lateral coronal ridge.

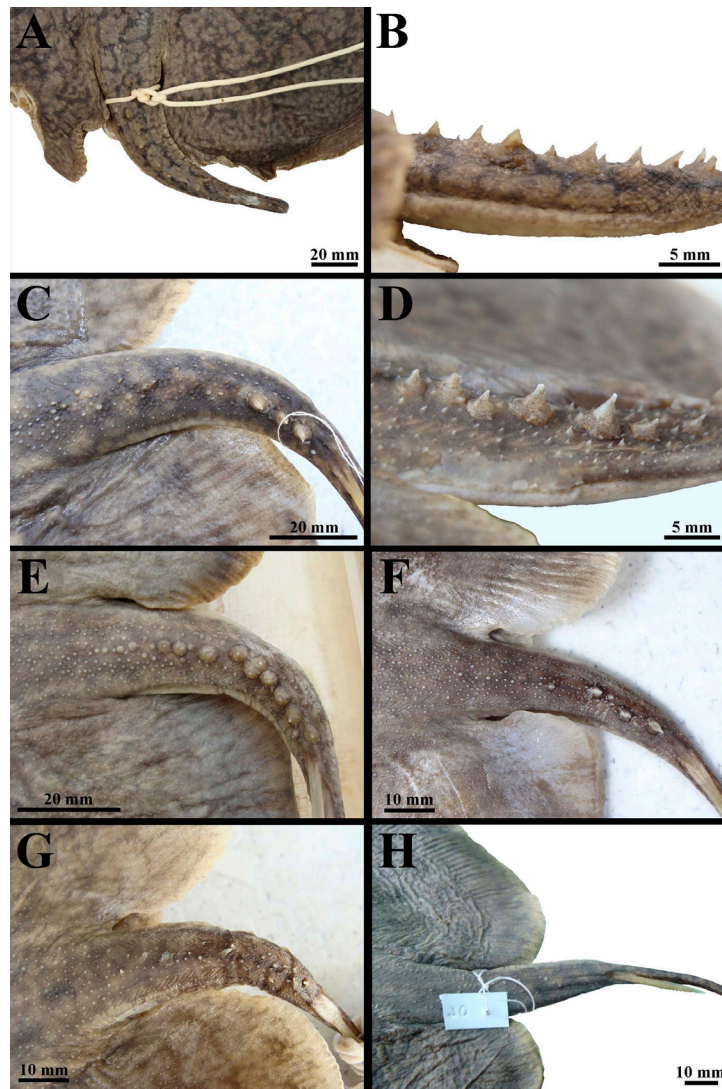


FIGURE 10 | Dorsal row of thorns on the tail of *Paratrygon orinocensis*. **A.** dorsal view of USNM 233944a (paratype). **B.** lateral view of USNM 233944a. **C.** dorsal view of IAvH-P 11939 (holotype). **D.** lateral-dorsal view of IAvH-P 11940 (paratype). **E.** dorsal view of IAvH-P 11943, juvenile female, 372 mm DW, from Orinoco river. **F.** dorsal view of IAvH-P 11938. **G.** dorsal view of IAvH-P 12444, juvenile female, 241 mm DW, from Orinoco river. **H.** dorsal view of ICN uncatalogued specimen, juvenile male, 240 mm DW.

Lateral line. Four principal ventral lateral line canals (hyomandibular, *HMD*; infraorbital, *IOC*; supraorbital, *SPO*; and nasal, *NAS*) connect at a unique point named junction of the four canals (*JFC*), located laterally to mouth (Fig. 12). Hyomandibular canal (*HMD*) extends posteriorly through its angular component (*ang*). After the angular component, the canal continues to descend, contouring externally the branchial basket toward the central region of the disc to the scapulocoracoid bar, where it is curved posteriorly forming its jugular component (*jug*). Close to the pelvic girdle, the hyomandibular canal makes a broad loop, the subpleural loop (*spl*), with two to five small posterior subpleural tubules (*pst*) that continue posteriorly; posteriormost tubule slightly

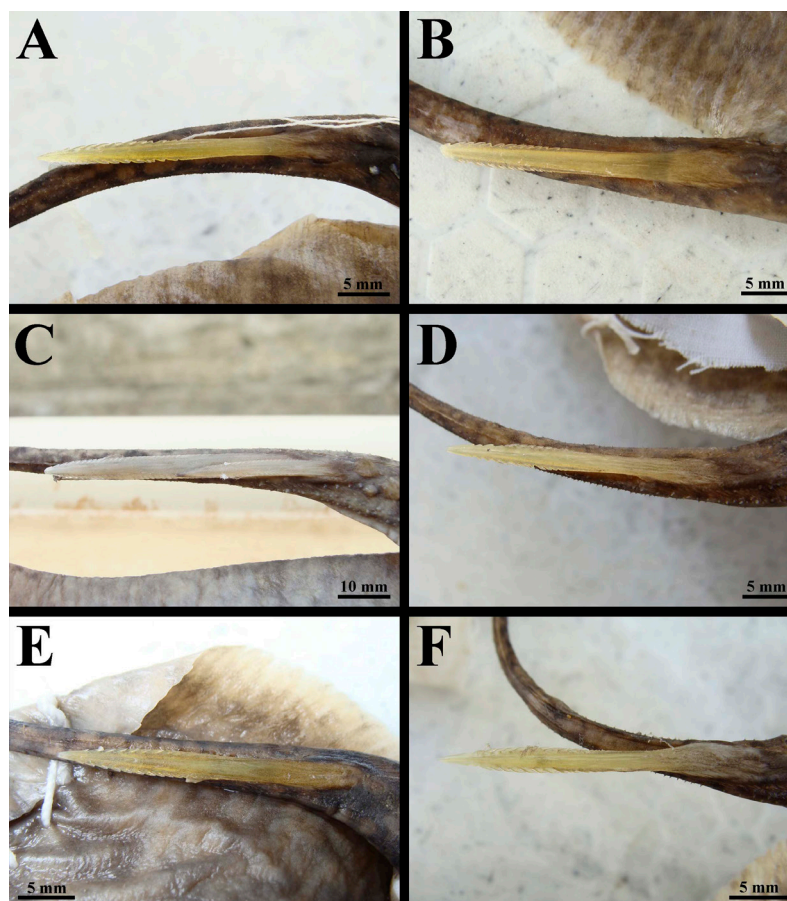


FIGURE 11 | Dorsal view of caudal sting of *Paratrygon orinocensis* in six specimens. **A.** IAvH-P 11939 (holotype). **B.** IAvH-P 11940 (paratype). **C.** IAvH-P 11943. **D.** IAvH-P 12440, juvenile female, 249 mm DW, from Bitá river. **E.** IAvH-P 12443. **F.** IAvH-P 12444.

larger than others. From the subpleural loop, the canal continues anteriorly as a big curve to the scapulocoracoid bar, where it turns again externally in direction to anterior margin of the disc, forming the subpleural component (*spc*) of the hyomandibular canal. Subpleural component extends anteriorly toward anterolateral margin of disc, where between the levels of mouth and branchial basket the first subpleural tubule (*spt*) detaches from the hyomandibular canal, extending toward disc margin. Subpleural component reaches disc margin at the level just anterior to the nostrils, and continues anteriorly very close to disc margin to connect with the nasal canal (*NAS*) in the mid region of anterior disc margin (not shown in Fig. 12). Dozens of small subpleural tubules connected to subpleural component of hyomandibular canal present on anterior disc margin, the posteriormost tubule longer than others (Fig. 12).

From the *JFC* the infraorbital canal (*IOC*) extends laterally, slightly curves anteriorly, and subdivides forming the ramifications of the suborbital component (*sub*). Suborbital component of infraorbital canal presents a honeycomb pattern; individual honeycombs greater posteriorly, smaller close to the subpleural component (*spc*) of hyomandibular canal and the anterior margin of the disc. Ramifications of the suborbital component

connected in at least two points with the prenasal component (*pnc*) of nasal canal near the mid anterior margin of disc region. Supraorbital canal (*SPO*) extends medially and anteriorly from *JFC*, forming its orbitonasal component (*orb*) that curves posteriorly anterior to nostrils forming the prenasal loop (*pnl*). From the prenasal loop, the canal extends posteriorly in direction to the nostrils, forming the more broadly curved nasointernal loop (*nil*). From the *nil*, the supraorbital canal extends anteriorly to the level of the *pnl*, where it connects to the prenasal component (*pnc*) of nasal canal, forming in this part its subrostral component (*sbr*) with close to a dozen vesicles of Savi (*vS*) (Fig. 12).

Nasal canal (*NAS*) extends anteromedially at a 45° angle from the *JFC* to next to the nostril, where it penetrates the disc; the canal emerges between the nostrils, making a small anterior curve and ascending straight to the anterior margin of disc, forming the prenasal component (*pnc*). Prenasal component connects with *sbr* of *SPO* next to nostrils, and with *sub* of *IOC* and *spc* of *HMD* next to anterior margin of disc. Mandibular canal (*MNC*) extends lateroexternally from median line of body very close to mouth, contouring posteriorly the *adductor mandibulae* muscle until close to the first gill slit, where it penetrates the body (Fig. 12).

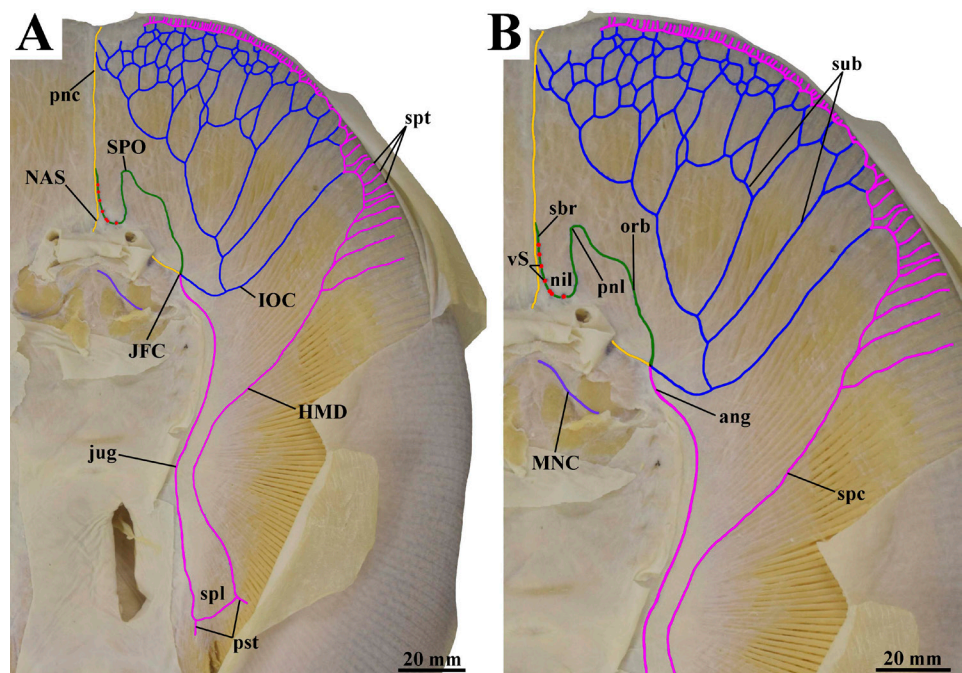


FIGURE 12 | Ventral canals of lateral line system in *Paratrygon orinocensis*, MZUSP 117220 (paratype).

A. distribution of all ventral canals. **B.** detail of the anterior central disc ventral canals. ang = angular component of hyomandibular canal, HMD = hyomandibular canal, IOC = infraorbital canal, JFC = junction of the four canals, jug = jugular component of hyomandibular canal, MNC = mandibular canal, NAS = nasal canal, nil = nasointernal loop, orb = orbitonasal component of supraorbital canal, pnc = prenasal component of nasal canal, pnl = prenasal loop, pst = posterior subpleural tubules, sbr = subrostral component of supraorbital canal, spc = subpleural component of hyomandibular canal, spl = subpleural loop, SPO = supraorbital canal, spt = subpleural tubule, sub = suborbital component of supraorbital canal, vS = vesicles of Savi.

Skeleton. Meristic counts of vertebrae and pectoral and pelvic radials are shown in Tab. 2. In dorsal view, neurocranium presents a “T” format, widest anteriorly at the nasal capsules (*NC*). Rostral projection (*RPJ*) minute and almost imperceptible in the anteriormost part of the neurocranium between the nasal capsules (Fig. 13). Nasal capsules oval, separated by a large internasal septum (*IS*), anteriorly surrounded by the first segment of propterygium (*FSP*) and laterally connected with propterygium (*PRO*) through a small and triangular antorbital cartilage (*ANT*). Preorbital process (*PRP*) posterodorsal to the nasal capsules, small, triangular, and not exceeding laterally the limits of nasal capsules (Fig. 13). Supraorbital crest (*SOC*) posterior to the preorbital process and extending dorsolaterally above all orbital region. Posterior portion of *SOC* with a small supraorbital process (*SP*) and a short but more developed postorbital process (*POP*). Roof of neurocranium with a large and spoon shaped fontanelle, from nasal capsules to posterior part of orbital region. Fontanelle divided into two components: an anterior, rounded and broad precebral component (*PCF*), and a posterior, long, narrow and “8”-shaped frontoparietal component (*FPF*) (Fig. 13).

Mandibular arch laterally extended, with long and proximally arched palatoquadrate (*PQ*) and Meckel’s cartilage (*MC*). Palatoquadrate not too slender, arched medially, with a dorsolateral process (*DLP*) close to its articulation with Meckel’s cartilage. Meckel’s cartilage with a pronounced arch in its proximal portion where it articulates with palatoquadrate and hyomandibula; proximal portion more robust than distal portion. *MC* with long lateral process (*LP*) that reaches the *DLP* of palatoquadrate (Fig. 13). Hyomandibula (*HYO*) long, slender and straight, with its distal portion anteriorly curved. This portion articulates with the posteroexternal corner of *MC* through the hyomandibular-Meckelian ligament (not shown in Fig. 13).

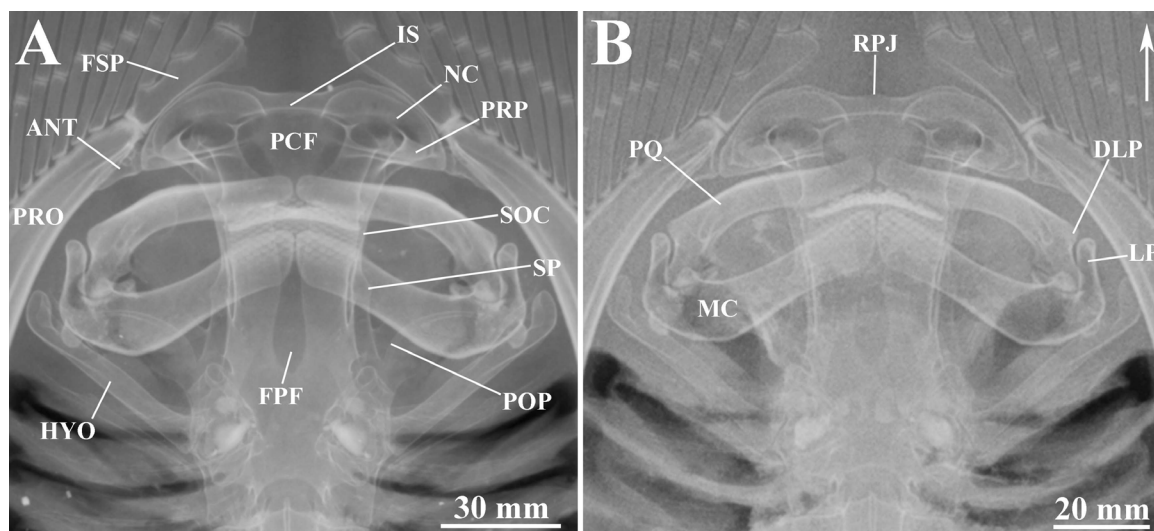


FIGURE 13 | Radiographs of neurocranium and mandibular arch of *Paratrygon orinocensis*, upper views. **A.** USNM 233944b (paratype). **B.** MZUSP 117220 (paratype). ANT = antorbital cartilage, DLP = dorsolateral process, FPF = frontoparietal component of fontanelle, FSP = first segment of propterygium, HYO = hyomandibula, IS = internasal septum, LP = lateral process, MC = Meckel’s cartilage, NC = nasal capsule, PCF = precebral component of fontanelle, POP = postorbital process, PQ = palatoquadrate, PRO = propterygium, PRP = preorbital process, RPJ = rostral projection, SOC = supraorbital crest, SP = supraorbital process. Arrow indicates to the anterior portion of specimens.

In dorsal view, synarcual cartilage with length similar to neurocranium and expanded laterally throughout its length, mainly posteriorly where it articulates with scapulocoracoid bar (Fig. 14). Dorsomedial crest (*DMC*) located over spinal nerve canal (*SNC*); *SNC* tubular. Dozens of spinal nerve foramina (*SNF*) present on lateral walls of *SNC* at its basal portion (Fig. 14). Posterior region of synarcual cartilage expanded laterally with three areas of contact with the scapulocoracoid bar: dorsal socket (*DS*) broad and with a slightly deep recess, and two ventral condyles, anterior ventral condyle (*AVC*) and posterior ventral condyle (*PVC*), with anterior condyle slightly larger than posterior condyle. From this region to mid portion of *SNC* a lateral stay (*LS*) projects laterally, almost reaching the widest point of synarcual cartilage (located at its articulation with scapulocoracoid bar) (Fig. 14).

Scapulocoracoid (shoulder girdle) composed of coracoid bar (*CB*) slightly arched in both anterior and posterior faces. Anterior surface with a more pronounced curvature than posterior aspect, and with a broad and triangular scapular process (*SCP*) articulating with the synarcual cartilage (Fig. 15). Scapular process with a dorsolateral crest (*DLC*) which projects anterolaterally from the region next to its articulation with the synarcual cartilage, and projects laterally beyond the mesocondyle (Fig. 15). In dorsal view, three condyles of *SCP* contact the basal elements of the pectoral fin. The procondyle (*PC*) in the anterolateral extremity of *SCP*, constituting the major condyle of *SCP*, articulates with the most anterior portion of the propterygium base and presents an inverted “L” shape (Fig. 15). The mesocondyle (*MSC*) in the posterolateral face of *SCP* next to the metacondyle articulates with the mesopterygium and is the most laterally projected condyle of *SCP*. The metacondyle (*MTC*) also in the posterolateral extremity of *SCP*, very next to *MSC*, articulates with the metapterygium (Fig. 15).

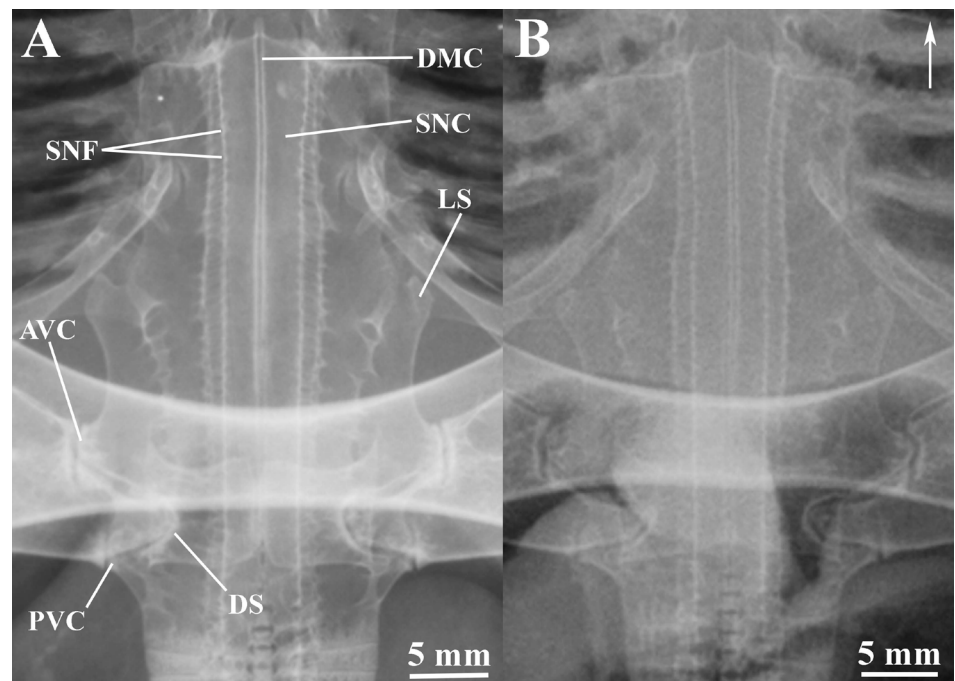


FIGURE 14 | Radiographs of synarcual cartilage of *Paratrygon orinocensis*, upper views. **A.** USNM 233944b (paratype). **B.** MZUSP 117220 (paratype). AVC = anterior ventral condyle, DMC = dorsomedial crest, DS = dorsal socket, LS = lateral stay, PVC = posterior ventral condyle, SNC = spinal nerve canal, SNF = spinal nerve foramen. Arrow indicates to the anterior portion of specimens.

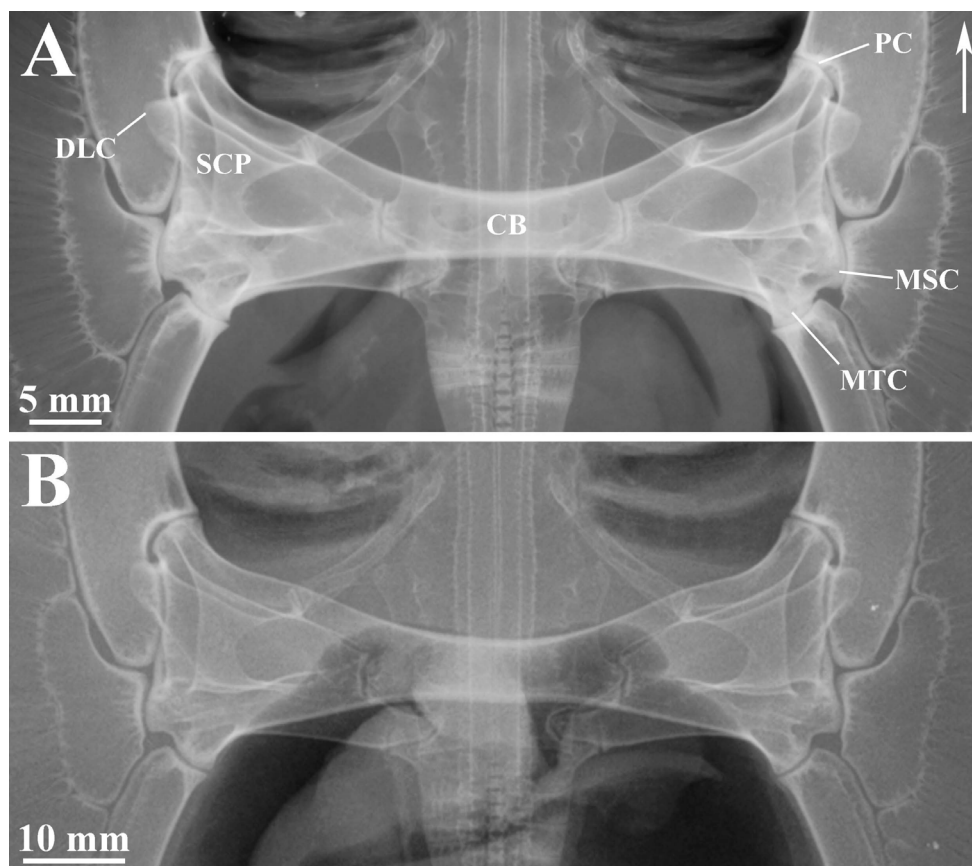


FIGURE 15 | Radiographs of scapulocoracoid of *Paratrygon orinocensis*, upper views. **A.** USNM 233944b (paratype). **B.** MZUSP 117220 (paratype). CB = coracoid bar, DLC = dorsolateral crest, MSC = mesocondyle, MTC = metacondyle, PC = procondyle, SCP = scapular process. Arrow indicates to the anterior portion of specimens.

The propterygium (*PPT*) articulates with *PC* at its anterior portion but posteriorly contacts the lateroexternal face of *SCP* between *PC* and *MSC*. The mesopterygium (*MSP*) articulates solely with *MSC*, and the metapterygium (*MTP*) articulates only with *MTC* (Fig. 16). Propterygium robust and arched, is the most developed basal element of the pectoral fin, with its posterior extremity broader than the anterior and curved and more slender distally (Fig. 16A). Anterior extremity of *PPT* articulates at its internal face with the antorbital cartilage (*ANT*), and its anterior tip with the first segment of propterygium (*FSP*). *FSP* one-fourth of *PPT* length, contouring externally the anterior portion of nasal capsules (*NC*) and articulating anteriorly with the first two rays of the propterygium. Posterior portion of *PPT*, where it articulates with scapulocoracoid, presents an inverted “L” shape, with its anterior part contacting the procondyle and the rest contacting the lateral external face (*LEF*) of *SCP* to next to the mesocondyle; this portion of *PPT* also contacts mesopterygium in two points: one on its external face near the tip, and other in the posterior extremity through a small articular surface (*SAS*) (Figs. 16A–B). Mesopterygium with length similar or slightly smaller than scapular process in anteroposterior aspect, being the smallest basal element of pectoral

fin (Figs. 15, 16B). Anterior portion of *MSP* anteriorly detached and more slender than posterior part. Posterior portion more developed with its internal face articulating with *MSC* and presenting anteriorly a pronounced concavity which contacts propterygium. Both extremities, anterior and posterior, contact respectively propterygium and metapterygium, and median radials (*JMR*) of pectoral fin (Fig. 16B). Metapterygium long, arched and slender, with its proximal portion about as wide or slightly less than half of width of proximal portion of *PPT* (Fig. 16B). Anterior portion of *MTP* slightly more robust than the rest, being articulated with *MTC* at its anterior tip, and contacting mesopterygium and *JMR* on its external anterior face. Posterior portion of *MTP* segmented in two or three posterior segments (*PSM*) at the level of pelvic girdle, with its posterior segments successively smaller than anterior segments (Fig. 16C).

Pelvic girdle composed of arched puboischiadic bar (*PB*) which possesses a very long prepelvic process on its anteromedial portion (not shown in Fig. 17). Puboischiadic bar highly arched, with its anterior portion more inclined and its posterior portion highly curved. Lateral extremities of *PB* possess two ventral processes and one dorsal, and three pairs of dorsoventrally situated obturator foramina (*OF*) (Fig. 17). Iliac process (*IP*) short, with same dimensions or slightly longer than ischial process, and located at posterolateral extremity of *PB*. Ischial process (*ISP*) triangular and broad, located at internal portion of lateral extremities of *PB*. Lateral prepelvic process (*LPP*) situated in lateral extremities of anterior margin of *PB*; *LPP* triangular, developed and projected dorsolaterally (Fig. 17).

Color in alcohol. Dorsal disc color beige, brown, gray or dark gray, with large dark spots concentrated between disc margins and central disc area, and also small light spots distributed through entire disc (Figs. 1A, 2A, C, 3A, C; S1A, C). Dark spots dark gray, dark brown or black, and in various shapes such as rounded, oval, polygonal, vermiculated or even axon shaped. Large dark spots in some specimens possess small

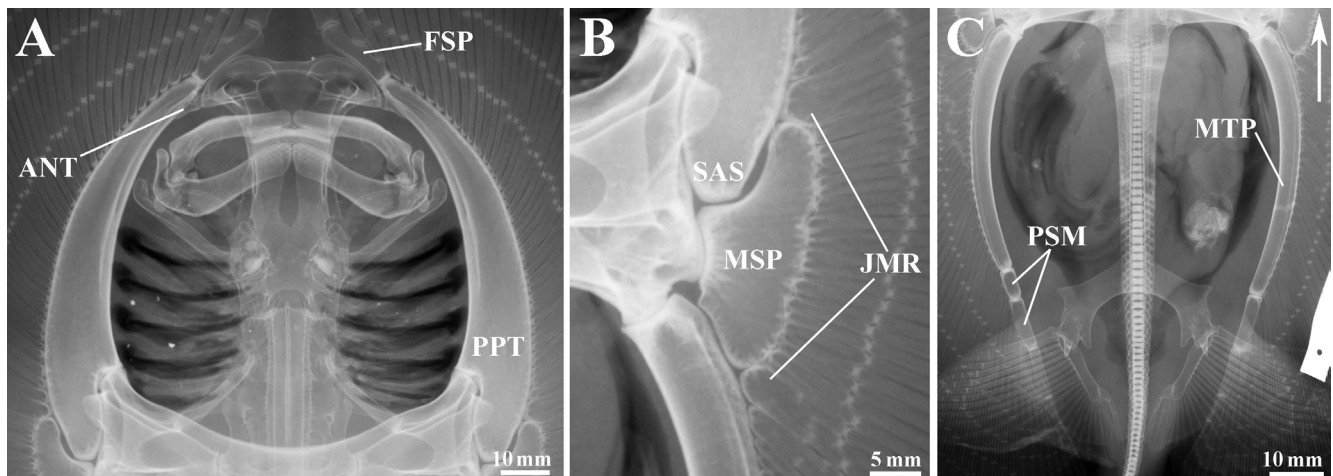


FIGURE 16 | Radiographs of basal elements of pectoral fin of *Paratrygon orinocensis*, USNM 233944b (paratype), upper views. **A.** propterygium region. **B.** mesopterygium region. **C.** metapterygium region. ANT = antorbital cartilage, FSP = first segment of propterygium, JMR = junction of medial radials, MSP = mesopterygium, MTP = metapterygium, PPT = propterygium, PSM = posterior segments of metapterygium, SAS = small articulation surface. Arrow indicates to the anterior portion of specimens.

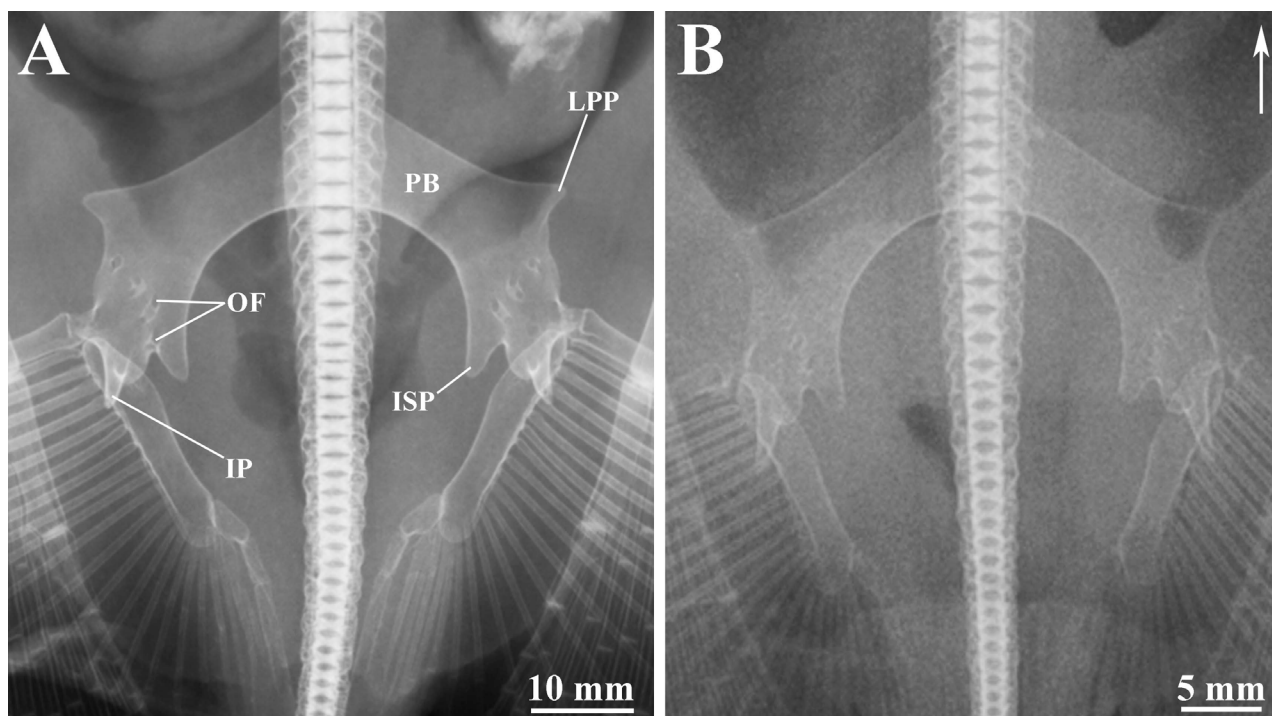


FIGURE 17 | Radiographs of pelvic girdle of *Paratrygon orinocensis*, upper views. **A.** USNM 233944b (paratype). **B.** MZUSP 117220 (paratype). IP = iliac process, ISP = ischial process, LPP = lateral prepelvic process, OF = obturator foramen, PB = puboischiadic bar. Arrow indicates to the anterior portion of specimens.

beige specks in its central area; when closer to disc margins, these spots become smaller. Large dark spots also occur in head and branchial basket regions. Small light gray or beige spots present polygonal shapes, and their sizes are generally similar to eye diameter but sometimes slightly greater. Dorsal caudal coloration from caudal base to caudal sting tip similar to dorsal disc coloration, with some dark spots on midline, and light spots laterally; post caudal sting region gray to dark gray with beige or light brown specks, but darker closer to tail tip.

Disc ventral coloration with two major patterns: one light, white color, predominant in practically all central disc area and anterior margin, and another darker pattern, gray color, present on lateral and posterior margins of disc (Figs. 1B, 2B, D, 3B, D; S1B, D). Gray pattern in most specimens also possesses small and vermiculate dark gray spots closer to disc margins, with these spots more visible in juvenile specimens. Ventral coloration of pelvic fins also present both patterns present on ventral disc, with light pattern located on anterior margins and central region of pelvic fin, and dark pattern located only at posterior margin. Claspers also with both patterns, with light one at its base, and dark pattern at its medial and terminal regions. Ventral coloration of tail in few specimens with same light pattern of disc occurring from its base to caudal sting tip; however, in most specimens tail region presents a light gray coloration with some darker gray rounded spots. Post-caudal sting region of tail, in all specimens, with dark gray color, progressively darker toward tail tip, and with small dark gray specks throughout. In live specimens, coloration similar but with dorsal and ventral patterns more clearly demarked.

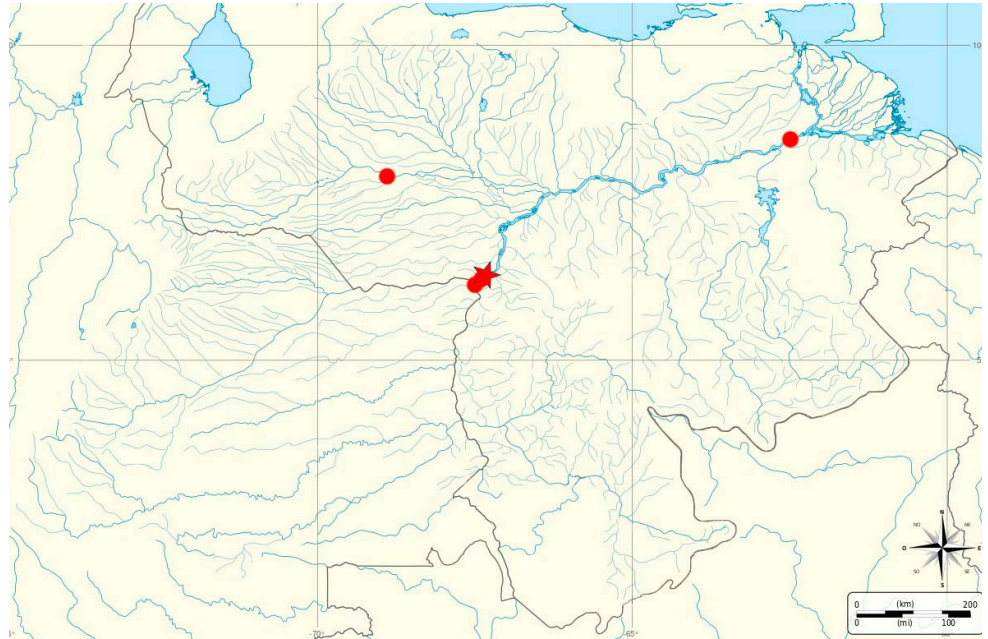


FIGURE 18 | Distribution of *Paratrygon orinocensis* throughout Orinoco basin. This species occurs in the mid and lower portion of Orinoco river, and mid portion of Apure river. See Discussion to a more complete discussion about its distribution. Star = holotype specimen (IAvH-P 11939) locality.

Geographic distribution. Endemic to the Orinoco basin, specimens of *Paratrygon orinocensis* analyzed in this study occur in the Apure, Bitá and Orinoco rivers (Fig. 18).

Etymology. The epithet *orinocensis* reflects the endemic distribution of this new species in the main rivers of the Orinoco basin. An toponym.

Paratrygon parvaspina, new species

urn:lsid:zoobank.org:act:5EF6A291-D95A-4E29-AD87-EDF4BFF635F8

(Figs. 19–31, Tabs. 3–4)

Paratrygon aiereba. —Maldonado-Ocampo *et al.*, 2006:117 [occurrence in the Tomo River, specimen IAvH-P 4684]. —Mejía-Falla *et al.*, 2007:125 [checklist of the species of sharks, rays and skates of Colombia, specimen IAvH-P 4684]. —Maldonado-Ocampo *et al.*, 2008:150 [checklist of the freshwater fishes of Colombia]. —Lasso, Sánchez-Duarte, 2012:134 [citation of specimen IAvH-P 4684].

Paratrygon sp. 2: —Loboda, 2016: vol.1. vii–ix, 33, 60, 75–76, 87, 97, 100, 112–123, 126–127, 142, 156, 190–192, 237–241, vol.2. xvi–xvii, 91–103, fig. 127, p. 91, fig. 128, p. 92, figs. 129–130, p. 93, figs. 131–132, p. 94, figs. 133–134, p. 95, fig. 135, p. 96, fig. 136, p. 97, fig. 137, p. 98, fig. 138, p. 99, figs. 139–140, p. 100, figs.

141–142, p. 101, figs. 143–144, p. 102, fig. 145, p. 103 [morphometry, morphological description, taxonomic revision, diagnosis, previous misidentifications, distribution].

Holotype. IAvH-P 12447, female, 450 mm DW, Colombia, State of Vichada, Municipality of Puerto Carreño, río Bitá, 06°06'07.2"N 67°29'11.9"W, 2 Feb 2014, C. Lasso & M. A. Morales-Betancourt.

Paratypes. (3 specimens). IAvH-P 12441, female, 225 mm DW, Colombia, State of Vichada, Locality of PNN El Tuparro, río Tomo, 05°21'09.8"N 67°55'04.4"W, 3 Mar 2014, C. Lasso & M. A. Morales-Betancourt. IAvH-P 12446, male, 212 mm DW, same data as previous specimen. MZUSP 117836, female, 266 mm DW, Venezuela, State of Amazonas, Municipality of Puerto Ayacucho, río Orinoco, 23 Jan 2013, F. Marques.

Non-type. IAvH-P 4684, female, 345 mm DW, Colombia, State of Vichada, Municipality of Cumaribo, Caño Peinilla, tributary of río Tomo, 05°35'08.3"N 68°0.3'44"W, 1 Feb, J. Maldonado-Ocampo.

Diagnosis. A species of *Paratrygon* diagnosed by the following combination of characters. Spiracular process extremely short and reduced, slightly more developed in adults, and with few dermal denticles (*vs. P. aiereba* with large and knob shaped spiracular processes that almost cover the spiracle aperture, and *P. orinocensis* with short and straight spiracular process with developed dermal denticles). Caudal sting very reduced, with mean of its length 6.2% DW [5.6–7.1% DW] (*vs. longer caudal stings in P. aiereba* and *P. orinocensis* with means and ranges, respectively, 11.3% DW [3–17.9% DW], and 11.9% DW [6.7–15.3% DW]). Tail short, with means of the pre-caudal sting region and the distance between cloaca and tail tip, respectively, 21.1% and 50.4% DW (*vs. longer tails in P. aiereba* and *P. orinocensis*, with means of the pre-caudal sting region and the distance between cloaca and tail tip, respectively, 23.5% and 87.8% DW in *P. aiereba*, and 25.2% and 115.4% DW in *P. orinocensis*). Anterior disc margin broadly rounded (*vs. P. aiereba* and *P. orinocensis* with well developed and visible concave anterior disc margins, especially the latter). Spiracles small and quadrangular, with mean length 5.2% DW [4.9–5.8% DW] (*vs. larger spiracles in P. aiereba*, with mean length 6% DW [4.4–11.6% DW], and *P. orinocensis* with triangular and slightly smaller spiracles, with mean spiracle length 5.6% DW [4.5–7.9% DW]). Rostral projection relatively large (*vs. small or minute in P. aiereba* and *P. orinocensis*, respectively). Preorbital processes more laterally projected, externally exceeding level of nasal capsules (*vs. preorbital processes less laterally projected, not exceeding level of nasal capsules in P. aiereba* and *P. orinocensis*). Lateral stay of synarcual cartilage long, exceeding the lateral level of anterior ventral condyle (*vs. short in P. aiereba* and *P. orinocensis* not exceeding the lateral level of anterior ventral condyle). Dorsolateral crest of scapular process not pronounced and not exceeding laterally the level of mesocondyle (*vs. pronounced dorsolateral crests that laterally exceed the level of mesocondyle in P. aiereba* and *P. orinocensis*). Propterygium robust (*vs. more slender in P. aiereba* and *P. orinocensis*). Concavity of the internal face of mesopterygium not so pronounced and curved (*vs. very pronounced and curved in P. aiereba* and *P. orinocensis*). Metapterygium robust and highly curved (*vs. metapterygium slender and more straight in P. aiereba* and *P. orinocensis*).

Description. For the general appearance of *Paratrygon parvaspina*, see Figs. 19–20, for morphological characters examined see Figs. 21–31. Measurements and counts are showed in Tabs. 3–4, respectively, and S3.

Paratrygon parvaspina presents a more rounded than oval disc format, with mean of disc length in 106.5% DW [104.9–110.4% DW]. Anterior margin of disc with an extremely reduced and discrete concavity in its medial portion (Figs. 19, 20). Disc briefly longer than *P. orinocensis*, distance from anterior margin of disc to cloaca with mean in 90.3% DW [87.6–98.6% DW].

Head with greater interorbital distance than *P. orinocensis*, with mean in 11.6% DW [10.5–12.2% DW]; interspiracular distance short, with mean 15.5% DW and [15–16.2% DW] (Tab. 3). Eyes moderately large (mean 2.2% DW) and little pedunculated (Figs. 4D–F, 21). Spiracles quadrangular, small, being narrow and slightly larger than eyes, with mean of its length 5.2% DW [4.9–5.8% DW] (Fig. 21). Spiracular process extremely short, underdeveloped, with few dermal denticles, being in juvenile specimens practically

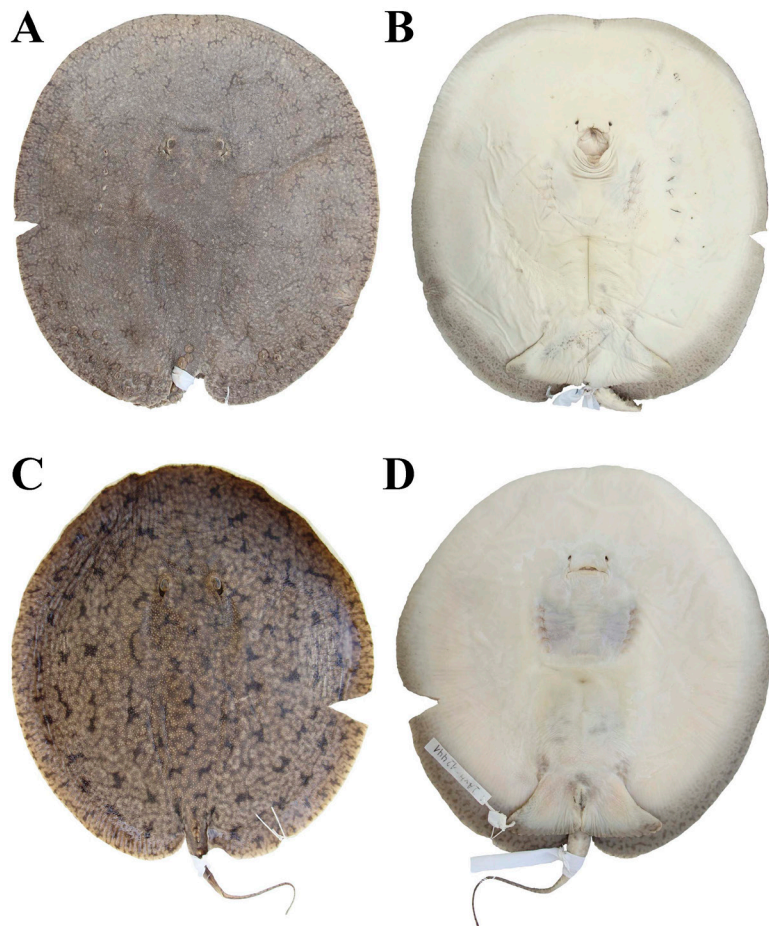


FIGURE 19 | Holotype and paratype of *Paratrygon parvaspina*. Holotype, IAvH-P 12447, adult female, 450 mm DW, from Bitá river. **A.** dorsal and **B.** ventral views. Paratype, IAvH-P 12441, juvenile female, 255 mm DW, from Tomo river. **C.** dorsal and **D.** ventral views.

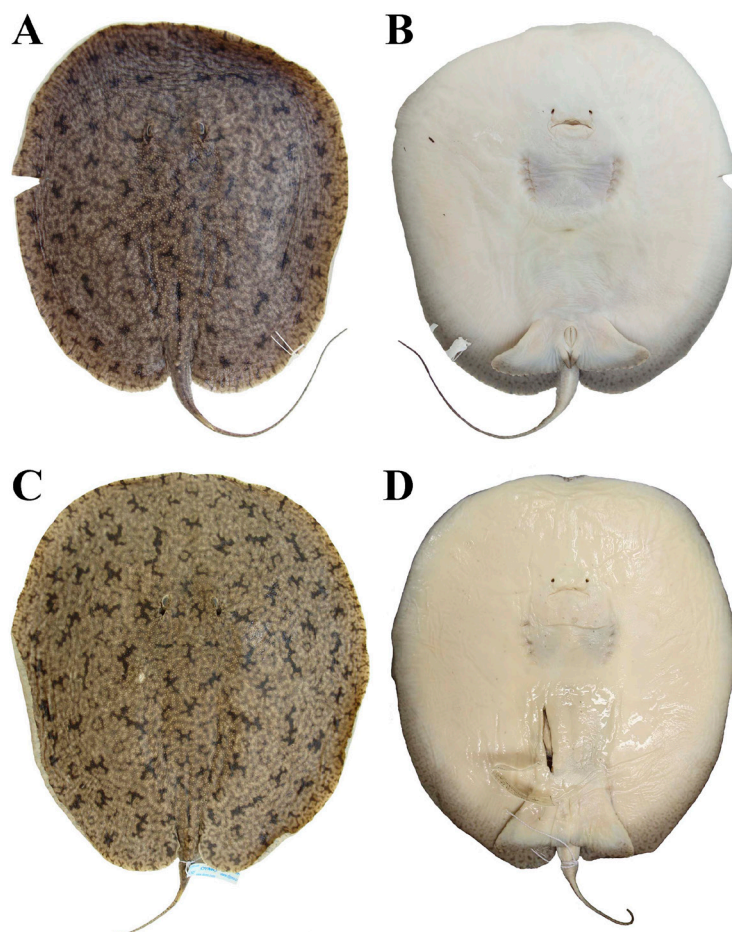


FIGURE 20 | Paratypes of *Paratrygon parvaspina*. IAvH-P 12446, juvenile male, 212 mm DW, from Tomo river. A. dorsal and B. ventral views. MZUSP 117836, juvenile female, 266 mm DW, from Orinoco river. C. dorsal and D. ventral views.

inconspicuous; however, some slight development occurs according to the maturity of specimens (Fig. 21). *Paratrygon parvaspina* with preorbital, prenasal and preoral distances greater than *P. orinocensis* (means respectively 32.2, 31.5 and 35% DW), being its head slightly farther from anterior margin of disc than that species. Mean internasal distance 8.1% DW, and mean mouth width 9.8% DW. Teeth triangular, cuspidate, arranged in quincunx in both jaws, and without size difference between teeth from lateral and central rows; teeth of central rows with more developed cusps than laterals, however cusps more similar in height with *P. aiereba*'s teeth and minor than *P. orinocensis* ones. Tooth rows of holotype (IAvH-P 12447, adult female) 31/22 (Tab. 4).

Branchial basket broad laterally, with mean of distance between first pair of gill slits (anterior part) 20.5% DW, and mean of distance between fifth pair of gill slits (posterior part) 17.6% DW; branchial basket also short, with mean of distance between first and fifth pair of gill slits 10.4% DW (Tab. 3). Pelvic fin triangular and dorsally covered by disc (Figs. 20B,D, 21B,D) its mean anterior margin length 16.6% DW; distances between distal portions of pelvic fins, and between axils of pectoral and pelvic

TABLE 3 | Measurements of specimens of *Paratrygon parvaspina*, including the holotype (IAvH-P 12447). Mean, Standard Deviation (SD) and ranges are expressed in millimeters (mm) and proportions of disc width (%DW); (N) corresponds to the number of specimens analyzed.

<i>Paratrygon parvaspina</i>	Holotype IAvH-P 12447		Mean		SD		Range				N
	mm	%DW	mm	%DW	mm	%DW	mm		%DW		
Total length	543	120.7	409.4	140.9	76.6	16.5	331	543	120.7	168.4	5
Disc length	497	110.4	320.6	106.5	100.8	2.1	223	497	104.9	110.4	5
Disc width	450	100.0	299.6	100.0	88.4	0.0	212	450	100.0	100.0	5
Interorbital distance	55	12.2	35.0	11.6	11.8	0.6	24	55	10.5	12.2	5
Interrespiracular distance	70	15.6	46.6	15.5	14.3	0.4	33	70	15.0	16.2	5
Eye length	9	2.0	6.4	2.2	1.4	0.4	5	9	1.7	2.8	5
Spiracle length	22	4.9	15.4	5.2	3.7	0.4	12	22	4.9	5.8	5
Preorbital length	163	36.2	98.6	32.2	36.7	2.6	61	163	28.8	36.2	5
Prenasal length	134	29.8	94.0	31.5	25.7	1.2	67	134	29.8	33.0	5
Preoral length	152	33.8	104.8	35.0	30.0	1.1	73	152	33.8	36.8	5
Internasal length	36	8.0	24.2	8.1	7.2	0.2	17	36	7.9	8.4	5
Mouth width	40	8.9	29.0	9.8	7.4	0.5	21	40	8.9	10.2	5
Distance between first gill slits	92	20.4	61.8	20.5	19.2	0.9	43	92	19.1	22.0	5
Distance between fifth gill slits	80	17.8	53.0	17.6	16.8	0.7	37	80	16.5	18.8	5
Branchial basket length	46	10.2	31.4	10.4	10.2	0.8	21	46	9.8	11.9	5
Length of anterior margin of pelvic fin	81	18.0	50.8	16.6	18.5	1.7	30	81	14.2	18.4	5
Pelvic fins width	209	46.4	129.4	42.5	47.1	3.5	90	209	37.2	46.4	5
External length of clasper	–	–	6.0	2.8	0.0	0.0	6	6	2.8	2.8	1
Internal length of clasper	–	–	14.0	6.6	0.0	0.0	14	14	6.6	6.6	1
Distance between cloaca and tail tip	113	25.1	136.0	50.4	21.4	19.3	113	175	25.1	82.5	5
Tail width	30	6.7	20.0	6.6	6.4	0.3	14	30	6.2	7.2	5
Distance between snout tip and cloaca	400	88.9	271.8	90.3	83.8	4.1	187	400	87.6	98.6	5
Distance between pectoral axil and posterior margin of pelvic fin	20	4.4	12.6	4.1	4.5	0.4	7	20	3.3	4.4	5
Distance between cloaca and caudal sting	–	–	55.3	21.1	13.2	2.3	46	78	17.3	23.1	4
Caudal sting length	–	–	16.3	6.2	2.9	0.5	13	21	5.6	7.1	4
Caudal sting width	–	–	2.3	0.9	0.4	0.1	2	3	0.8	0.9	4
Dorsal pseudosiphon length	–	–	–	–	–	–	–	–	–	–	0
Ventral pseudosiphon length	–	–	–	–	–	–	–	–	–	–	0

fins respectively 42.5 and 4.1% DW (Tab. 3). Single male specimen of *P. parvaspina* examined, IAvH-P 12446 (juvenile specimen) with external and internal clasper lengths respectively 2.8 and 6.6% DW (Tab. 3).

Tail reduced compared to *P. orinocensis* and *P. aiereba*, with narrow base, and short pre-caudal sting portion; post-caudal sting portion prolonged and filiform. Mean distance between cloaca and caudal sting insertion 21.1% DW; mean tail width 6.6% DW (Tab. 3). Distance from cloaca to tail's tip measured in all specimens, show a proportional decrease from juveniles to adult specimen (holotype IAvH-P 12447):

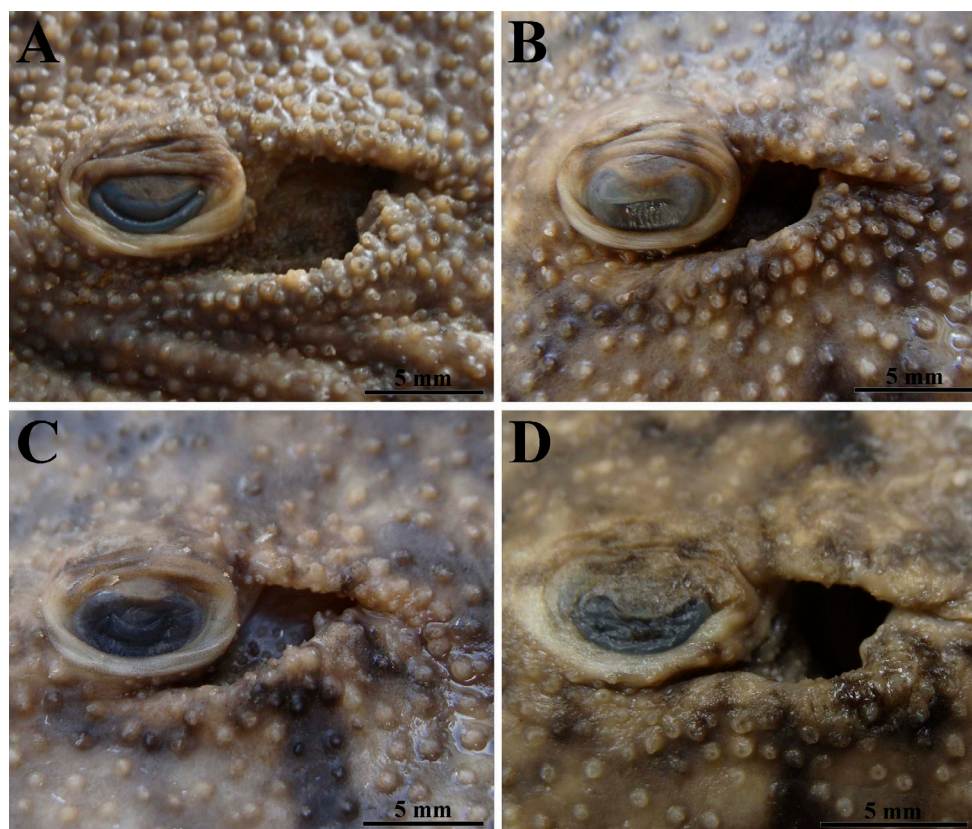


FIGURE 21 | Lateral view of spiracles and spiracles process of *Paratrygon parvaspina*. A. IAvH-P 4684, adult female, 345 mm DW, from Tomo river. B. IAvH-P 12441 (paratype). C. IAvH-P 12446 (paratype). D. MZUSP 117836 (paratype).

TABLE 4 | Meristic data taken from two specimens of *Paratrygon parvaspina* radiographed.

<i>Paratrygon parvaspina</i>	Holotype IAvH-P 12447	MZUSP 117836
Precaudal vertebrae	–	43
Caudal vertebrae	–	79
Total vertebrae	–	122
Diplospodylic vertebrae	–	77
Propterygial radials	–	45
Mesopterygial radials	–	24
Metapterygial radials	–	38
Total radials	–	107
Pelvic radials	–	24
Tooth rows of upper jaw	31	–
Tooth rows of lower jaw	22	19
Symphysis of upper jaw	–	–
Symphysis of lower jaw	5	–

with range in juveniles from 40.3 to 82.5% DW, whereas adult possess 25.1% DW (S3). Lateral tail folds slightly developed, from tail's base to caudal sting insertion; dorsal and ventral folds also present and poorly developed, more easily recognizable in region immediately after caudal sting, with dorsal fold more evident. Some specimens with medial ventral groove in tail more developed than others, occurring from tail base to origin of ventral fold.

Squamation. Dermal denticles scattered throughout the dorsal disc and tail (Fig. 22A). Dermal denticles in central region of disc bigger, more concentrated and visible than denticles on disc margins. Posterior margins of disc with notable concentration of developed thorns with large basal plate (*bp*) (Figs. 22B–C); some of these thorns may exceed 10 mm in diameter and five mm in height, and possess some minute dermal denticles in its *bp*. On the tail, dermal denticles occur only in pre-caudal sting portion. Dermal denticles in central disc generally with 0.5 mm in diameter, presenting a high and narrow crown

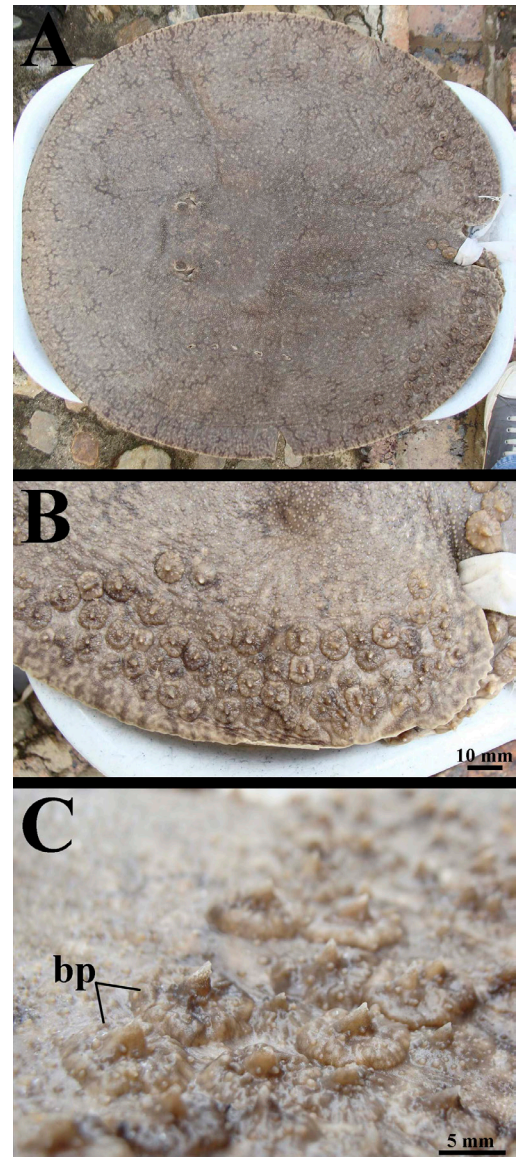


FIGURE 22 | Dermal denticles on the dorsal disc and tail of *Paratrygon parvaspina*, IAvH-P 12447 (holotype). **A.** distribution of dermal denticles. **B.** detail of some thorns with tubercular base on the posterior margin of the disc and tail's basis. **C.** detail of basal plates of these tubercular spines. bp = basal plate.

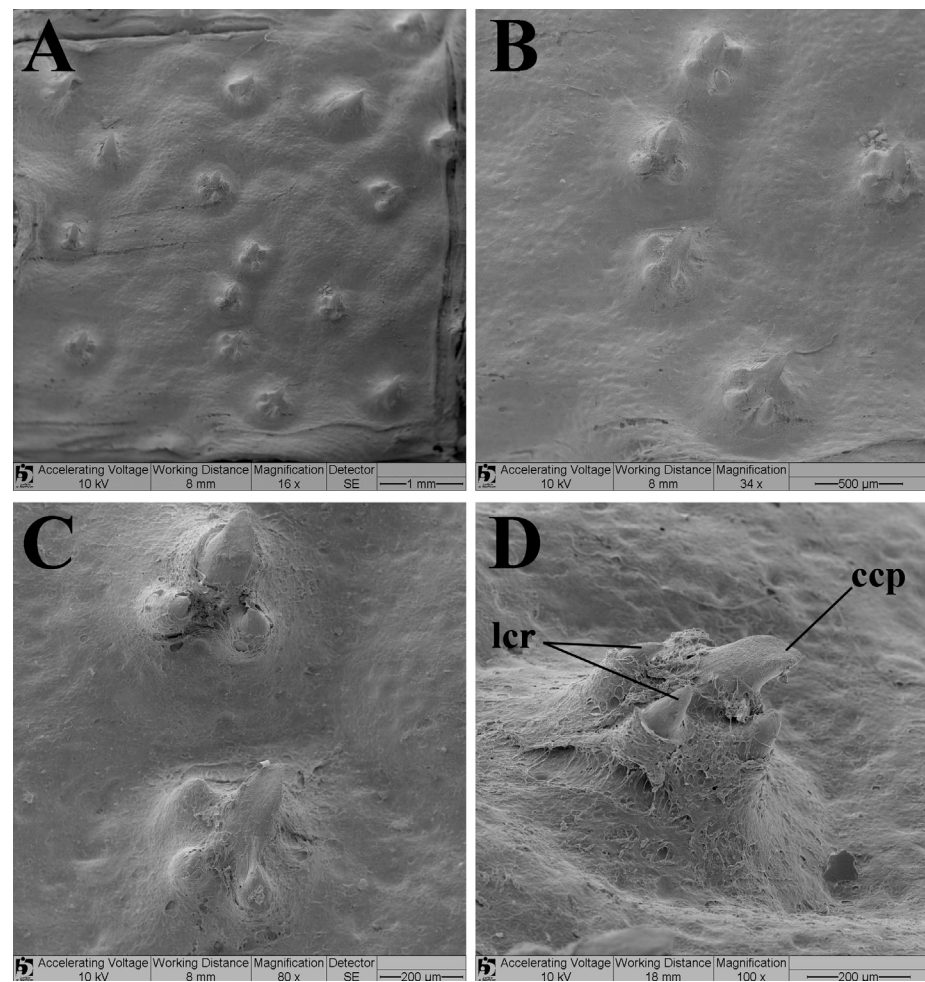


FIGURE 23 | Dorsal view and details of central disc dermal denticles of *Paratrygon parvaspina*, MZUSP 117836 (paratype) (SEM images). **A.** and **B.** dorsal view of some denticles. **C.** dorsal and **D.** lateral details of central dermal denticles. ccp = central coronal plate, lcr = lateral coronal ridge.

(Fig. 23). Central coronal plate (*ccp*) well developed, high and with pointed format; lateral coronal ridges (*lcr*) small, pointed and generally in number from two to five (Fig. 23D).

Female adult specimen (holotype IAvH-P 12447) with just one dorsal and one lateral rows of thorns on tail (Figs. 24A–B). Thorns developed, high and with a broad tubercular base throughout all extension of dorsal row, which originates at tail base and reaches caudal sting insertion. Lateral rows begin just before medial portion of tail and reach caudal sting insertion level; thorns of lateral rows very similar to dorsal ones, also well developed, high and with a broad tubercular base (Figs. 24A–C). Juveniles with just the dorsal row developed, only in pre-caudal sting portion; thorns developed but smaller than in adults, also with tubercular base (Figs. 24D–F).

Caudal sting very reduced, its mean length 6.2% DW [5.6–7.1% DW] (smallest caudal sting among the three species of *Paratrygon*); mean sting width 0.9% DW [0.8–0.9% DW] (Tab. 3). One female adult specimen (IAvH-P 4684) with lateral serrations of

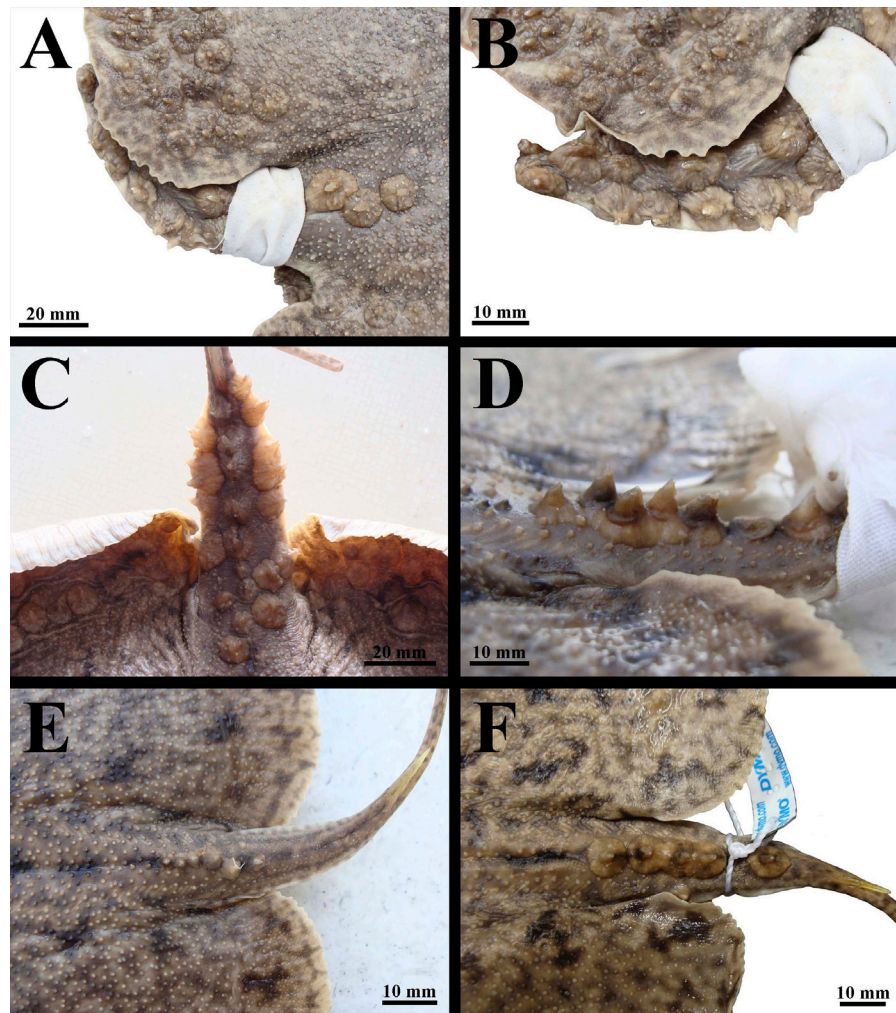


FIGURE 24 | Dorsal and lateral rows of thorns in *Paratrygon parvaspina*. **A.** and **B.** IAvH-P 12447 (holotype). **C.** IAvH-P 4684. **D.** detail of dorsal pointed spines on the tail of IAvH-P 12441 (paratype). **E.** IAvH-P 12446 (paratype). **F.** MZUSP 117836 (paratype).

caudal sting poorly developed and present only on medial and distal portions (Fig. 25A). Juveniles with very few and poor developed lateral serrations, present only on third final portion of spine (Figs. 25B–D).

Lateral line. Junction of four canals (*JFC*) of ventral lateral line in *Paratrygon parvaspina* longer than in *P. orinocensis*, with its posterior part formed by connection of hyomandibular (*HMD*) and infraorbital (*IOC*) canals, and its anterior extremity by the supraorbital (*SPO*) and nasal (*NAS*) canals connection (Fig. 26). Angular (*ang*) and jugular (*jug*) components of *HMD* descend straight to posterior portion of disc, while in *P. orinocensis* these components show a conspicuous curve. Subpleural loop (*spl*) not so wide as in *P. orinocensis*, and with three short posterior subpleural tubules (*pst*), with most central one subdivided. Subpleural component (*spe*) ascends in straight line and begins an external curvature just before scapular girdle level. Subpleural tubules (*spt*) begin detaching from *HMD* at level of third pair of gill slits (Fig. 26).

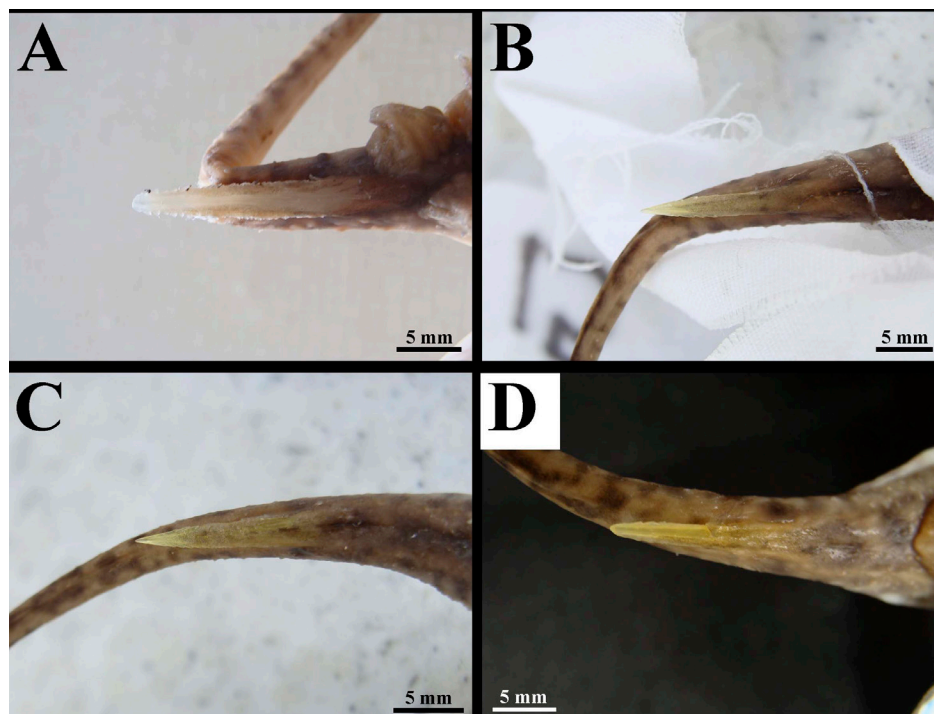


FIGURE 25 | Dorsal view of caudal stings of *Paratrygon parvaspina*. **A.** IAvH-P 4684. **B.** IAvH-P 12441 (paratype). **C.** IAvH-P 12446 (paratype). **D.** MZUSP 117836 (paratype).

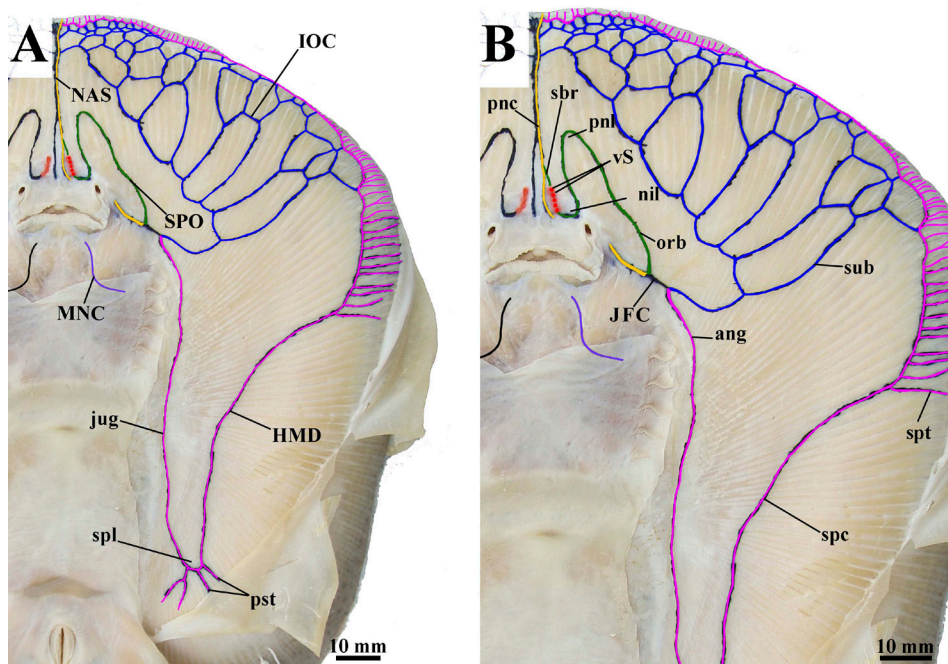


FIGURE 26 | Ventral canals of lateral line system in *Paratrygon parvaspina*, IAvH-P 12446 (paratype). **A.** distribution of all ventral canals. **B.** detail of the anterior central disc ventral canals. Abbreviations see Fig. 12.

Infraorbital canal (*IOC*) descends from *JFC* as in *P. orinocensis*; suborbital component (*sub*) with less honeycomb ramifications (mainly the small and anterior ones) than *P. orinocensis*; *sub* presents two connection points with prenasal component (*pnc*) of nasal canal (Fig. 26). Supraorbital canal (*SPO*) with orbitonasal component (*orb*) slightly curved, a broad prenasal loop (*pnl*), and with a nasointernal loop (*nil*) similar to *P. orinocensis*; subrostral component (*sbr*) shorter than *P. orinocensis*, and with just five vesicles of Savi (*vS*) occurring next to *nil* (Fig. 26).

Nasal canal (*NAS*) ascends from *JFC* similar as in *P. orinocensis*; prenasal component (*pnc*) with a slightly internal curvature next to vesicles of Savi level. Mandibular canal (*MNC*) descends posteriorly from Meckel's cartilage in straight line and externally curved next to *adductor mandibulae* muscle (Fig. 26).

Skeleton. Meristic counts of vertebrae and radials of pectoral and pelvic fins just from MZUSP 117836 specimen (Tab. 4). Differently from *P. orinocensis*, neurocranium of *P. parvaspina* not with an evident letter "T" format in dorsal view, with its preorbital process (*PRP*) extending laterally beyond nasal capsules (*NC*) level, being the widest portion of anterior part of neurocranium; orbit and otic capsules regions slightly more robust in this species than in *P. orinocensis*, these regions not showing a clear difference in width with *NC*. Rostral projection (*RPJ*) also broad and with half circle format, with its tip reaching anterior level of *NCs*. Nasal capsules oval and separated by a large internasal septum (*IS*), not so encircled by first segment of propterygium (*FSP*) as in *P. orinocensis* (Fig. 27). Supraorbital crest (*SOC*) with very evident small and triangular supraorbital process (*SP*). Frontoparietal component of fontanelle (*FPF*) in spoon format (posteriorly oriented), with its posterior portion wider than anterior and, broader and more developed than *FPF* of *P. orinocensis* (Fig. 27). Mandibular arch very similar to *P. orinocensis*, with palatoquadrate (*PQ*) and Meckel's cartilage (*MC*) slightly straighter in *P. parvaspina*, and *MC* slightly robust, with its proximal portion (extremity which articulates with *PQ* and hyomandibula) wider than in that species. Hyomandibula (*HYO*) slightly curved in its medial part, and more robust than *P. orinocensis* (Fig. 27).

Synarcual cartilage shorter and wider than *P. orinocensis*, with wider spinal nerve canal (*SNC*) than in that species. Dorsomedial crest (*DMC*) does not reach synarcual tip as in *P. orinocensis*; dorsal socket (*DS*) in posterior region of synarcual cartilage deeper and tapered, anterior ventral condyle (*AVC*) with a convex surface (whereas *AVC* in *P. orinocensis* with straight surface), and posterior ventral condyle (*PVC*) also smaller than *AVC*. Lateral stay (*LS*) more expanded anterolaterally than in *P. orinocensis* (Fig. 28). Scapulocoracoid with more robust and thicker coracoid bar (*CB*) than *P. orinocensis*; anterior and posterior faces of *CB* respectively straight and curved in its central portions. Dorsolateral crest (*DLC*) of scapular process (*SCP*) not so pronounced as in *P. orinocensis*, and not passing laterally mesocondyle (*MSC*) level. Mesocondyle and metacondyle (*MTC*) slightly smaller and less projected than in *P. orinocensis* (Fig. 29).

Propterygium (*PPT*) slightly more robust than in *P. orinocensis*, and slightly more arched in its distal portion. First segment of propterygium (*FSP*) one-fourth of *PPT* length, with just one pectoral radial directly connected (*P. orinocensis* with two radials), and not encircling anteriorly the nasal capsules (*NC*) so closely as in *P. orinocensis* (Fig. 30A). Contact between small articulation surface (*SAS*) of *PPT* with mesopterygium (*MSP*) not so evident as in *P. orinocensis* (Figs. 30A–B). Concavity of proximal face of

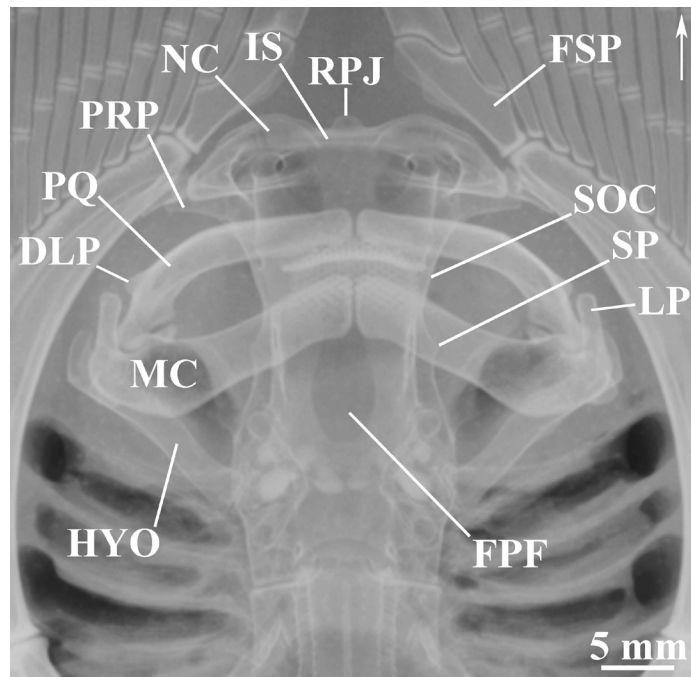


FIGURE 27 | Radiograph of neurocranium and mandibular arch of *Paratrygon parvaspina*, MZUSP 117836 (paratype), upper view. Abbreviations see Fig. 13. Arrow indicates to the anterior portion of specimen.

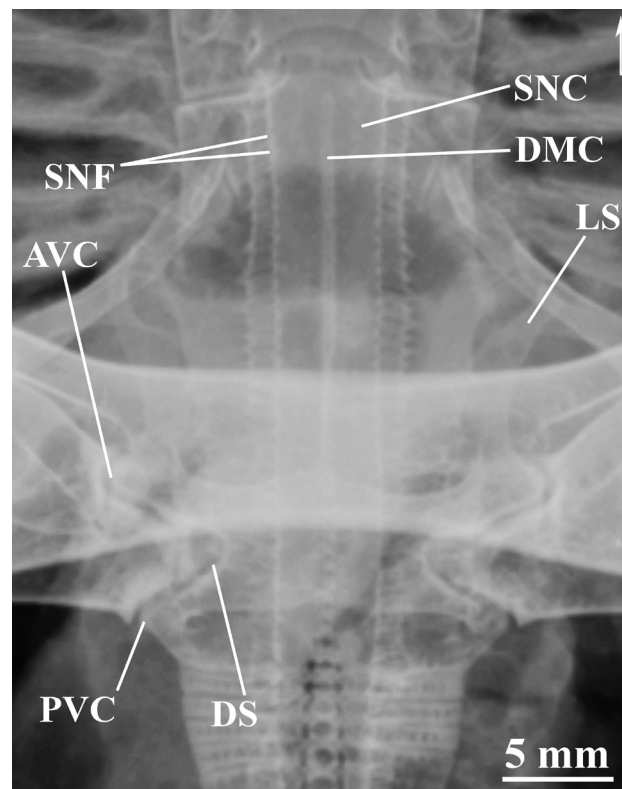


FIGURE 28 | Radiograph of synarcual cartilage of *Paratrygon parvaspina*, MZUSP 117836 (paratype), upper view. Abbreviations see Fig. 14. Arrow indicates to the anterior portion of specimen.

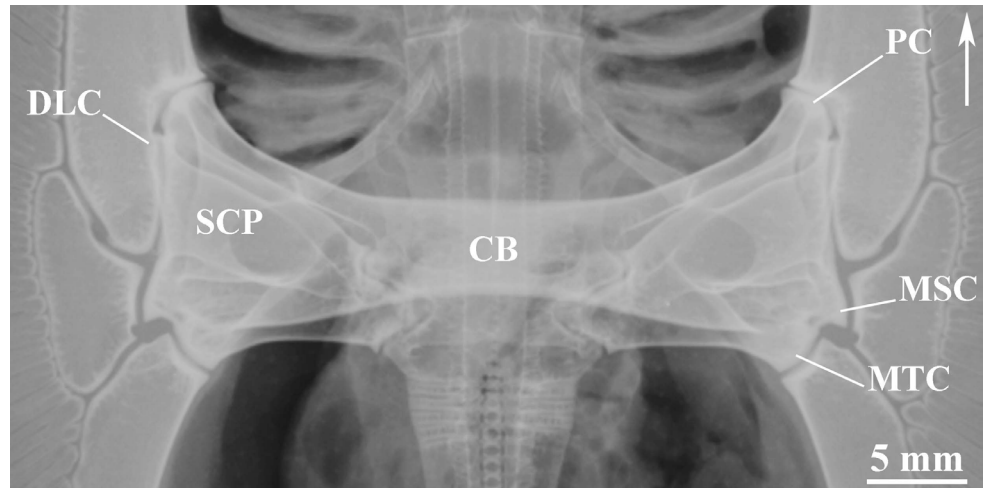


FIGURE 29 | Radiograph of scapulocoracoid of *Paratrygon parvaspina*, MZUSP 117836 (paratype), upper view. Abbreviations see Fig. 15. Arrow indicates to the anterior portion of specimen.

MSP not so curved and pronounced as in *P. orinocensis*; both extremities, anterior and posterior, contact respectively propterygium and metapterygium, however, junctions of medial radials (*JMR*) of pectoral fin appear only in anterior extremity of *MSP* (Fig. 30B). Metapterygium (*MTP*) more robust (mainly in its proximal portion), arched and slightly shorter than in *P. orinocensis*; posterior segments (*PSM*) also in pelvic girdle level (Fig. 30C).

Puboischiadic bar (*PB*), as in *P. orinocensis*, with arched shape, inclined and rectilinear in its anterior portion, and, its posterior portion presenting a curvature as a half circle (however slightly more closed than in that species). Iliac process (*IP*), ischial process (*ISP*) and lateral prepelvic process (*LPP*) slightly less developed than *P. orinocensis*, and with more rounded tips. Three pairs of obturator foramina (*OF*) on lateral extremities of its *PB* (Fig. 31).

Color in alcohol. Dorsal disc coloration gray or beige, with big dark and small light spots scattered all over dorsal disc (Figs. 19A, C, 20A, C). Dark spots in dark gray, dark brown or even black, with vermicular or dendritic format, slender or slightly thick in its central portions; spots more concentrated and smaller on disc margins. Light spots in light gray or light beige with rounded, oval or polygonal formats. Dorsal coloration of tail similar to disc, gray or beige with dark spots occurring from tail's base to caudal sting insertion; posterior to caudal sting, tail in light beige or light gray with many small and dark gray, dark brown or even black specks. Ventral disc coloration in two tones: one light and predominant, white color, occurring on all central region, anterior margin and anterior portion of lateral margins of disc; and another one, slightly darker, beige or gray, occurring on posterior margins and posterior portion of lateral margins of disc; in this darker pattern occur numerous small and dark gray spots, with various formats, rounded, oval or vermicutale (Figs. 19B, D, 20B, D). Pelvic fins also with both tones present on disc, with light tone on anterior margin and on all central portion of pelvic fin, and darker one as a thin

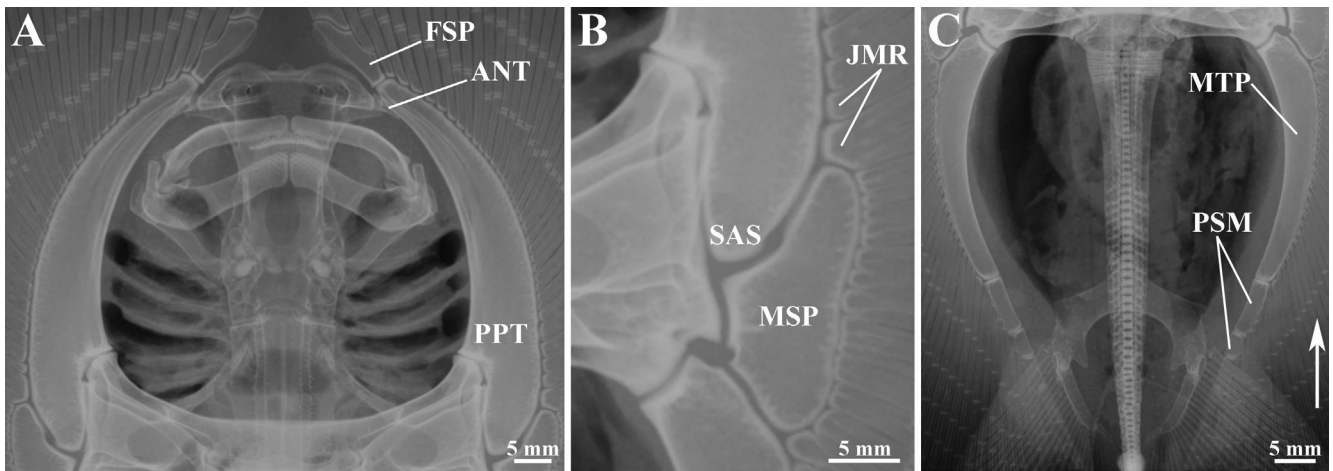


FIGURE 30 | Radiographs of basal elements of pectoral fin of *Paratrygon parvaspina*, MZUSP 117836 (paratype), upper view. Abbreviations see Fig. 16. Arrow indicates to the anterior portion of specimen. **A.** Propterygium region. **B.** Mesopterygium region. **C.** Metapterygium region.

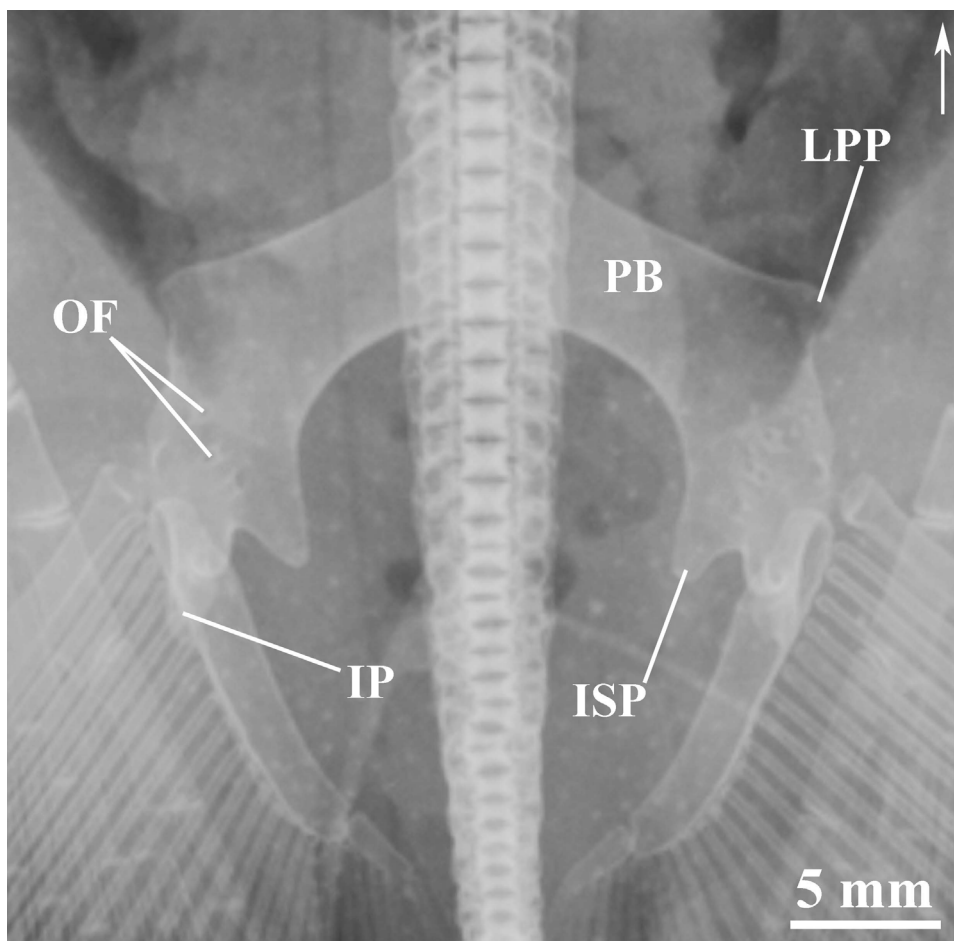


FIGURE 31 | Radiograph of pelvic girdle of *Paratrygon parvaspina*, MZUSP 117836 (paratype), upper view. Abbreviations see Fig. 17. Arrow indicates to the anterior portion of specimen.

strip on posterior margin, slightly wider on posterior corner; darker areas also show small dark spots on pelvic fins as well as on disc. Clasper also with these two tones, with light one occurring just on base, and darker occurring on medial and terminal portions; darker tone on clasper without small dark spots. Ventral coloration on pre-caudal sting portion of tail with same light tone of disc; some specimens with gray spots. Posterior to caudal sting, ventral coloration of tail beige or gray, darker close to tail tip; tail tip with numerous small dark gray specks. As in *P. orinocensis*, the dorsal and ventral coloration of *P. parvaspina* is more intense and evident than in preserved specimens, especially concerning dorsal marks and spots.

Geographic distribution. *Paratrygon parvaspina* is also endemic to the Orinoco basin, however with a more restricted distribution than *P. orinocensis*. Specimens analyzed in this study were collected in middle portion of the Orinoco River and its main affluents, the Bitá and Tomo rivers (Fig. 32).

Etymology. From the Latin *parvus*, meaning small, and *spina* for spine; the epithet *parvaspina* refers to the diagnostic reduced caudal sting of this new species. Gender feminine. An adjective.

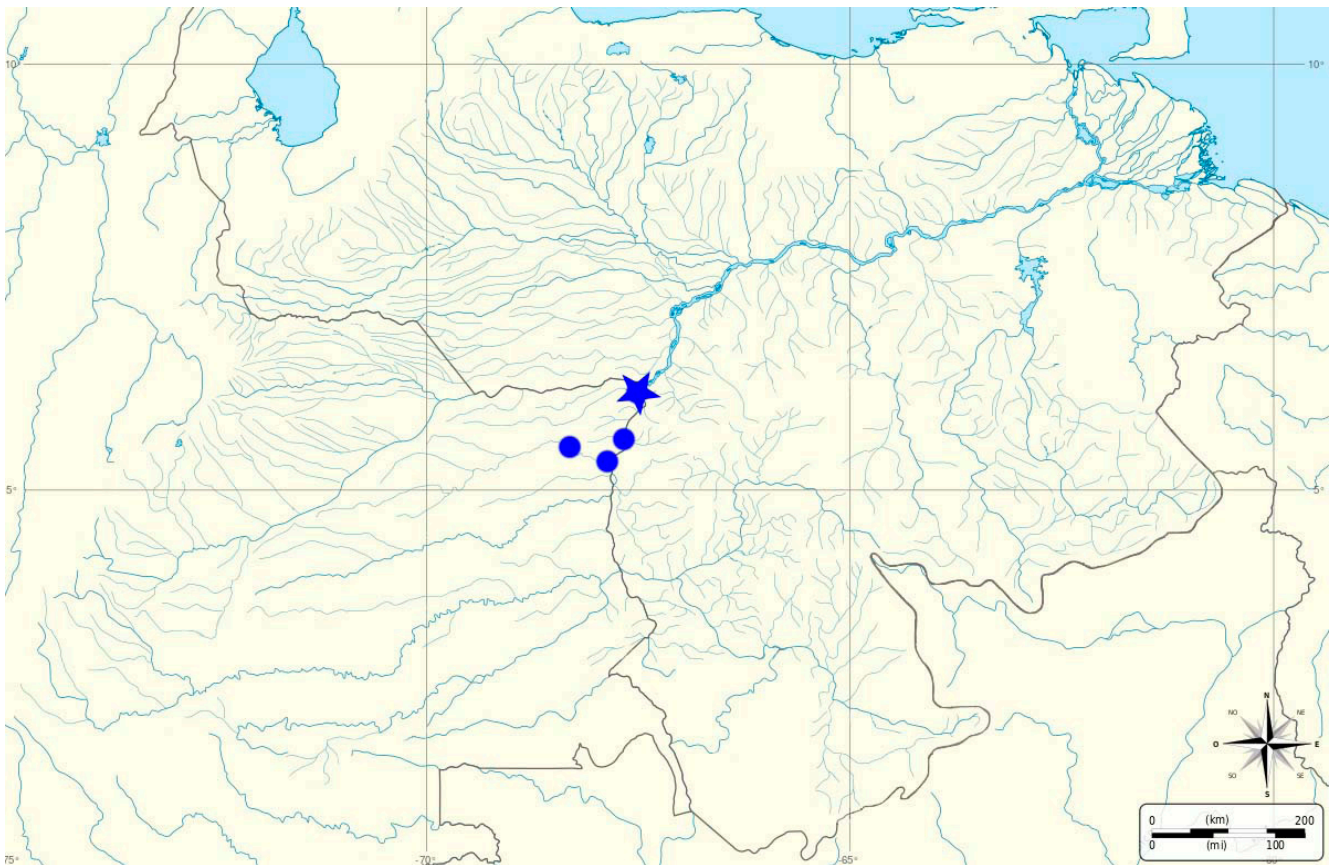


FIGURE 32 | Distribution of *Paratrygon parvaspina* throughout Orinoco basin. This species occurs in the mid portion of Orinoco river, and in some tributaries of this portion. Star = holotype specimen (IAvH-P 12447) locality.

Paratrygon aiereba (Müller & Henle, 1841)

(Figs. 33–58; Tabs. 5–6)

- Trygon aiereba* Müller & Henle, 1841:160, 196 [original description, not figured, type locality: ‘Brasilien’ [=Brazil]; one type specimen originally deposited in the Zoologische Staatssammlung München (“*Ein Exemplar im zoologischen Museum zu München*”, p. 196), presently considered lost].
- Trygon (Paratrygon) aiereba*. —Duméril, 1865:594–595 [synonymy, description, distribution].
- Disceus strongylopterus* [sic]. —Garman, 1877:208–209 [synonymy, description, distribution in Belém, Manaus and Óbidos (Brazilian locations)].
- Paratrygon strongylopterus* [sic]. —Jordan, 1887:557 [citation]. —Eigenmann, Eigenmann, 1891:24 [citation, distribution]. —Eigenmann, 1910:378 [synonymy, distribution].
- Paratrygon orbicularis*. —Eigenmann, 1912:118 [synonymy, brief description; note that *Raja orbicularis* Bloch, Schneider, 1801 is based on the “*Aiereba*” of Marcgrav, 1648, intended for a marine stingray and considered a *nomen dubium* by Rosa, 1991].
- Elipesurus stroglylopterus*. —Garman, 1913:425–426 [synonymy, description]. —Fowler, 1951:4–5 [synonymy, distribution].
- Disceus thayeri* Garman, 1913:426–427, plates 34, 54 (fig. 2), 57 (fig. 2), 70 (fig. 3) [synonymy, original description, distribution in Belém, Manaus, Óbidos and rio Juruá; type locality: Amazon (in the following localions: Manaus, Óbidos and Belém [“*Para*”]) and Juruá rivers; type specimens (syntypes): MCZ 563-S (female, from Belém), MCZ 297-S (female, from Manaus) and MCZ 606-S (male, from Óbidos)]. —Fowler, 1951:10, fig. 4 [synonymy, distribution]. —Castex, 1964:33–34 [brief description, distribution].
- Potamotrygon strongylopterus*. —Castex, 1964:22 [synonymy, brief description, distribution].
- Disceus stroglylopterus*. —Castex & Castello, 1969:21, 22, 24, 26–29 [taxonomic discussion, description, distribution].
- Paratrygon aiereba*. —Rosa, 1985a:363–372, 365–394, 405–407, 413–431, 433–434, 437–438, 454, 460–462, figs. 87–96, fig. 97b, fig. 99, [synonymy, diagnosis, taxonomic discussion, description, distribution, phylogenetic analysis]. —Taniuchi, Ishihara, 1990:10–12, 14–15, fig. 1 [morphological description of clasper]. —Rosa, 1991:425–430, 433–435, figs. 1–2, fig. 5 [synonymy, description, taxonomic discussion, distribution]. —Compagno, Cook, 1995:72–73, 80–81 [distribution]. —Lovejoy, 1996:214–217, 219–221, 224–225, 227–230, 234, 236–237, 240–246, 249, fig. 4c, figs. 6e, 6f, fig. 8d, fig. 9d, fig. 10c, fig. 11f, figs. 15–16 [morphological description, analysis, phylogenetic discussion]. —Carvalho *et al.*, 2003:22–23 [synonymy, taxonomic discussion, brief biological aspects, distribution]. —Carvalho *et al.*, 2004:10, 17, 49, 76, 78, 81, 84–86, 90, 93–99, 101, 103, 105, 107–109, 118, 134–135 figs. 43–47, fig. 51 [morphological description, analysis, phylogenetic discussion]. —Santos *et al.*, 2004:138, 184, 188, 214 [list of species of the Tocantins River, Tucuruí region, brief description of external morphology]. —Rosa *et al.*, 2010:246–247, 253–256, 259–260, 262, 276–277, fig. 5.2, fig. 5.A.1 [identification key, taxonomy, phylogenetic discussion, feeding habits]. —Carvalho, Lovejoy,

2011:16–17 [list of analyzed specimens; characters discussed in relation to *Heliotrygon*; phylogenetic discussion]. —Frederico *et al.*, 2012:73–79, figs. 1–3 [phylogeography, molecular analysis, conservation]. —Mojica *et al.*, 2012:42 [list of endangered species of fishes of Colombia]. —García-Villamil *et al.*, 2013:288–294, figs. 4–6 [molecular systematics, phylogenetic discussion]. —Sánchez-Duarte *et al.*, 2013:319, 322, 330, 332 [comercialization]. —Silva, 2014: vol 1., 24, 277–280, 370, 383, 412, 418, 483, vol2., ix, 148, 188, fig. 148, fig. 188 [morphological description of scapulocoracoid, pelvic girdle, skeletal elements of paired fins, phylogenetic discussion]. —Fontenelle, Carvalho, 2016:1–3, 8–11, figs. 1–2, fig. 9b, fig. 10b, fig. 11 [brain morphology, phylogenetic discussion]. —Garcia *et al.*, 2016:4483–4489, figs. 2–5 [molecular systematics, phylogenetic discussion]. —Loboda, 2016: vol.1., vi, viii, 2–5, 7, 14–18, 21–58, 60–61, 65–66, 68–71, 73, 75, 79–87, 91, 94–96, 100, 105, 108–113, 117, 119–123, 126–127, 130–131, 133–136, 142, 147–148, 151–154, 156, 164–168, 189–192, 195, 198, 204–211, vol.2., viii–x, 2–31, 75, figs. 2–38 [morphometry, morphological description, taxonomic revision, diagnosis, synonymy, distribution, morphological characters discussion]. —Carvalho, 2016b:3, 55, 57–59 fig. 49c, p. 57 [occurrence in lower portion of the Tapajós River, identification key]. —Carvalho, 2016c:624 [species account, identification, illustration, distribution]. —Sánchez-Duarte *et al.*, 2016:151–156, figs. 15–17 [biological data, habitat].

Holotype. Formerly in the ZSM, considered lost (Rosa, 1985a; Loboda, 2016), probably during a bombing raid in April 1944 (Rosa, 1991) (see Discussion below).

Neotype. MZUSP 117155, male, 603 mm DW, Brazil, State of Pará, municipality of Colares, Marajó Bay, 00°55'34"S 48°17'25"W, 16 Aug 2007, F. P. L. Marques, M. Cardoso & V. M. Bueno. **Neotype herein designated** (see Discussion below).

Diagnosis. *Paratrygon aiereba* is distinguished from congeners by a combination of characters. An evident pair of big and dark spots on the preorbital region of the disc that resembles the shape of “eyebrows” or a “mustache” (*vs. P. orinocensis* and *P. parvaspina* lacking this pair of preorbital spots). Spiracular process great and knob-shaped in neonates, juveniles, subadults and adults, being more developed (almost covering the entire spiracle aperture) and with some small dermal denticles in adults (*vs. P. orinocensis* has short and straight spiracular process with developed dermal denticles, *P. parvaspina* has an extremely short and reduced spiracular process, being just more visible in adult specimens, which possesses few dermal denticles). Spiracles large and quadrangular, mean spiracle length 6% DW [4.4 to 11.6% DW] (*vs. P. orinocensis* has triangular and slightly smaller spiracles, mean spiracle length in 5.6% DW [4.5–7.9% DW], and *P. parvaspina* has very small and quadrangular spiracles, with mean spiracle length 5.2% DW [4.9 to 5.8% DW]). Few tooth rows in the upper and lower jaws 16–26/14–20 (*vs. P. orinocensis* with 22–35/20–29, and *P. parvaspina* with 31/19–22). Frontoparietal component of fontanelle very large, with its posterior extremity very broad and rounded (*vs. P. orinocensis* with a very narrow frontoparietal component with a number eight shape, and *P. parvaspina* that has a broad frontoparietal component but narrower than in *P. aiereba*). Propterygium not very curved, straighter at its posterior portion (*vs. P. orinocensis* and *P. parvaspina* with a more curved propterygium, including at their posterior portions).

Description. For general appearance of *P. aiereba*, see Figs. 33–34, 38–40, for morphological characters examined see Figs. 4G–I, 35–37, 41–58. Measurements and counts presented in Tabs. 5–6, respectively, and S4–S5. In the description below, *P. aiereba* is directly compared to the Orinoco *Paratrygon* species.

Among the three species of *Paratrygon*, *P. aiereba* is the species that reaches the largest dimensions (Tabs. 1, 3 and 5), with means of total length, disc length, and disc width, respectively, 594.7, 398.2, and 362.2 mm, and the maximum size of these measurements reaching, respectively, 1270, 867 and 786 mm. *Paratrygon orinocensis* is the largest species of the genus in the Orinoco basin reaching a total length of 866 mm, and disc dimensions of 634 DL and 573 mm DW (Tab. 1). *Paratrygon parvaspina* is the smallest species of the genus, with means of 409.4 TL, 320.6 DL, and 299.6 mm DW (Tab. 3), with its disc width not exceeding 500 mm in the greatest specimen measured (holotype, IAvH-P 12447).

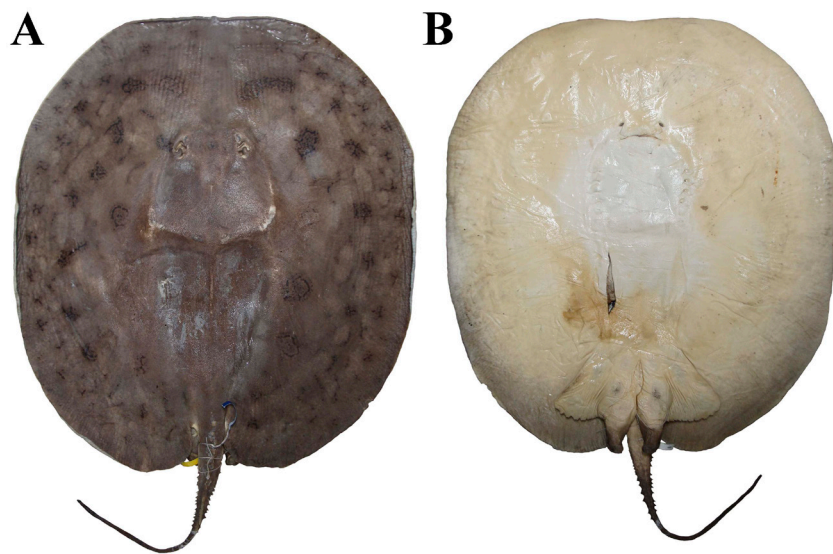


FIGURE 33 | Neotype of *Paratrygon aiereba*, MZUSP 117155, adult male, 603 mm DW, from Marajó bay. **A.** dorsal and **B.** ventral views.



FIGURE 34 | *Paratrygon aiereba*, dorsal view of the specimen MZUSP 104896, adult female, 560 mm DW, from Javari river. Note the concavity in the anterior margin of the disc.

As in the other two new species of the genus, *P. aiereba* also has a subcircular to oval disc, with mean of disc length in 110.3% DW [103.7 to 117.7% DW]. However, both new species from the Orinoco basin present a more rounded disc, with *P. parvaspina* presenting the roundest disc among all three species, with mean of its disc length 106.5% DW (Tabs. 1, 3, 5). The median concavity of the anterior disc margin of *P. aiereba* is more pronounced and visible in adult and subadult specimens (Figs. 33–34, 38–40; **S4**); all specimens of *P. orinocensis* (from juveniles to adults) possess this concavity very pronounced (Figs. 1–3; **S1**); on the other hand, in *P. parvaspina* this concavity is extremely reduced (Figs. 19–20). *Paratrygon orinocensis* possesses a shorter disc than *P. aiereba* and *P. parvaspina*, with the mean distance between anterior margin of disc and cloaca 85.6% DW (*P. aiereba* 89.5% DW and *P. parvaspina* 90.3%; Tabs. 1, 3, 5).

TABLE 5 | Measurements of specimens of *Paratrygon aiereba* examined, including the neotype (MZUSP 117155). Mean, Standard Deviation (SD) and ranges are expressed in millimeters (mm) and proportions of disc width (%DW); (N) corresponds to the number of specimens analyzed.

<i>Paratrygon aiereba</i>	Neotype MZUSP 117155		Mean		SD		Range				N
	mm	%DW	mm	%DW	mm	%DW	mm		%DW		
Total length	937	155.4	594.7	178.8	207.6	44.4	271	1270	111.0	283.7	43
Disc length	645	107.0	398.2	110.3	181.3	3.1	171	857	103.7	117.7	45
Disc width	603	100.0	362.2	100.0	166.7	0.0	147	786	100.0	100.0	45
Interorbital distance	62	10.3	38.6	10.8	17.4	0.7	19	84	9.3	12.9	45
Interrespiracular distance	88	14.6	56.5	16.0	23.7	1.6	31	114	13.6	22.4	45
Eye length	7	1.2	5.7	1.7	1.7	0.5	3	11	0.9	2.7	45
Spiracle length	29	4.8	20.9	6.0	8.8	1.4	10	47	4.4	11.6	45
Preorbital length	179	29.7	113.0	31.2	51.7	1.9	47	243	25.3	35.0	45
Prenasal length	167	27.7	105.8	29.5	46.1	1.3	43	212	27.0	32.4	45
Preoral length	185	30.7	118.5	33.0	51.9	1.4	49	237	30.2	36.3	45
Internasal length	50	8.3	29.5	8.3	13.8	0.5	11	63	7.3	9.5	44
Mouth width	59	9.8	37.0	10.2	17.7	0.7	14	80	8.7	12.3	43
Distance between first gill slits	113	18.7	77.8	21.4	38.1	1.2	31	180	18.7	24.3	43
Distance between fifth gill slits	–	–	66.9	18.6	34.0	1.0	25	167	16.8	21.2	42
Branchial basket length	64	10.6	40.6	11.3	18.5	0.7	17	87	10.0	13.6	45
Length of anterior margin of pelvic fin	99	16.4	64.0	17.6	30.5	2.1	22	130	14.1	22.9	45
Pelvic fins width	238	39.5	143.5	40.2	67.4	4.5	49	327	30.8	48.9	44
External length of clasper	49	8.1	21.7	4.7	19.9	2.8	4	60	2.3	10.4	25
Internal length of clasper	97	16.1	46.6	10.9	36.4	4.5	11	113	6.7	21.5	24
Distance between cloaca and tail tip	402	66.7	265.2	87.8	97.2	43.0	82	545	19.5	183.0	42
Tail width	36	6.0	23.7	6.6	11.6	0.8	11	55	5.0	8.8	45
Distance between snout tip and cloaca	504	83.6	318.4	89.5	146.6	3.2	139	720	83.6	97.1	44
Distance between pectoral axil and posterior margin of pelvic fin	30	5.0	17.0	4.6	9.7	1.1	5	40	2.3	7.5	45
Distance between cloaca and caudal sting	127	21.1	79.8	23.5	35.9	3.0	42	191	17.5	31.3	41
Caudal sting length	45	7.5	36.8	11.3	15.0	2.8	17	80	3.0	17.9	38
Caudal sting width	4	0.7	3.3	1.0	1.5	0.3	1	7	0.4	1.5	40
Dorsal pseudosiphon length	12	2.0	8.4	1.5	3.7	0.5	1	12	0.4	2.0	11
Ventral pseudosiphon length	37	6.1	30.4	5.4	12.8	1.7	7	52	2.1	7.6	9

In relation to head proportions, *P. parvaspina* possesses the largest mean interorbital distance of 11.6% DW, *P. aiereba* has 10.8% DW, and *P. orinocensis* has the smallest mean at 9.9% DW. In relation to interspiracular distance, *P. aiereba* possess the largest mean with 16% DW, whereas *P. orinocensis* has 15.8% DW and *P. parvaspina* has 15.5% DW. All three species possess pedunculate, small eyes (Figs. 4, 5, 21, 35), however, *P. parvaspina* has the greatest mean eye length at 2.2% DW, whereas *P. orinocensis* has 1.9% DW and *P. aiereba* has 1.7% DW (Tabs. 1, 3, 5). Spiracles possess different shapes among the three species: *P. aiereba* possesses large, quadrangular spiracles (Figs. 4G–I, 35) with mean length 6% DW [4.4 – 11.6% DW]; *P. orinocensis* has triangular and slightly smaller spiracles (Figs. 4A–C, 5) with mean length 5.6% DW [4.5–7.9% DW]; and *P. parvaspina* possesses very small and quadrangular spiracles (Figs. 4D–F, 21), with mean length 5.2% DW [4.9–5.8% DW]. Spiracular process in *P. aiereba* great, knob-shaped in neonates, juveniles and adult specimens, being more developed and almost covering the entire spiracle aperture in adults; dermal denticles on this process very small in *P. aiereba*, even in adults (Fig. 35). *Paratrygon orinocensis* has short and straight spiracular processes with developed dermal denticles (Fig. 5). *Paratrygon parvaspina* has extremely short and reduced spiracular processes, being just more visible in adult specimens, and with few dermal denticles present (Fig. 21).

Paratrygon aiereba has intermediate values of preorbital, prenasal and preoral distances proportions compared with the new species, with its preorbital, prenasal and preoral means, respectively, 31.2%, 29.5% and 33% DW (Tab. 5). Head closer to the anterior margin of the disc in *P. orinocensis*, with means of preorbital, prenasal and preoral distances respectively 29.9%, 27.5% and 30.9% DW. *Paratrygon parvaspina* has the greatest preorbital, prenasal and preoral distances among the three species with means, respectively, 32.2%, 31.5% and 35% DW; even the ranges of these measurements between the two sympatric species of the Orinoco basin are very contrasting, mainly in prenasal and preoral distances (Tabs. 1, 3). Mouth and nostrils proportionally similar in all three species: *P. aiereba* has means of internasal distance and mouth width, respectively, 8.3% and 10.2% DW, *P. orinocensis* 8.3% and 10% DW, and *P. parvaspina* 8.1% and 9.8% DW (Tabs. 1, 3, 5).

Teeth triangular, large, cuspidate, and arranged in quincunx in both jaws in all three species (Figs. 6, 36, 37), with teeth in central rows presenting more developed cusps. Adult specimens of *P. orinocensis* possesses more developed and higher cusps than *P. aiereba* and *P. parvaspina* (Fig. 6). *Paratrygon aiereba* has fewer tooth rows in upper and lower jaws than both new species with 16–26/14–20, whereas *P. orinocensis* has 22–35/20–29 and *P. parvaspina* has 31/19–22; however, *P. aiereba* has more exposed teeth at symphysis, 3–6/3–5, vs. 2–4/3–4 in *P. orinocensis* (Tabs. 2, 4, 6).

Paratrygon aiereba has a large and laterally expanded branchial basket with means of distance between first pair of gill slits, distance between fifth pair, and branchial basket length, respectively, 21.4%, 18.6%, and 11.3% DW. Both new species of the Orinoco basin have proportionally smaller branchial baskets than *P. aiereba*, with means in *P. orinocensis*, respectively, 20.1%, 17.3%, and 10.9% DW, and in *P. parvaspina* 20.5%, 17.6%, and 10.4% DW (Tabs. 1, 3, 5).

Pelvic fins triangular and dorsally covered by the disc in all three species of *Paratrygon* (Figs. 1B, 2B, D, 3B, D, 19B, D, 20B, D, 33B, 38B, 39B, D, 40B, D; S1B, D, S4B, D). Proportions of pelvic fin measurements very similar among the three species: means of

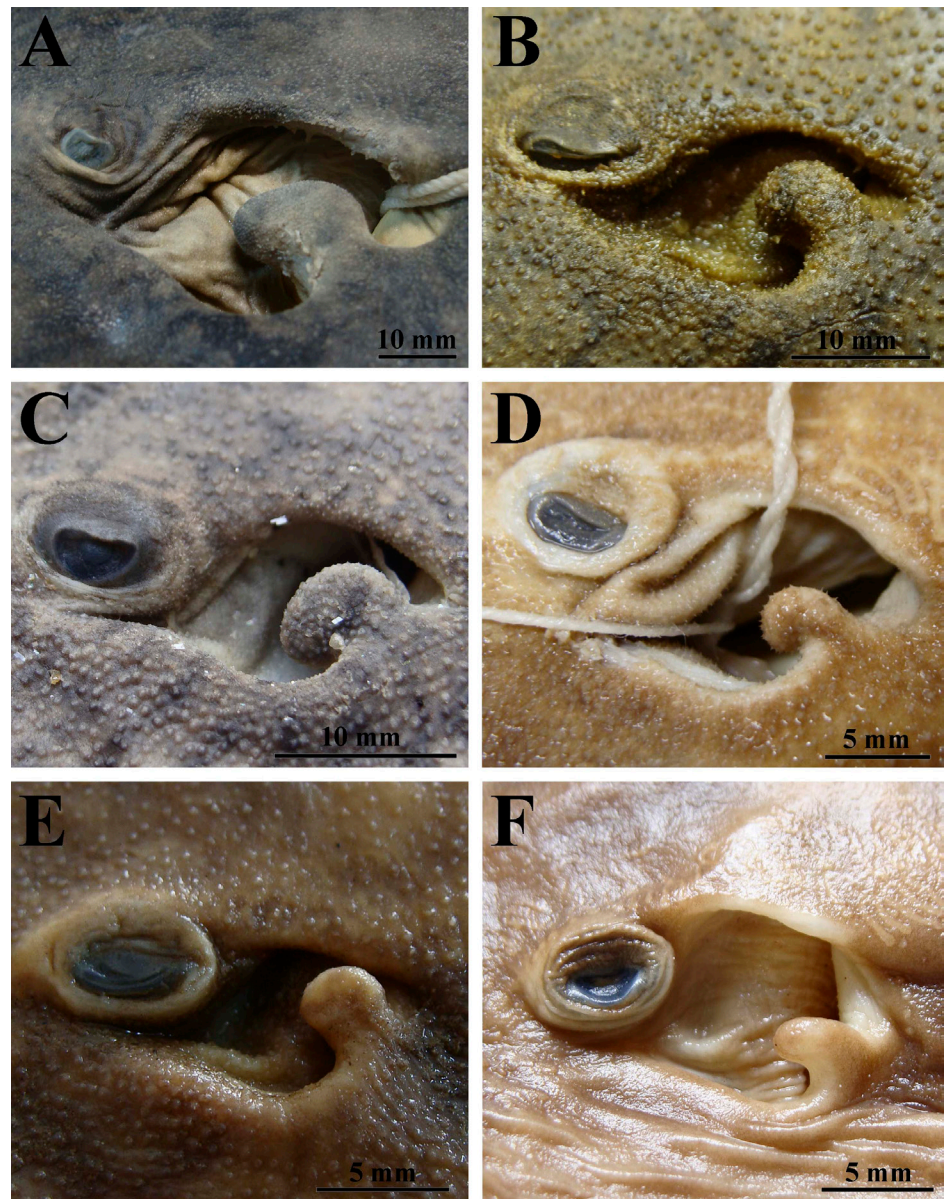


FIGURE 35 | Lateral view of spiracles and spiracles process of *Paratrygon aiereba*. **A.** MPEG uncatalogued, adult female, 786 mm DW, from Marajó island. **B.** AMNH 59878, subadult male, 383 mm DW, from Itenez river. **C.** IAVH-P 11929, juvenile male, 366 mm DW, from Putumayo river. **D.** MNHN A.2269, juvenile male, 285 mm DW, from Solimões river. **E.** MUSM 1389, neonate female, 204 mm DW. **F.** MZUSP 101015, neonate female, 150 mm DW, from Breu river.

length of anterior margin, pelvic fin length, and distance between the axils of pelvic and pectoral fins in *P. aiereba*, respectively, 17.6%, 40.2%, and 4.8% DW; in *P. orinocensis*, 16.9%, 38.7%, and 3.8% DW; and in *P. parvaspina*, 16.6%, 42.5%, and 4.1% DW (Tabs. 1, 3, 5). Male adult specimens of *P. aiereba* and *P. orinocensis* with short, robust and cylindrical claspers presenting rounded tips (Fig. 33B, and also see fig. 3 of Moreira *et al.*, 2018 for more external details). Means of external and internal lengths of clasper in all male

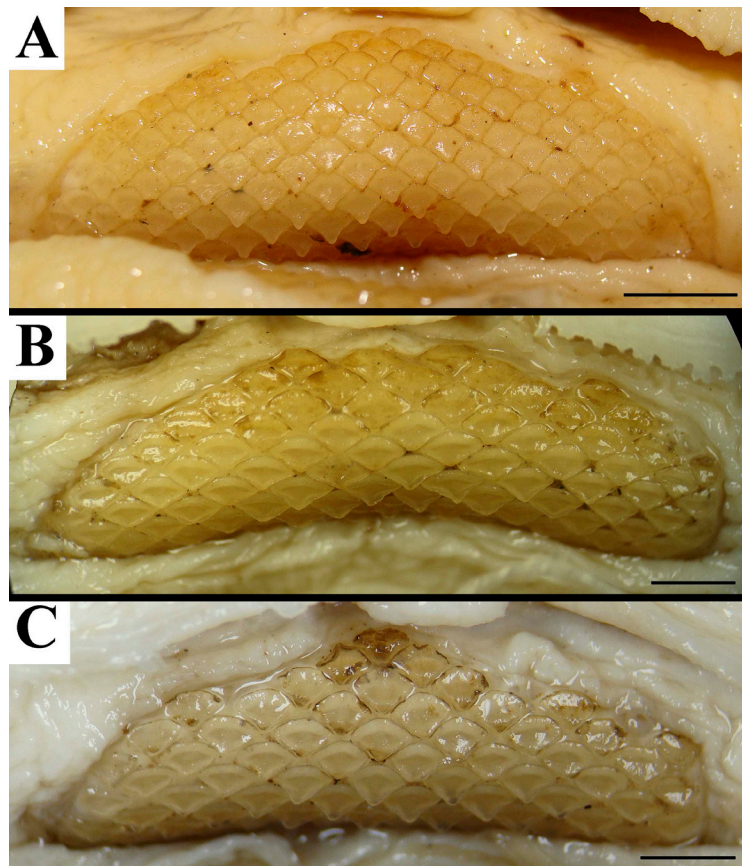


FIGURE 36 | Upper teeth of *Paratrygon aiereba*. **A.** MZUSP 104895, adult female, 590 mm DW, from Javari river. **B.** MNHN A.1019, juvenile female, 324 mm DW, from Solimões river. **C.** MNHN A.2269. Scale bars, **A.** = 5 mm, **B.** and **C.** = 2 mm.



FIGURE 37 | Upper (above) and lower (below) teeth of *Paratrygon aiereba*, MNHN A.2269. Scale bars = 2 mm.

TABLE 6 | Meristic data taken from specimens of *Paratrygon aiereba* from radiographs or dissected specimens; “M” corresponds to the mode, and “N” corresponds to the number of specimens.

<i>Paratrygon aiereba</i>	M	Range	N
Precaudal vertebrae	40	39 – 45	5
Caudal vertebrae	62	62 – 80	4
Total vertebrae	–	101 – 120	4
Diplospodylic vertebrae	–	56 – 81	4
Propterygial radials	–	43 – 49	5
Mesopterygial radials	–	24 – 26	5
Metapterygial radials	42	41 – 44	5
Total radials	–	110 – 117	5
Pelvic radials	17	17 – 22	5
Tooth rows of upper jaw	20	16 – 26	13
Tooth rows of lower jaw	17	14 – 20	10
Symphysis of upper jaw	4	3 – 6	13
Symphysis of lower jaw	4	3 – 5	9

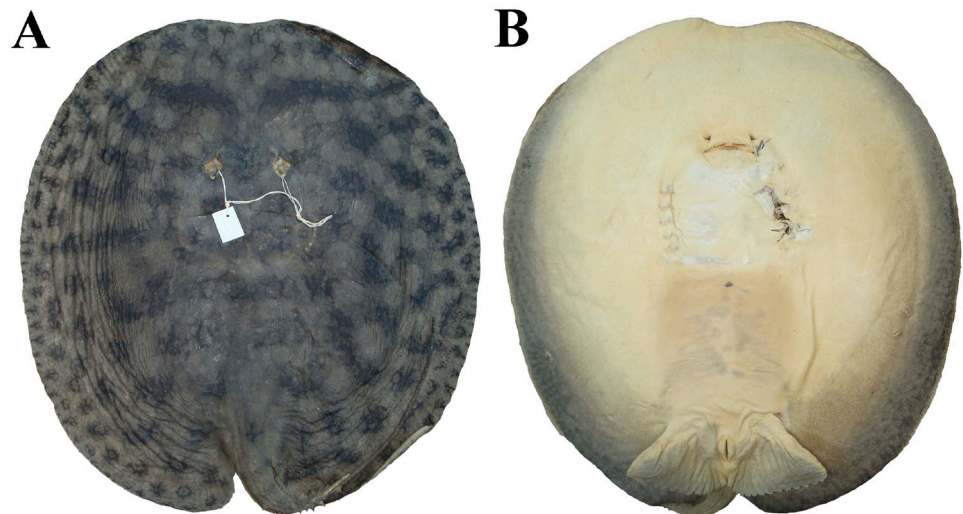


FIGURE 38 | Non-type specimen of *Paratrygon aiereba*, MPEG uncatalogued, adult female, 786 mm DW, from Marajó island. A. dorsal and B. ventral views.

specimens (including neonates, juveniles and subadults) of both species, respectively, 4.7% and 10.9% DW in *P. aiereba*, and, 3.4% and 8.9% DW in *P. orinocensis* (Tabs. 1, 5); only a single juvenile male specimen of *P. parvaspina* was measured (see Tab. 3). Claspers show a significant size increment from neonates to adults; however its growth is greater between subadult and adult specimens (S2 and S5, respectively, for *P. orinocensis* and *P. aiereba*); range of external and internal lengths of clasper in neonates of *P. aiereba*, respectively, 2.4 to 2.7% and 6.7 to 7.5%; in juveniles 2.3 to 4.4% and 6.8 to 11.7%; and in adults 6.6 to 10.4% and 15.1 to 21.5% DW (S5). Pseudosiphon and ventral pseudosiphon also show this size increment from neonates to adults in these both species (S2, S5). Pseudosiphon small, located in the medial region of internal lateral portion of clasper; ventral pseudosiphon

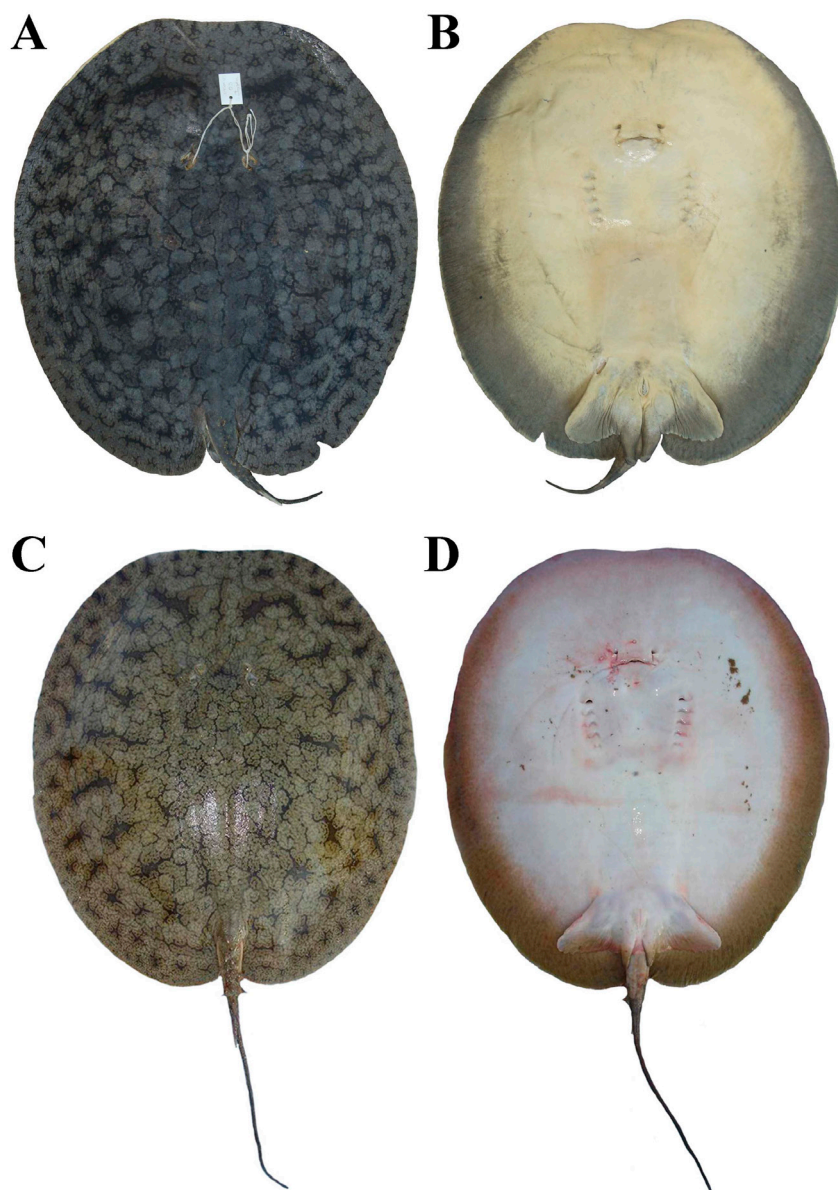


FIGURE 39 | Non-types of *Paratrygon aiereba*. MPEG uncatalogued, adult male, 681 mm DW, from Marajó island. **A.** dorsal and **B.** ventral views. MZUSP 104029, juvenile male, 436 mm DW, from Juruá river. **C.** dorsal and **D.** ventral views.

larger, occurring in the external lateral portion of clasper from the same level of anterior margin of pseudosiphon to clasper tip. Spermatic groove dorsally located from the same level of posterior margin of pelvic fins to the distal extremity of clasper; at the level between the two pseudosiphons, this groove curves toward the external lateral portion (see fig. 3 of Moreira *et al.*, 2018 for clasper of *P. aiereba*).

Paratrygon aiereba and *P. orinocensis* possess long tails with mean distances between cloaca and caudal sting insertion (pre-caudal sting portion) in both species 23.5% DW, and mean distances between cloaca and tail tip (post-caudal sting portion), respectively, 87.8% and 100.7% DW (Tabs. 1, 5). *Paratrygon parvaspina* has a shorter tail, with means

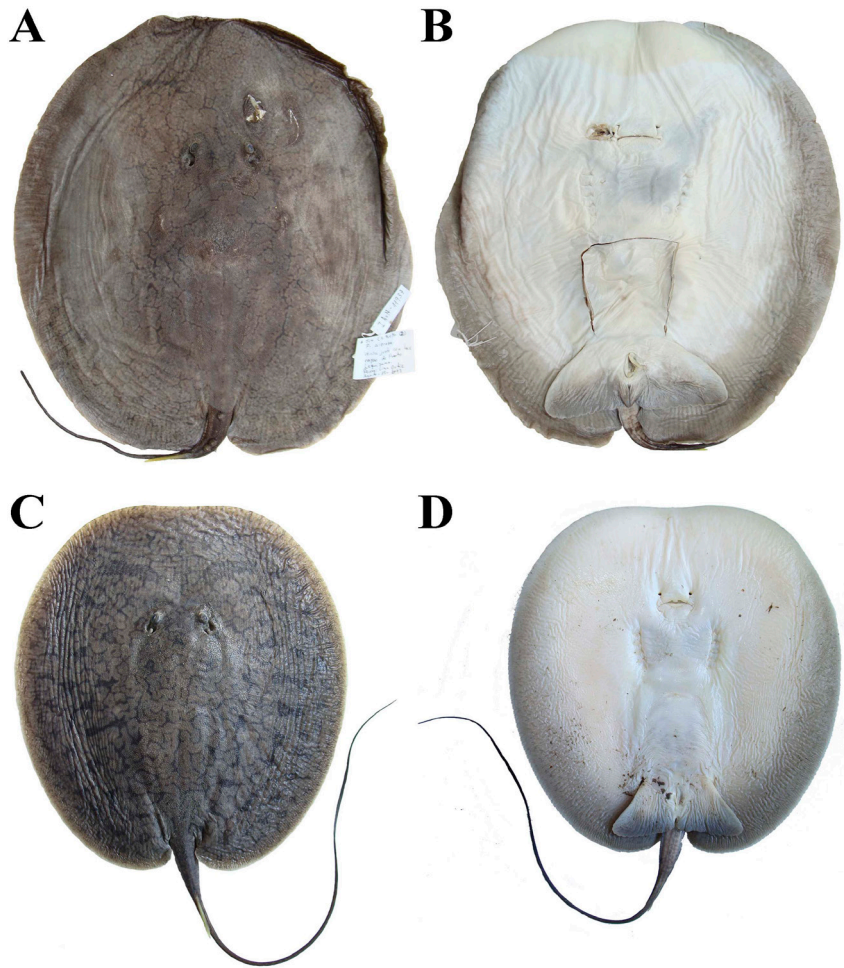


FIGURE 40 | Non-types of *Paratrygon aiereba*. IAvH-P 11927, juvenile male, 408 mm DW, from Putumayo river. **A.** dorsal and **B.** ventral views. IIAP uncatalogued, juvenile female, 208 mm DW, from Napo river. **C.** dorsal and **D.** ventral views.

of precaudal sting and distance between cloaca and tail tip, respectively, 21.1% and 50.4% DW (Tab. 3). However, tail width in all three species very similar, with means around 6.5 DW (Tabs. 1, 3, 5). All three species present a decrease of tail length (pre- and postcaudal sting portions) from neonates to adult specimens (see values of tail measurements in S2, S3 and S5). Tail folds in the three species lack morphological differences, with lateral tail folds slightly developed and occurring from base of tail to caudal sting insertion, and dorsal and ventral tail folds present just on postcaudal sting portion and poorly developed.

Color in alcohol. *Paratrygon aiereba* presents dorsal disc coloration in gray or brown tones, with dark and light spots spread over disc; dark spots larger and more conspicuous than light spots (Figs. 33A, 34, 38A, 39A, C, 40A, C; S4A, C). *Paratrygon orinocensis* and *P. parvaspina* present a similar pattern, in gray and brown tones with large dark and small

light spots on disc; however specimens of both Orinoco basin species also have beige on dorsal disc, mainly *P. parvaspina* (Figs. 1A, 2A, C, 3A, C, 19A, C, 20A, C; S1A, C). Dark spots of *P. aiereba* dark brown, dark gray or black, generally large, vermiculate or rounded, and sometimes axon shaped, being more evident and larger near disc margin; some adults present small gray rings within the largest dark spots on central disc, and the great majority of specimens of *P. aiereba* also have an evident and diagnostic preorbital pair of dark spots extremely developed on preorbital region that resembles a pair of eyebrows or a mustache shape. *Paratrygon orinocensis* has a similar pattern of dark spots, with various shapes and dark tones (see pags. 18–19), however smaller than in *P. aiereba*, and generally rounded with small beige specks inside largest dark spots in adults; dark spots in this species larger near the central disc region. *Paratrygon parvaspina* presents dark spots with vermicular or slender dendritic shapes, spread and more or less evenly spaced (mainly in adult specimens) over disc, and small and more concentrated near disc margins. No specimen of both new Orinoco basin species present the preorbital pair of developed dark blotches observed in *P. aiereba*. Light spots of *P. aiereba* light gray, beige or light brown, rounded and not as evident as the dark spots, intermingled in some specimens. *Paratrygon orinocensis* has these spots polygonal and generally about same size as eye diameter; *P. parvaspina* with rounded, oval or polygonal light spots. Dorsal coloration of tail in *P. aiereba* similar to color pattern present from dorsal disc to caudal sting insertion, with dark spots occurring laterally on tail, and light spots on central dorsal area; postcaudal sting portion with very dark tone. The opposite occurs in the precaudal sting portion of *P. orinocensis* with dark spots present on central dorsal area and light spots occurring laterally; postcaudal sting portion also dark, but with some beige specks. *Paratrygon parvaspina* also has dorsal tail coloration similar to dorsal disc, with dark spots spread on the precaudal sting portion, and postcaudal sting tail light beige or light gray presenting many and small dark specks.

Paratrygon aiereba possess a similar pattern of ventral coloration of the two new species, with two tones present on the disc: one light (white or light beige), predominant on central area of disc and anterior margin, and another one dark (brown, gray or beige) occurring on the lateral and posterior margins of disc; also in all three species, some specimens possess small and rounded, oval or vermiculate darker spots close to disc margins (Figs. 1B, 2B, D, 3B, D, 19B, D, 20B, D, 33B, 38B, 39B, D, 40B, D; S1B, D, S4B, D). Pelvic fins and claspers with similar pattern among the three species: the same tones of ventral disc occur on pelvic fins and claspers, with light tone present on anterior margin of pelvic fins and clasper base, and dark tone present posteriorly. Ventral coloration of tail also similar among the three species on precaudal sting portion, presenting the same light tone on central disc with some gray spots. Coloration on postcaudal sting portion darker and similar in *P. aiereba* and *P. orinocensis*; *P. parvaspina* presents on this portion lighter, either beige or gray tone, slightly darker near tail tip; ventrally numerous small dark gray specks present in *P. parvaspina*.

Squamation. *Paratrygon aiereba* possess dermal denticles scattered throughout dorsal disc and tail as *P. orinocensis* and *P. parvaspina*, with denticles on disc center greater and more visible than at margins; on tail, denticles greater on precaudal sting portion, and on postcaudal sting portion denticles minute and scarce (*P. parvaspina* without denticles on postcaudal sting portion of tail).

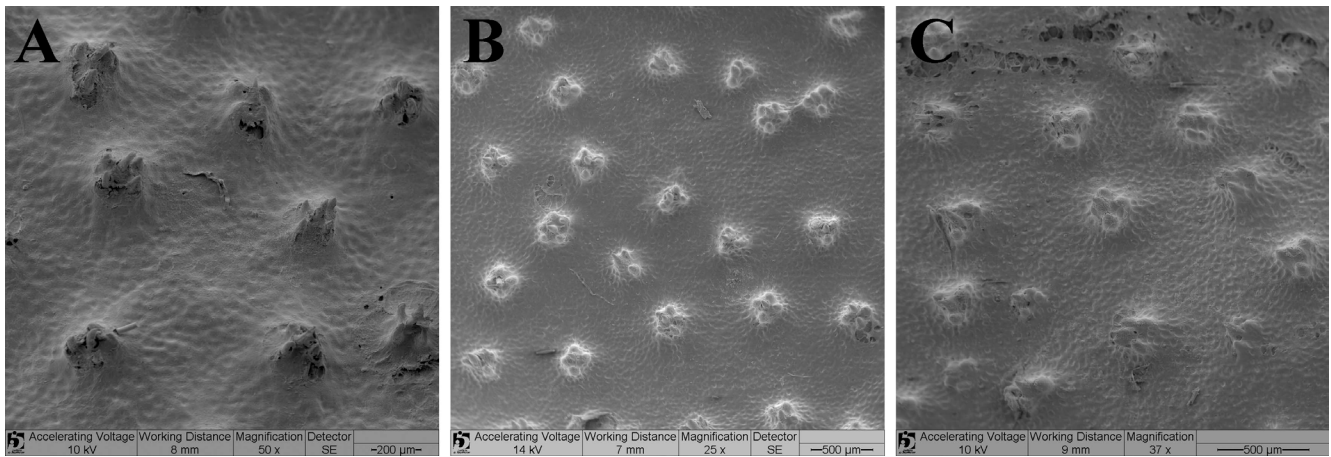


FIGURE 41 | Dorsal view of dermal denticles in central disc of *Paratrygon aiereba* (SEM images). **A.** INPA 1331, juvenile female, 255 mm DW, from Solimões river. **B.** MUSM 47105, juvenile male, 214 mm DW, from Urubamba river. **C.** MZUSP 117831, neonate female, 200 mm DW, from Nanay river.

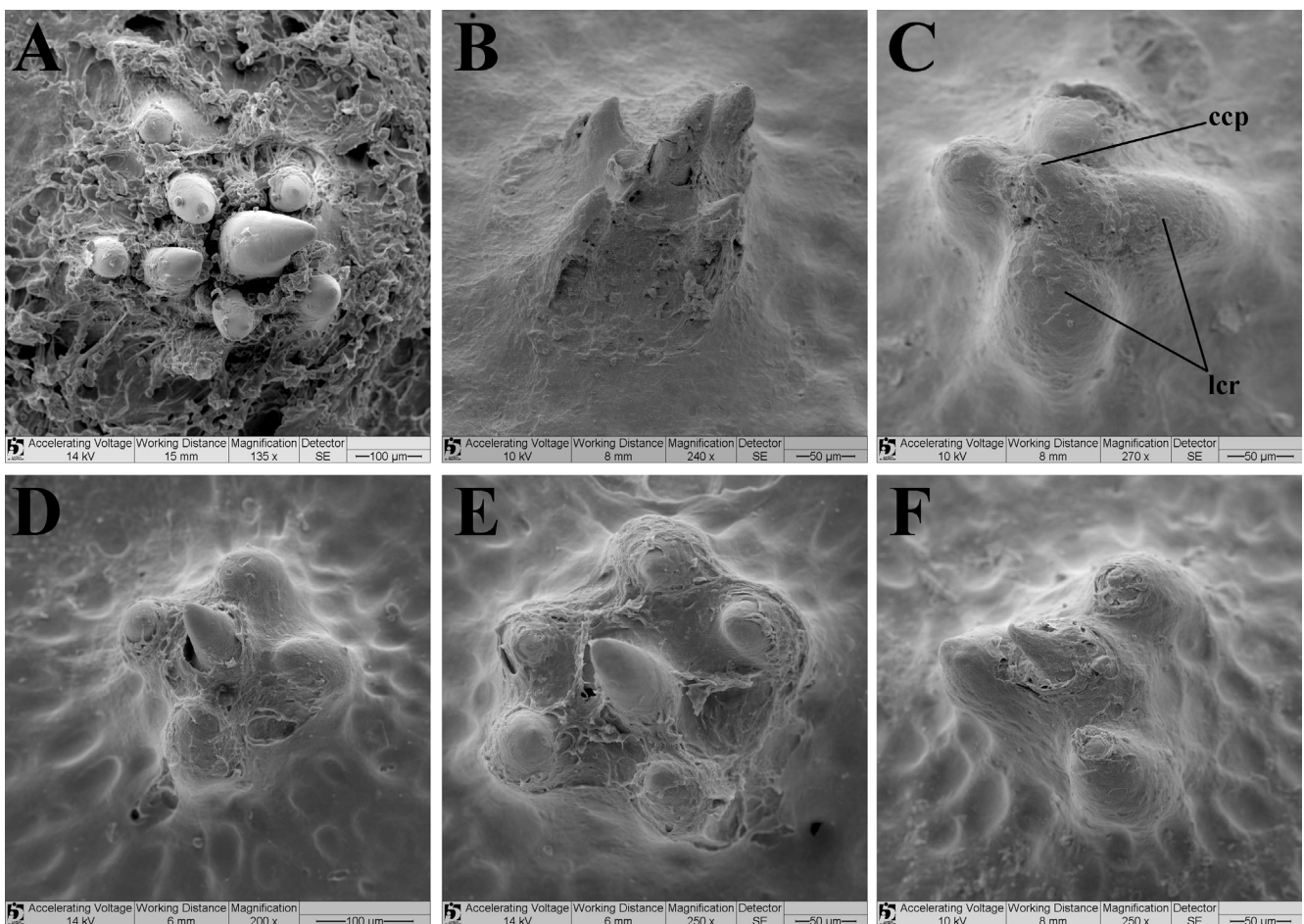


FIGURE 42 | Details of dermal denticles in central disc of *Paratrygon aiereba* (SEM images) in dorsal view. **A.** MZUSP 103896, adult male, 508 mm DW, from Tapajós river. **B.** and **C.** INPA 1331. **D.** and **E.** MUSM 47105. **F.** MZUSP 117831. ccp = central coronal plate, lcr = lateral coronal ridge.

Paratrygon aiereba has small dermal denticles, even on disc where they reach their greatest size, their diameters not reaching one mm (Figs. 41–42). *Paratrygon orinocensis* possesses larger denticles on disc center than *P. aiereba*, with diameters reaching two mm (Fig. 7), whereas *P. parvaspina* has small denticles with diameters 0.5 mm on central disc (Fig. 23). On central disc region in *P. aiereba*, dermal denticles have a high and narrow crown, with a higher and pointed central coronal plate (*ccp*) surrounded by smaller, pointed or rounded lateral coronal ridges (*lcr*) vary in number between three and six depending on their size; adult specimens present crowns with more lateral ridges (Fig. 42). *Paratrygon orinocensis* has dermal denticles on central disc with wide and high crowns, presenting a central coronal plate morphologically very similar to its lateral coronal ridges; *lcr* in adult specimens more than 12 (Fig. 7). Dermal denticles on central disc of *P. parvaspina* morphologically similar to *P. aiereba* (Fig. 23). Dermal denticles on disc margins in *P. aiereba* more scattered, mainly on lateral margins (Fig. 43). Morphology of dermal denticles on anterior and lateral margins similar to central disc (Figs. 43A–B), however with fewer lateral crown ridges; dermal denticles on anterior margin have a more pointed *ccp* than central denticles (Figs. 43A, 44A). Dermal denticles on posterior margins with a very developed and pointed *ccp* (Fig. 44D). Some specimens of *P. aiereba* present on their posterior disc margins well-developed thorns, much greater than dermal denticles; these thorns have a large basal plate (*bp*), generally with some denticles, and a very high and developed pointed crown (*cr*) (Figs. 44E–F). *Paratrygon aiereba* has dermal denticles on tail base with morphology similar to thorns, larger than dermal denticles from other parts of disc (their basal plates reach one mm), with a very developed *ccp* (reaching one mm high), and presenting small and pointed lateral crown ridges (Fig. 45). *Paratrygon orinocensis* has two morphological types of dermal denticles on tail base (Fig. 9): one similar to dermal denticles on central disc area (Figs. 9A, C–D), and another similar to typical dermal denticles of tail base of *P. aiereba* (Figs. 9A–B).

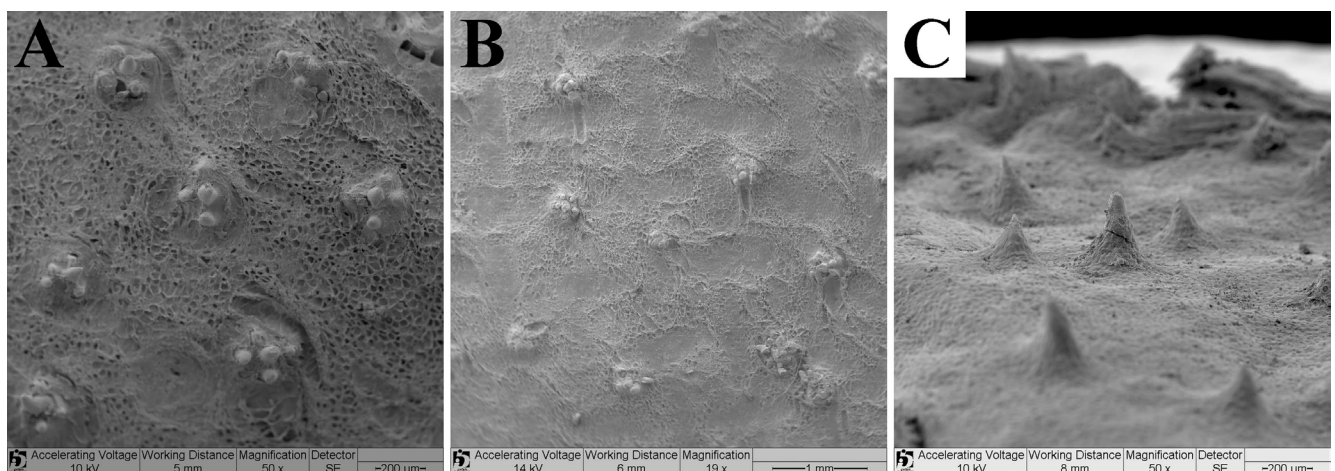


FIGURE 43 | Dermal denticles in the disc margins of *Paratrygon aiereba*, MZUSP 103896 (SEM images). **A.** dorsal view of anterior margin denticles. **B.** dorsal view of lateral margin denticles. **C.** lateral view of posterior margins denticles.

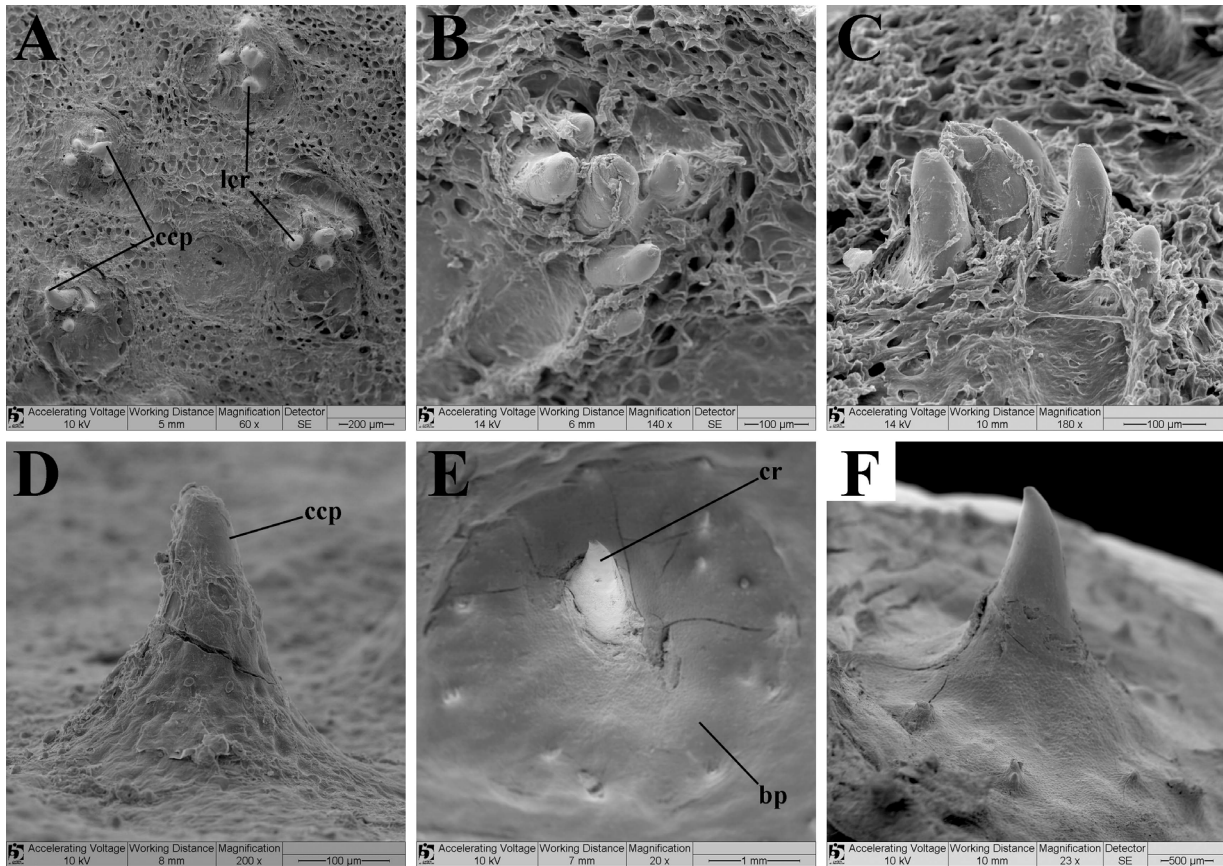


FIGURE 44 | Details of dermal denticles in the disc margins of *Paratrygon aiereba*, MZUSP 103896 (SEM images). **A.** dorsal view of anterior margin denticles. **B.** dorsal and **C.** lateral detail of lateral margin denticle. **D.** lateral view of a posterior margin denticle. **E.** dorsal and **F.** lateral detail of a thorn in the posterior margin of disc. bp = basal plate, ccp = central coronal plate, cr = crown, lcr = lateral coronal ridge.

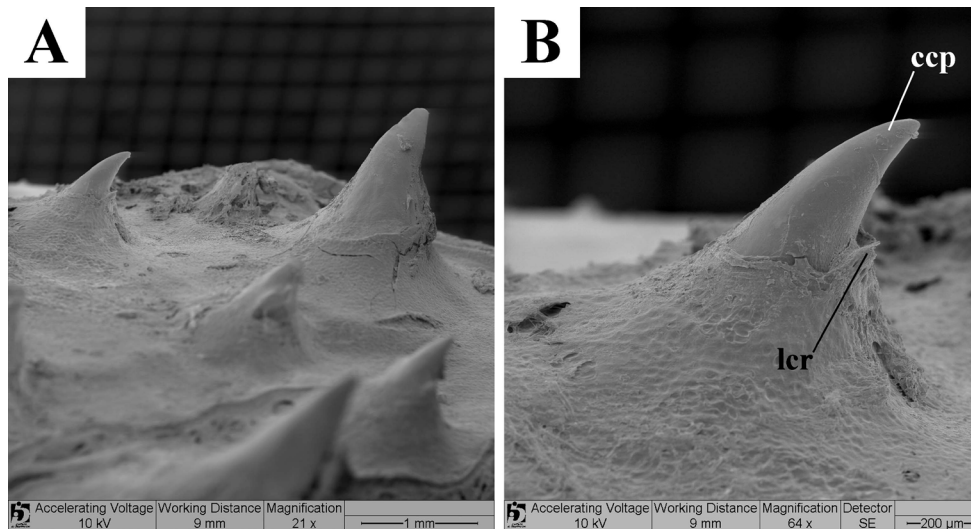


FIGURE 45 | Details of dermal denticles and thorns in the tail basis of *Paratrygon aiereba*, MZUSP 103896 (SEM images). **A.** dermal denticles and one thorn (right superior corner) in the tail basis of MZUSP 103896. **B.** detail of pointed dermal denticles of left superior corner in the Fig. 45a. image. ccp = central coronal plate, lcr = lateral coronal ridge.

Paratrygon aiereba has dorsal and lateral rows on tail (Fig. 46). Adult specimens have two or three dorsal rows with developed, high and broad-based thorns; some specimens also have tubercular ones. Dorsal rows extend from tail base and reach caudal sting insertion. Adults also with developed lateral rows, generally a single row, extending from the medial portion of tail to the region just posterior to caudal sting tip; lateral rows also with developed thorns, more developed than dorsal thorns in some specimens (Fig. 46A). Large juvenile specimens present dorsal and lateral rows very similar to adults, however with thorns not as developed (Figs. 46B–C). Most juvenile specimens have only dorsal rows, with few small thorns; lateral rows less developed and occurring in few specimens (Figs. 46D–E). Neonates only with incipient dorsal rows on the tail base; however some specimens lack thorns (Fig. 46F). *Paratrygon orinocensis* presents only dorsal rows on tail, lacking lateral rows (Fig. 10). Adult specimens with one or two dorsal rows of developed and high thorns with broad base (Figs. 10A–B). Subadults and larger juveniles generally with only one row, with thorns high and with broad base (Figs. 10C–E). Most juvenile specimens with only part of this single dorsal row with small thorns (Figs. 10F–G). Neonates with only a poorly developed row of minute thorns on tail base (Fig. 10H). *Paratrygon parvaspina* has dorsal and lateral rows of thorns on tail (Fig. 24). Adult specimens with just one dorsal and one lateral row. Dorsal row in adult and large juvenile specimens extends from tail base to caudal sting insertion; dorsal thorns developed, high and with broad tubercular bases (Figs. 24A–C). Lateral rows in these specimens extend from just anterior to medial portion of tail and reach caudal sting insertion; lateral thorns very similar to dorsal ones. Juveniles only present a dorsal row with thorns slightly less developed than adult specimens, and with broad tubercular bases (Figs. 24D–F).

Paratrygon aiereba with long and slightly broad caudal sting (Fig. 47); *P. orinocensis* with similar caudal sting as *P. aiereba*, whereas *P. parvaspina* has a diagnostic small and slender caudal sting (Figs. 11, 25). Mean caudal sting length in *P. aiereba* 11.3% DW and range between 3 and 17.9% DW; caudal sting mean width 1% DW and range between 0.4 and 1.5% DW (Tab. 5). Adults possess one or two very developed caudal stings, with lateral serrations along their length, with larger serrations closer to tip; a dorsal medial groove present in caudal sting, from sting base to its distal third (Figs. 47A–B). Subadult specimens have a caudal sting similar to adults, however its serrations occur on the distal two-thirds of sting and lack a dorsal medial groove. Larger juvenile specimens also have one or two stings, with serrations only present on the distal two-thirds (Fig. 47C). Most juveniles have only one caudal sting with few lateral serrations present on distal two-thirds (Figs. 51D–F). *Paratrygon orinocensis* has a mean caudal sting length 12% DW [6.7–15.3% DW], and caudal sting width with mean 1% DW [0.6–1.7% DW] (Tab. 1). *Paratrygon parvaspina* has a very reduced caudal sting, with mean length 6.2% DW [5.6–7.1% DW], and mean width 0.9% DW (Tab. 3).

Lateral line. *Paratrygon aiereba* has the junction of four canals (*JFC*) very small, its posterior portion the junction point of hyomandibular (*HMD*) and infraorbital canals (*IOC*), and its anterior portion the junction of supraorbital (*SPO*) and nasal (*NAS*) canals (Fig. 48B). *JFC* in *P. orinocensis* very small (Fig. 12), and *P. parvaspina* has the largest *JFC* among the three species (Fig. 26).

From *JFC*, hyomandibular canal (*HMD*) extends posteriorly through its angular component (*ang*), which contours externally the *adductor mandibulae*; *P. aiereba* has a

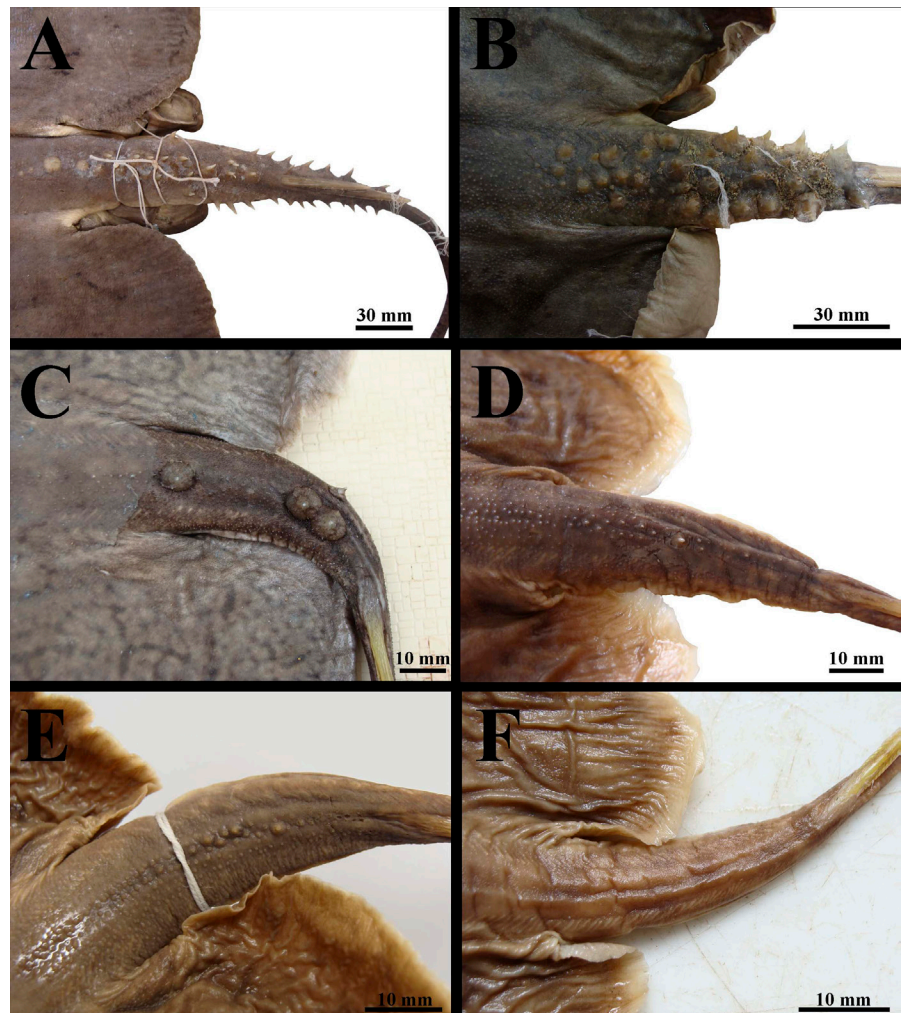


FIGURE 46 | Dorsal view of dorsal and lateral rows of thorns in *Paratrygon aiereba*. **A.** MZUSP 117155 (neotype). **B.** MUSM 9423, juvenile male, 428 mm DW, from Las Piedras river. **C.** IAvH-P 11927. **D.** MUSM 1389, juvenile male, 207 mm DW. **E.** MZUSP 14772, juvenile female, 221 mm DW, from Ucayali river. **F.** MZUSP 101015.

straight angular component (Fig. 48A), whereas *P. orinocensis* and *P. parvaspina* have a more curved component (Figs. 12B, 26B). Hyomandibular canal continues to descend and externally surrounds the branchial basket at about central region of disc, forming the jugular component (*jug*); *P. aiereba* and *P. parvaspina* have this component straighter and posteriorly directed (Figs. 26A, 48A) whereas in *P. orinocensis* the *jug* component more directed to central disc region (Fig. 12A). Jugular component descends farther and posterior to the level of scapulocoracoid; this canal posteriorly extends slightly away from central disc until it reaches a region slightly anterior to level of pelvic girdle; in this part, the jugular component forms the subpleural loop (*spl*). *Paratrygon orinocensis* has a wide *spl* with two short posterior subpleural tubules (*pst*) (Fig. 12A); *P. aiereba* and *P. parvaspina* have a short *spl* with three short *pst*, with some of them branched (Figs. 26A, 48A). After the *spl*, hyomandibular canal ascends anteriorly and parallel to jugular component until

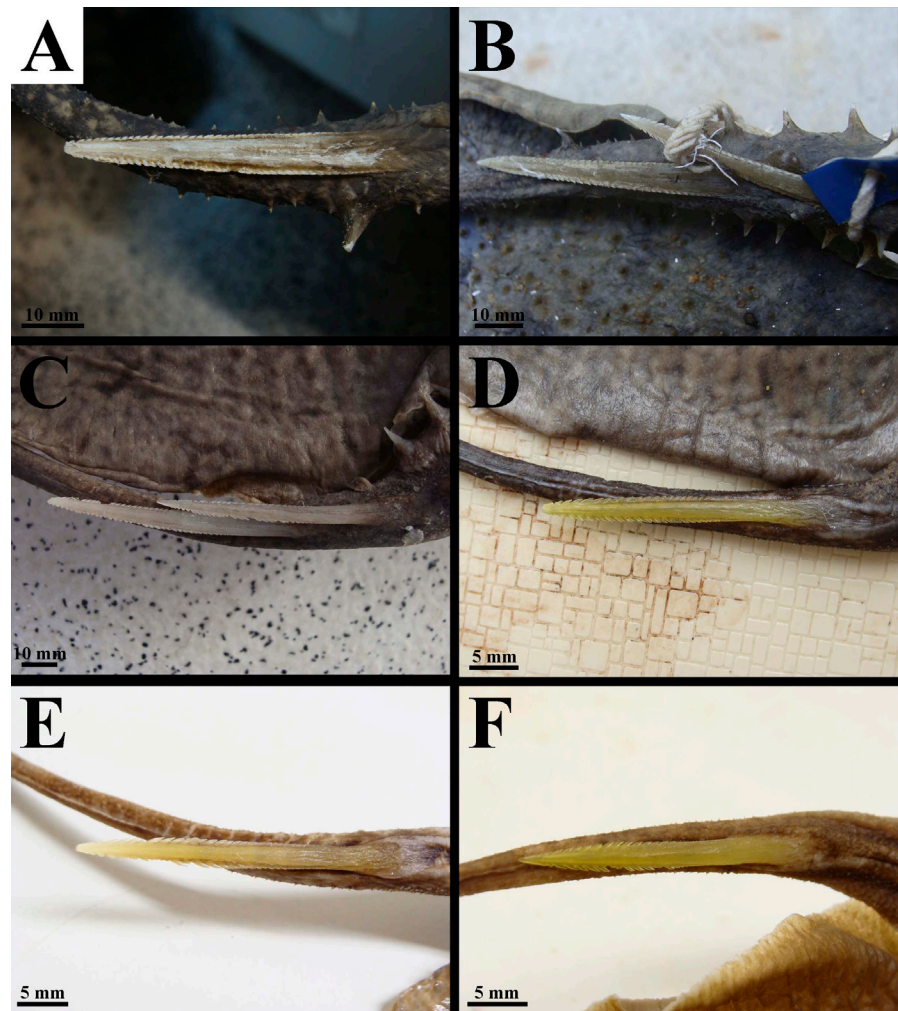


FIGURE 47 | Dorsal view of caudal stings of *Paratrygon aiereba*. **A.** MPEG uncatalogued, adult male, 681 mm DW. **B.** MZUSP 103907, adult male, 606 mm DW, from Tapajós river. **C.** IAvH-P 11894, juvenile female, 472 mm DW. **D.** IAvH-P 11937, juvenile male, 280 mm DW, from Putumayo river. **E.** MNHN A.2289. **F.** USNM 264005, juvenile male, 184 mm DW, from Tambopata river.

level of fourth pair of branchial slits, where the canal directs anterolaterally to disc margin, forming its subpleural component (*spc*). *Paratrygon aiereba* has part of this component extending to level of fourth pair of gill slits slightly straighter than the other two species (Fig. 48A); *P. orinocensis* has the same portion of its *spc* directed to central disc region (Fig. 12A), and *P. parvaspina* has its entire *spc* as a big curvature directed toward anterolateral disc margin (Fig. 26A). At mouth level, subpleural component continues approaching anterolateral margin of disc, and from there proceeds anteriorly, parallel and very close to margin, until it reaches the junction with prenasal component of nasal canal (*pnc*); this entire portion of *spc* presents subpleural tubules (*spt*) which are longer at lateral margins, reducing in size close to the anterior margin. *Paratrygon aiereba* and *P. orinocensis* have the beginning of the *spt* at level of mouth (Figs. 12, 48), whereas *P. parvaspina* has the beginning of its *spts* at level of second pair of gill slits (Fig. 26).

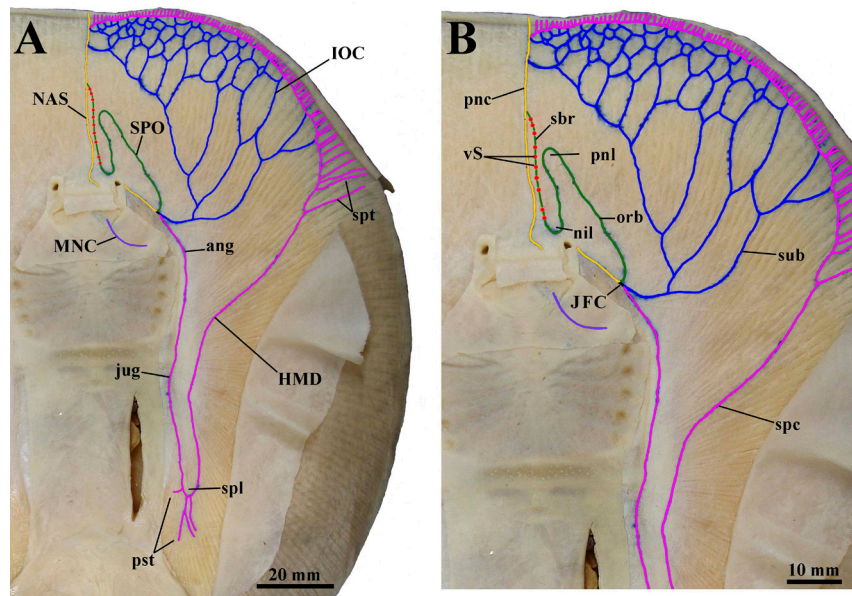


FIGURE 48 | Ventral canals of lateral line system in *Paratrygon aiereba*, MZUSP 117831. **A.** distribution of all ventral canals. **B.** detail of the anterior central disc ventral canals. Abbreviations see Fig. 12.

From the *JFC*, infraorbital canal (*IOC*) extends laterally and distally to just anterior to level of mouth, and subsequently ramifies into its suborbital component (*sub*). Suborbital component of *IOC* with honeycomb-shaped ramifications, which are greater posteriorly and smaller close to subpleural component of *HMD* and to the anterior disc margin; *sub* ramifications connect in various points with subpleural component of *HMD*, and in only two points with prenasal component of *NAS*. *Paratrygon aiereba* and *P. orinocensis* have more honeycomb-shaped ramifications (Figs. 12, 48) than *P. parvaspina* (Fig. 26).

Supraorbital canal (*SPO*) emerges from the *JFC* directed anteriorly and inclined (in a 45° angle) to anteromedial region of disc, forming orbitonasal component (*orb*). At level between the nostril and anterior margin of disc, *SPO* continues anteriorly to form the prenasal loop (*pnl*), before turning posteriorly again. Orbitonasal component in *P. aiereba* extends straight to the *pnl* (Fig. 48); *P. orinocensis* has a small curvature anteriorly directed in its *orb* (Fig. 12), whereas *P. parvaspina* has a smooth and small curvature posteriorly directed in its *orb* (Fig. 26). Also *P. parvaspina* has a slightly wide *pnl* compared to the other two species (Fig. 26B). From *pnl*, *SPO* extends posteriorly close to the nostrils where it forms a new central loop, the nasointernal loop (*nil*) directed anteriorly. After *nil*, *SPO* extends anteriorly until up to half prenasal distance where it connects with the prenasal component of *NAS*; in this region, named subrostral component of *SPO* (*sbr*), the vesicles of Savi (*vS*) occur. *Paratrygon aiereba* has a longer *sbr* than the other two new species, and the number of *vS* of *P. parvaspina* is smaller (around six *vS*; Fig. 26B) than in *P. aiereba* and *P. orinocensis* (around 12 *vS*; Figs. 12B, 48B).

Nasal canal (*NAS*) extends anteromedially from the *JFC* next to external margin of nostril in a 45° angle, where it penetrates the disc. The canal emerges in region between nostrils, next to longitudinal midline of body, and makes a small curvature in direction of anterior disc, where it ascends straight to anterior margin of disc, forming in this

portion its prenasal component (*pnc*). At the *pnc*, the *NAS* connects with the other three canals. Connection of *SPO* with *NAS* in *P. aiereba* is located more anteriorly than in the two new species (Figs. 12B, 26B, 48B).

Mandibular canal (*MNC*) extends posteriorly from midline of disc next to mouth and contours posteriorly the *adductor mandibulae* muscle until just anterior to level of first gill slit, where it enters the body; *MNC* makes a central posterior curve in *P. aiereba* (Fig. 48), descends in a straight fashion at a 45° angle in *P. orinocensis* (Fig. 12), and descends straight in almost a 90° angle in *P. parvaspina*, where at the level of first pair of gill slits it makes an external curve surrounding the *adductor mandibulae* muscle (Fig. 26).

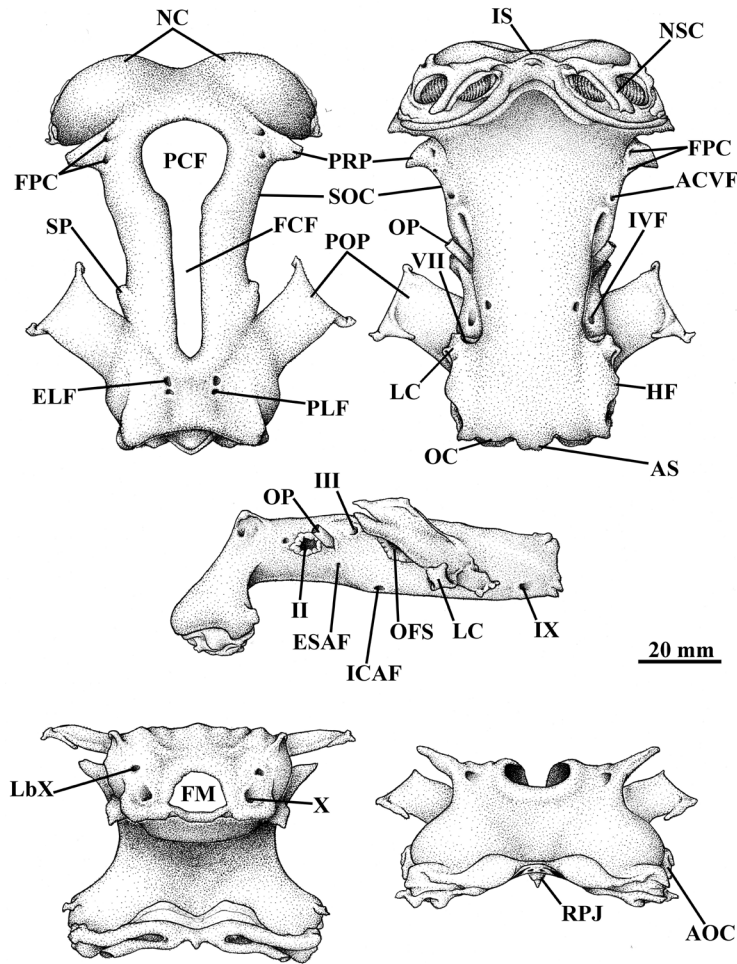


FIGURE 49 | Neurocranium of *Paratrygon aiereba*, MZUSP 103896, in dorsal, ventral, lateral, caudal and frontal views (from top to bottom, and from left to right). ACVF = anterior cerebral vein foramen, AOC = antorbital cartilage condyle, AS = articular surface, ELF = endolymphatic foramina, ESAF = efferent spiracular artery foramen, FCF = frontoparietal component of fontanelle, FM = foramen magnum, FPC = foramen of preorbital canal, ICAF = internal carotid artery foramina, HF = hyomandibular facet, IVF = interorbital vein foramen, IS = internasal septum, LC = lateral commissure, NC = nasal capsule, NSC = nasal cartilage, OC = occipital condyle, OFS = orbital fissure, OP = optic pedicel, PCF = precerebral component of fontanelle, PLF = perilymphatic foramina, POP = postorbital process, PRP = preorbital process, RPJ = rostral projection, SOC = supraorbital crest, SP = supraorbital process, II = optic nerve foramen, III = oculomotor nerve foramen, VII = hyomandibular ramus of facial nerve foramen, IX = glossopharyngeal nerve foramen, X = vagus nerve foramen, LbX = lateralis branch of vagus nerve foramen.

Skeleton. Mersitic counts of vertebrae and pectoral and pelvic radials of *P. aiereba* shown in Tab. 6.

Neurocranium of *P. aiereba* with length similar to synarcual cartilage (Figs. 49, 50). Nasal capsules (NC) and anterior region of neurocranium well inclined ventrally in a 45° angle in lateral view (Fig. 49). Neurocranium widest at postorbital process (POP) and nasal capsules, whereas orbital region, anterior to supraorbital process (SP), is the narrowest portion. In dorsal view, neurocranium of *P. aiereba* more similar to *P. parvaspina* than to *P. orinocensis*, which has an evident “T” shape and a more slender orbital region than *P. aiereba* and *P. parvaspina* (Figs. 13, 27, 50).

Nasal capsules broad, oval and inclined, with a relatively large internasal septum (IS); IS larger in *P. orinocensis* and narrower in *P. aiereba*; NC in *P. aiereba* laterally surrounded by first segment of propterygium (FSP), as in *P. orinocensis*, and different from *P. parvaspina* in which the FSP does not directly contact the lateral surface of NC (Figs. 13, 27, 50). Between nasal capsules, at the anteroventral tip of neurocranium, a small rostral projection (RPJ) is present (Figs. 49, 50); RPJ minute and not developed in *P. orinocensis*, whereas *P. parvaspina* has a large and circular RPJ (Figs. 13, 27). Posterolaterally NC articulates with the antorbital cartilage condyle (AOC). Nasal cartilages (NSC) present ventral to the NC apertures (Fig. 49).

Preorbital processes (PRP) just posterior to NC and dorsally positioned, triangular and not very projected laterally beyond level of NC (Figs. 49, 50) in *P. aiereba*, as in *P. orinocensis*; however, *P. parvaspina* has PRP very projected and extending externally beyond level of NC (Figs. 13, 27). Base of PRP with two foramina of preorbital canal (FPC) visible dorsally and ventrally, the anterior more developed than posterior (Fig. 49). Posterior to PRP, on dorsolateral portion of neurocranium, the supraorbital crest (SOC) covers entire dorsal part of lateral walls of orbital region from the PRP to supraorbital process (Figs. 49, 50); *P. aiereba* has a slightly more developed SOC than the two species from Orinoco basin (Figs. 13, 27, 50).

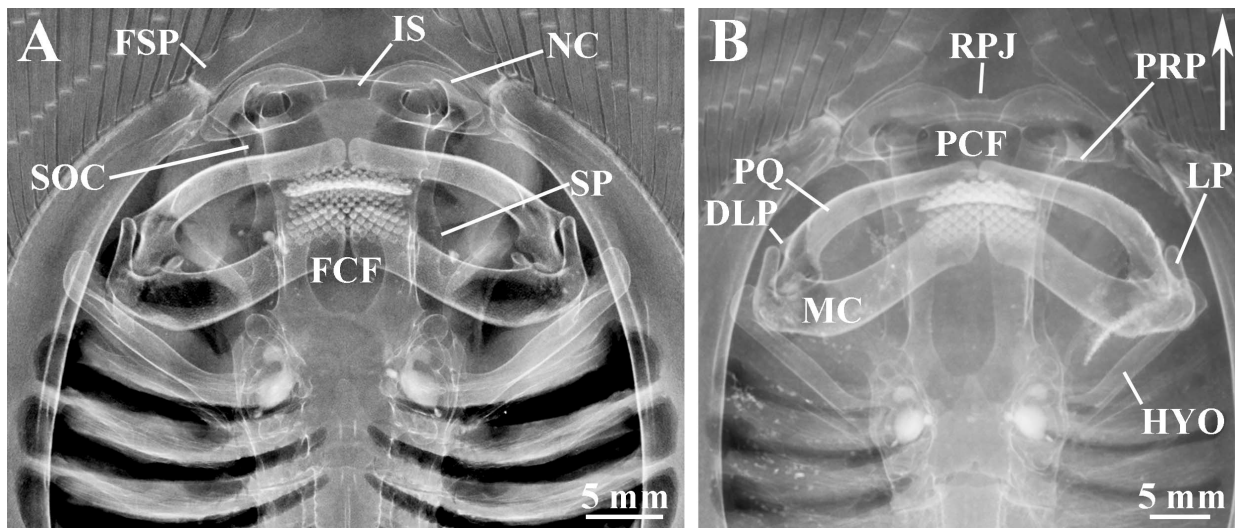


FIGURE 50 | Radiographs of neurocranium and mandibular arch of *Paratrygon aiereba*, upper views. A. ZSM 34500, neonate female, 204 mm DW, from San Martin river. B. USNM 264005. Abbreviations see Fig. 13. Arrow indicates to the anterior portion of specimens.

The anterior cerebral vein foramen (*ACVF*) is found on lateral wall of orbital region of neurocranium; optic nerve foramen (*II*) large and posterior to *PRP*, close to it; both foramina are positioned slightly dorsally on lateral wall of orbital region (Fig. 49). Optic pedicel (*OP*) closely adjacent to *II*; oculomotor nerve foramen (*III*) dorsal to *OP*; efferent spiracular artery foramen (*ESAF*) ventral to *OP*. Supraorbital process (*SP*) level with *OP*. Orbital fissure (*OFS*) posterior to *III*, and ventral to it is the interorbital vein foramen (*IVF*); *IVF* easy to visualize in ventral view of neurocranium (Fig. 49). Orbital fissure located at junction of orbit with otic capsule; just dorsal to *OFS* is the wing shaped postorbital process (*POP*); in dorsal view *POP* projects laterally from lateral wall of neurocranium at a 45° angle just posterior to *SP* (Figs. 13, 49). Posterior and ventral to *OFS* is the arch shaped lateral commissure (*LC*); immediately anterior to *LC* is the hyomandibular ramus of facial nerve foramen (*VII*). The glossopharyngeal nerve foramen (*IX*) and the hyomandibular facet (*HF*) (Fig. 49) are located on lateral wall of otic capsule, posterior and near ventral face of neurocranium.

Roof of neurocranium from *NC* to *POP* with a large, spoon-shaped fontanelle composed of anterior, rounded precerebral component (*PCF*) and posterior, narrow and straight frontoparietal component (*FCF*) in between the *PRP* and *POP* (Figs. 13, 27, 49, 50). *Paratrygon aiereba* has the largest *FCF*, with its posterior extremity very broad and rounded (Fig. 50); *P. parvaspina* also has a broad *FCF*, however slightly less wide than in *P. aiereba* (Fig. 27). *Paratrygon orinocensis* has narrowest *FCF*, with a “8” shape (Fig. 13). Posteriorly to fontanelle and above otic capsule, two pairs of lymphatic foramina occur: anterior and larger endolymphatic foramina (*ELF*), and the posterior perilymphatic foramina (*PLF*) (Fig. 49).

Basal plate of neurocranium with a pair of internal carotid artery foramina (*ICAF*) located next and below *OFS* (Fig. 49). A large and circular foramen magnum (*FM*) stands out in posterior view of neurocranium in the occipital region; vagus nerve foramen (*X*) lateral to *FM*, and dorsolaterally to these foramina is the lateralis branch of vagus nerve foramen (*LbX*). Ventral to *FM* is the articular surface (*AS*), and lateral to it is a pair of occipital condyles (*OC*) for the articulation with the synarcual cartilage (Fig. 49).

Mandibular arch laterally extended in *P. aiereba*, with long and proximally arched palatoquadrate (*PQ*) and Meckel’s cartilage (*MC*) (Figs. 50, 51); these cartilages are slightly thinner in *P. aiereba* than in the two Orinoco basin species (Figs. 13, 27, 50). Palatoquadrate straight, slightly arched near its proximal portion, and with a small dorsolateral process (*DLP*) near its articulation with Meckel’s cartilage (Figs. 13, 27, 50, 51). Meckel’s cartilage with proximal portion slightly more robust and curved, where it articulates with *PQ* and also with hyomandibular–Meckelian ligament (*L*); *MC* presents a long lateral process (*LP*) which almost reaches dorsal level of *PQ* (Figs. 13, 27, 50, 51), and also a ventrolateral process (*VLP*) on its distal extremity (Fig. 51).

Hyomandibula (*HYO*) rectangular, with its dorsal extremity tapered (Fig. 51). In dorsal view, *HYO* is long, slender and straight in all three species, slightly more robust and curved at its medial part in *P. parvaspina* (Figs. 13, 27, 50). Hyomandibular–Meckelian ligament (*L*) slightly robust despite being reduced, without any type of embedded calcified elements; the ligament possesses a wide connection to *HYO*, with this part of the ligament broad, contacting almost the entire proximal end of the cartilage (Fig. 51).

As in the Orinoco basin species, *P. aiereba* has a synarcual cartilage similar in length to neurocranium and laterally expanded mainly at its posterior portion where it articulates

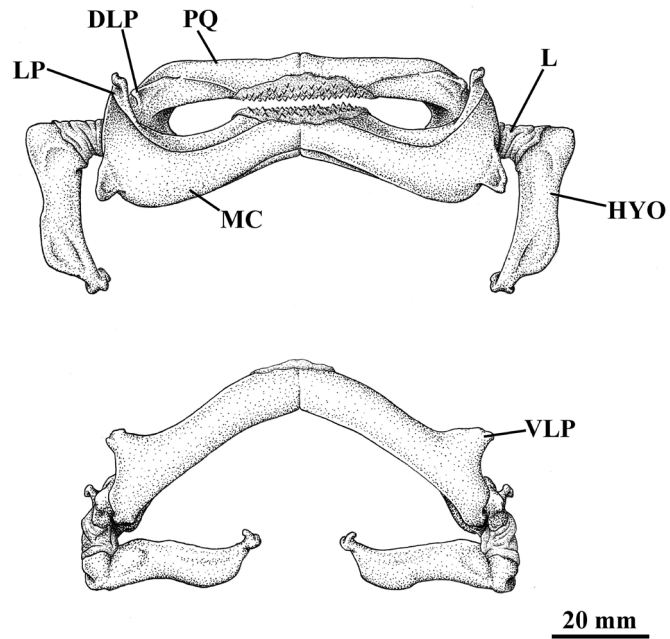


FIGURE 51 | Mandibular and hyoid archs of *Paratrygon aiereba*, MZUSP 103896, in frontal and ventral views (from top to bottom). L = Hyomandibular-Meckelian ligament, VLP = ventrolateral process. Other abbreviations see Fig. 13.

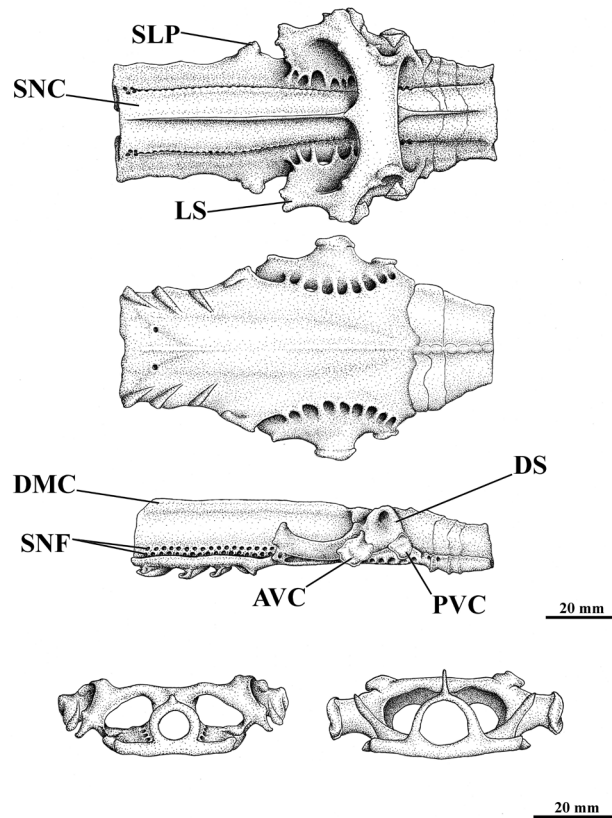


FIGURE 52 | Synarcual cartilage of *Paratrygon aiereba*, MZUSP 103896, in dorsal, ventral, lateral, caudal and frontal views (from top to bottom, and from left to right). SLP = small lateral projection. Other abbreviations see Fig. 14.

with scapulocoracoid (Fig. 52). Dorsomedial crest (*DMC*) low and occurring over the anterior and medial portions of the spinal nerve canal (*SNC*); *SNC* also contains along its total length and next to its basal portion several spinal nerve foramina (*SNF*). Medial portion of synarcual with a small lateral projection (*SLP*) of its lateral basal surface. On posterior region of synarcual, dorsal socket (*DS*) broad, with a deep and concave surface positioned above the two ventral condyles which articulate with scapulocoracoid: a large and convex anterior ventral condyle (*AVC*), and a smaller posterior ventral condyle (*PVC*) are present; as *P. parvaspina*, *AVC* in *P. aiereba* has a convex surface, whereas *P. orinocensis* has a straight *AVC* (Figs. 14, 28, 52). Lateral stay (*LS*) of synarcual cartilage projects anteriorly from its articulation with scapulocoracoid; among the three species, *P. parvaspina* has the longest and most laterally projected *LS* (Figs. 14, 28, 52).

Paratrygon aiereba presents scapulocoracoid with coracoid bar (*CB*) slightly arched at anterior face, and straight posteriorly. Broad scapular process (*SCP*) quadrangular in lateral view and triangular in dorsal view, its articular region with synarcual cartilage extending laterally (Figs. 53, 54). Coracoid bar in *P. orinocensis* more slender than in *P. aiereba*, with curved anterior and posterior faces, whereas *P. parvaspina* has a more broad *CB* with a more straight anterior face than in the other two species (Figs. 15, 29, 53, 54).

Scapular process dorsally with a small dorsolateral crest (*DLC*), more pronounced anterolaterally (Figs. 53, 54); in some specimens of *P. aiereba*, *DLC* exceeds laterally to level of mesocondyle (*MSC*) (Fig. 54). *Paratrygon orinocensis* also has a very pronounced *DLC* exceeding the *MSC* laterally, however, *P. parvaspina* has a short and not so pronounced *DLC* which does not exceed *MSC* (Figs. 15, 29). Laterally in central region

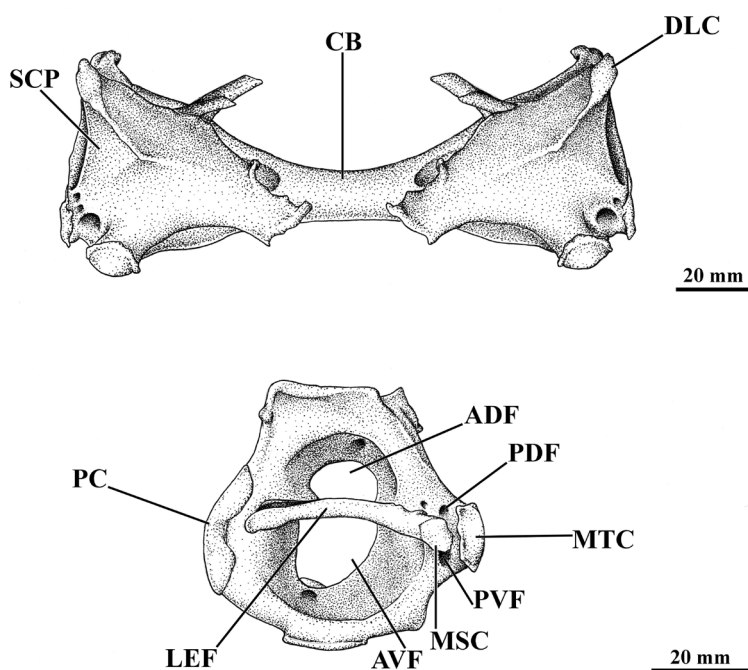


FIGURE 53 | Scapulocoracoid of *Paratrygon aiereba*, MZUSP 103896, in dorsal and ventral views (from top to bottom). ADF = anterodorsal fenestra, AVF = anteroventral fenestra, PDF = postdorsal fenestra, PVF = postventral fenestra, LEF = lateral external face. Other abbreviations see Fig. 15.



FIGURE 54 | Radiograph of scapulocoracoid of *Paratrygon aiereba*, ZSM 34500, upper view. Abbreviations see Fig. 15. Arrow indicates to the anterior portion of specimen.

of SCP, *P. aiereba* has two broad and deep fenestrae separated from one another by the lateral external face (LEF) of SCP: anterodorsal fenestra (ADF) smaller and deeper, and anteroventral fenestra (AVF) very wide, encompassing almost the entire ventral area of the LEF. Posteriorly and separated by MSC are the postdorsal fenestra (PDF) and the postventral fenestra (PVF), both small, but with the PVF slightly larger (Fig. 53).

The condyles that articulate with basal elements of pectoral girdle are positioned on horizontal axis of lateral face of SCP (Figs. 53, 54). On the anterior extremity of SCP is the dorsoventrally elongated procondyle (PC). Procondyle articulates with the anteriormost part of the base of propterygium (PPT), which presents an inverted “L” format (Fig. 54). Between procondyle and mesocondyle is the long LEF of the SCP, which separates the two major fenestrae (ADF and AVF) and where it contacts the posterior and greater part of the PPT base (Fig. 53, 54). Mesocondyle (MSC) anteriorly and next to metacondyle (MTC), both condyles positioned and laterally projected on posterior extremity of horizontal axis of the lateral face of SCP; MSC small and rounded, separates the two small fenestrae (PDF and PVF) and articulating with mesopterygium (MSP); MTC slightly dorsoventrally elongated, situated in the posterior corner of horizontal axis of SCP and articulates with metapterygium (MTP) (Figs. 53, 54). *Paratrygon aiereba* presents the three condyles slightly larger and more pronounced than in the two Orinoco species, whereas *P. parvaspina* has the smallest condyles (Figs. 15, 29, 53, 54).

Paratrygon aiereba possesses three basal elements of pectoral fin, propterygium (PPT), mesopterygium (MSP), and metapterygium (MTP) articulated with their respective condyles of SCP: PPT with the anterior part of its base articulated with PC and its posterior and greater part contacting the LEF surface; MSP articulates only with MSC; and MTP only contacts the MTC (Figs. 54, 55).

Propterygium in *P. aiereba* robust, slightly arched in its anterior portion where it articulates with the antorbital cartilage (ANT), and, as in the other two species, with its posterior extremity broader than anterior (Fig. 55A). Articulation base of PPT with the

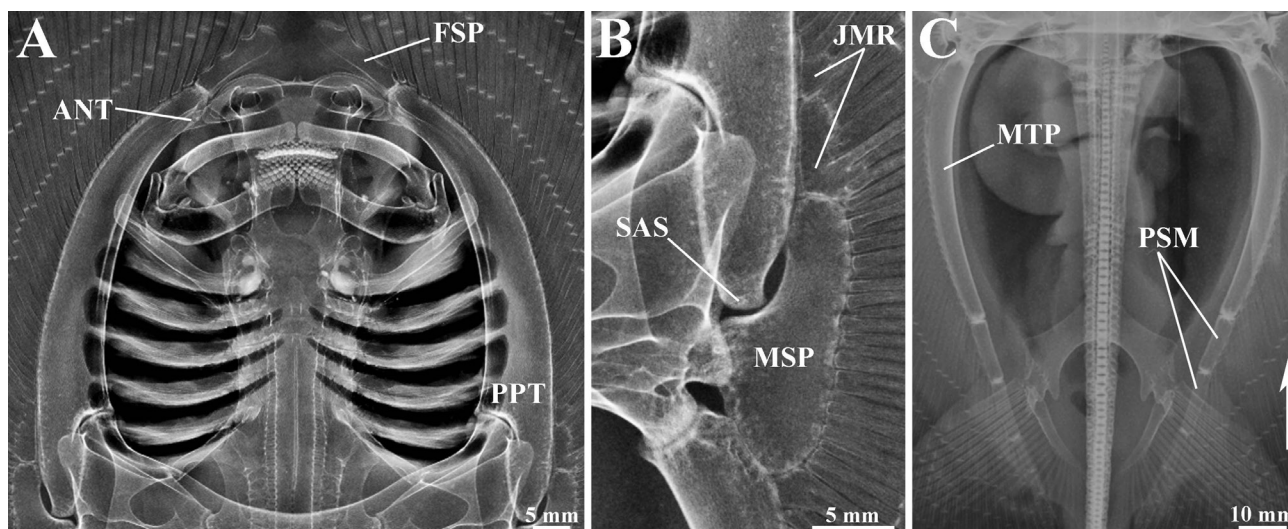


FIGURE 55 | Radiographs of basal elements of pectoral fin of *Paratrygon aiereba*, ZSM 34500, upper views. Abbreviations see Fig. 16. Arrow indicates to the anterior portion of specimen. **A.** Propterygium region. **B.** Mesopterygium region. **C.** Metapterygium region.

scapulocoracoid with an inverted “L” format, with its anterior portion articulated with *PC* and its posterior and greater portion contacting the *LEF* surface of *SCP*. In addition, *PPT* also articulates with mesopterygium through a small articular surface (*SAS*) on its posterior extremity. First segment of propterygium (*FSP*) one-fourth length of *PPT*, extending anteriorly to level of slightly less than half of the anterior portion of nasal capsules, and articulates anteriorly with the first two robust rays of pectoral fin (Fig. 55A).

Propterygium more curved in both Orinoco species than in *P. aiereba*; *P. parvaspina* has the most robust *PPT* among the three species, whereas *P. aiereba* has the anterior portion of *PPT* less tapered and unequal in relation to its posterior portion (Figs. 16, 30, 55). *Paratrygon orinocensis* and *P. aiereba* has its *FSP* contacting externally the nasal capsules (contact surface is larger in *P. orinocensis*), whereas in *P. parvaspina* this contact does not occur. Small articulation surface (*SAS*) of the *PPT* in *P. orinocensis* larger than *P. aiereba* and *P. parvaspina* (Figs. 16, 30, 55).

Mesopterygium in *P. aiereba* slightly shorter or equal to *SCP* at its anteroposterior axis (Fig. 55B). Posterior portion of *MSP* more developed, and with the articulation point with *MSC* at its proximal extremity. Anteriorly and next to this articulation point, *MSP* has a pronounced concavity where it contacts the *SAS* of *PPT*. Anterior portion of *MSP* thinner than posterior portion and slightly wider than half of posterior portion. Anterior and posterior extremities of *MSP* contact respectively *PPT* and *MTP* and junctions of median radials (*JMR*) of pectoral fin. *JMR* located at the anterior extremity of *MSP* larger and more numerous (Fig. 55B).

Concavity of *MSP* more pronounced in *P. aiereba* and *P. orinocensis* than in *P. parvaspina*; *JMR* more numerous in *P. aiereba* than in the two species, and the *JMR* in *P. parvaspina* occurs in the anterior extremity of *MSP* (Figs. 16, 30, 55).

Metapterygium in *P. aiereba* long, arched and slender, with its medial portion between half or little more than half the width of the *PPT*. Anterior part of *MTP* more robust than posterior, being articulated with *MSC* of *SCP* at its anterior extremity,

and contacting *MSP* (Fig. 55C). Posterior portion of *MTP* segmented in three or four posterior segments (*PSM*), being the posterior *PSM* successively smaller than the anterior segments (Fig. 55C).

Paratrygon parvaspina has the most robust *MTP* among the three species, with its anterior part much larger and robust than the other two; *MTP* in *P. parvaspina* also has more unequal extremities than *P. aiereba* and *P. orinocensis*, with its *MTP* more tapered from anterior to posterior portions than the other species (Figs. 16, 30, 55).

Paratrygon aiereba has an arched puboischial bar (*PB*), with its anterior portion straighter, and posterior margin half-circle shaped; some specimens possess a *PB* with an inverted “V” format, with the anterior portion more inclined than other specimens (Figs. 56, 57). Lateral extremities of *PB* possess two ventral processes, each with a dorsal projection, besides three pairs of dorsoventral obturator foramina (*OF*). Iliac process (*IP*) well developed, in rectangular shape, located on external posterior portion of lateral extremity of *PB*, forming the posteriormost extremity of pelvic girdle. The dissected specimen of *P. aiereba* (MZUSP 103896) has a small foramen (*SF*) in the external face of *IP* next to its insertion on *PB* (Fig. 56). Ischial process (*ISP*) small, triangular, located on the internal portion of lateral extremities of *PB*, delineating the half-circle shape of the posterior margin. Lateral prepelvic process (*LPP*) dorsal to lateral extremities of *PB*, small and triangular (Figs. 56, 57). Anterior portion of *PB* stands out the long and very developed prepelvic process (*PPP*) with an equivalent length to the width of *PB* (Fig. 56).

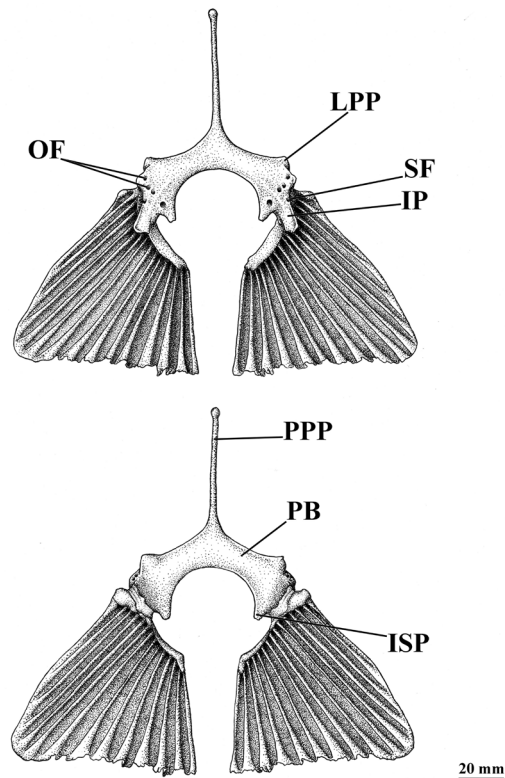


FIGURE 56 | Pelvic girdle and fins of *Paratrygon aiereba*, MZUSP 103896, in dorsal and ventral views (from top to bottom). PPP = prepelvic process, SF = small foramen. Other abbreviations see Fig. 17.

Paratrygon parvaspina possesses less developed *IP*, *ISP* and *LPP* than the other two species, and their tips are more rounded; *IP* much more developed and long in *P. aiereba* than in the other two species (Figs. 17, 31, 56, 57). Clasper skeleton of *P. aiereba* composed of the following elements divided into basal, axial and terminal groups: basal elements - two basal segments or intermediate cartilages, basal 1 (*B1*) and basal 2 (*B2*), and beta cartilage (β); axial elements - axial cartilage (*AX*), dorsal marginal cartilage (*DM*), and ventral marginal cartilage (*VM*); and terminal elements - dorsal terminal 1 (*DT1*), dorsal terminal 2 (*DT2*), and accessory terminal 1 (*AT1*) (Fig. 58).

In dorsal view, β cartilage is the anteriormost skeletal element, its anterior extremity articulated with *B1* and *B2*, its posterior extremity connected with *DM*; β cartilage long and cylindrical, slender and slightly curved. Dorsal marginal posterior to the β cartilage, connecting posteriorly with the *DT2*, with a flat shape, and projecting laterally and externally to central axis of clasper. Dorsal terminal 2 and *AT1* form the distal portion of clasper skeleton; *DT2* with cylindrical shape in dorsal view, its ventral portion more wide and flat; in ventral view *DT2* covers *AT1* (Fig. 58).

In ventral view, the small and cylindrical *B1* and *B2* cartilages contact β cartilage at proximal tip of clasper; *B2* slightly larger than *B1*. *AX* cartilage posterior to *B2*, also cylindrical, but slender and long, and constituting the principal cartilage of axial group; posteriorly *AX* connects with *DT2* and *AT1*. Ventral marginal cartilage articulates almost along its entire length with *AX* and is positioned more externally in relation to central axis of clasper; *VM* wraps around *AX*, its lateral aspect visible in dorsal view. Ventrally, posterior tip of clasper with large *DT1* cartilage, rectangular in shape and covering *DT2* and *AT1*, its lateral extension also visible in dorsal view (Fig. 58).

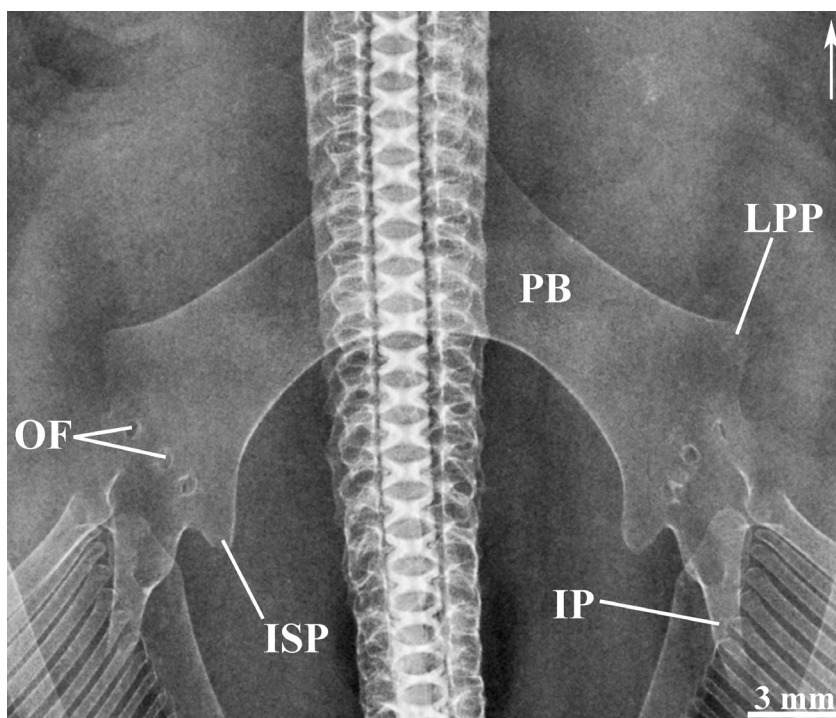


FIGURE 57 | Radiograph of pelvic girdle of *Paratrygon aiereba*, ZSM 34500, upper view. Abbreviations see Fig. 17. Arrow indicates to the anterior portion of specimen.

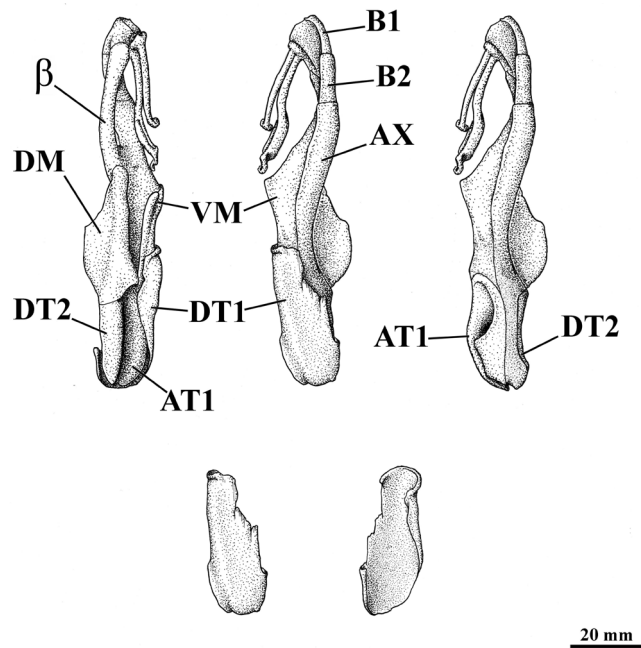


FIGURE 58 | Skeletal elements of right clasper of *Paratrygon aiereba*, MZUSP 103896, in dorsal, ventral, ventral without dorsal terminal 1 (top, left to right), and (below, left to right) dorsal and ventral views of dorsal terminal 1. AT1 = accessory terminal 1, AX = axial cartilage, B1 = basal 1, B2 = basal 2, β = beta cartilage, DM = dorsal marginal cartilage, DT1 = dorsal terminal 1, DT2 = dorsal terminal 2, VM = ventral marginal cartilage.

Geographic distribution. *Paratrygon aiereba* is herein restricted to the Amazon basin, occurring along the central channel of Solimões–Amazonas river, and also through its main affluents in the upper portion of Amazon basin: headwaters of Caqueta, Madeira, Purus, Putumayo and Ucayali rivers; the distribution of this species covers the territories of Bolivia, Brazil, Colombia, Ecuador, and Peru (Fig. 59).

Etymology. *Aiereba* comes from the old Tupi language (a classical indigenous language from Brazil) word *aíereba* that designates a specific type of marine stingray (possibly *Styracura schmardae*; see Ferrão, Soares, 1993, p. 37), which occurs on the coast of northeastern Brazil. This name was first made known during the period of Dutch occupation (1630–1654) when Marcgrav (1648) used it (possibly from the Tapuya nation) to designate this marine stingray species. As an adjective in the same language *aiereba* also means smooth, unmarked, shallow (Navarro, Suassuna, 2013).

Material examined. *Paratrygon aiereba*: **Bolivia**: AMNH 59865, male, 281 mm DW, AMNH 59878, male, 383 mm DW, ZSM 34500, female, 204 mm DW. **Brazil**: IAvH-P 11894, female, 472 mm DW, INPA 1331, female, 255 mm DW, MCZ 297-S, female, 281 mm DW (syntype of *Disceus thayeri* Garman, 1913), MCZ 563-S, female, 303 mm DW (syntype of *Disceus thayeri* Garman, 1913). MCZ 606-S, male, (syntype of *Disceus thayeri*), MNHN A.1019, female, 324 mm DW, MNHN A.1020, male, 299 mm DW, MNHN A.2269, male, 285 mm DW, MNHN A.2270, male, 147 mm DW,

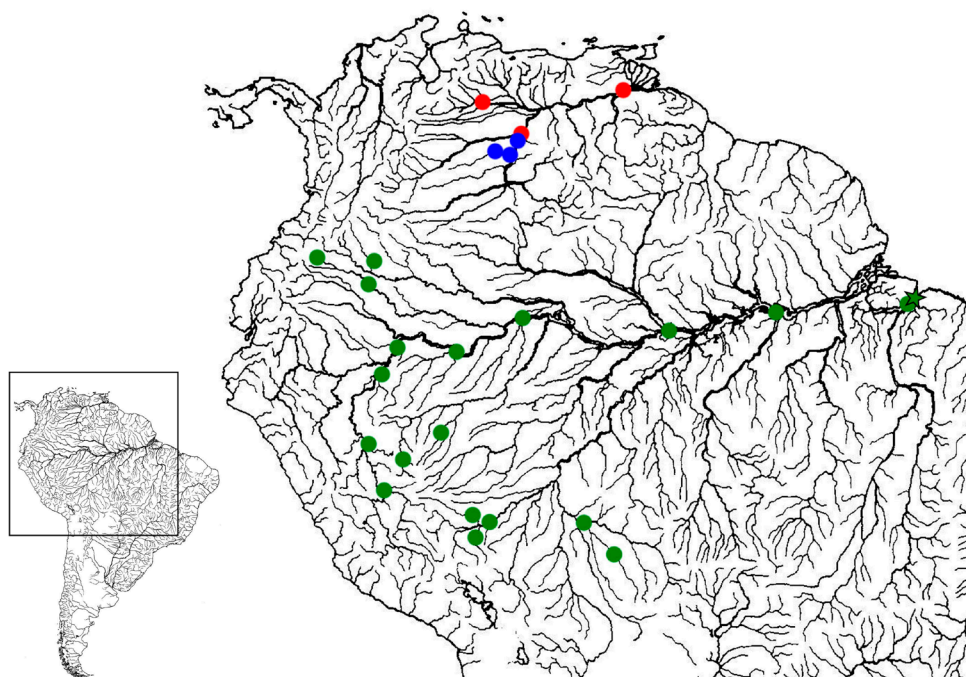


FIGURE 59 | Distribution of the three species of genus *Paratrygon* throughout the Amazon and Orinoco basins. *Paratrygon aiereba* (green) is restricted to Amazon basin, and *Paratrygon orinocensis* (red) and *Paratrygon parvaspina* (blue) are restricted and sympatric in the Orinoco basin. Star = neotype specimen (MZUSP 117155) locality.

MNHN 1997-0495, female, 285 mm DW, MPEG uncatalogued, 6, 3 females and 3 males, 255–786 mm DW, MUSM uncatalogued, male, 220 mm DW, MZUSP 14774, female, 256 mm DW, MZUSP 51680, male, 610 mm DW, MZUSP 101015, female, 150 mm DW, MZUSP 103896, male, 508 mm DW, MZUSP 103907, male, 606 mm DW, MZUSP 104029, male, 436 mm DW, MZUSP 104985, female, 590 mm DW, MZUSP 104986, female, 560 mm DW, MZUSP 104987, male, 568 mm DW, NMW 79194, female, 314 mm DW, UFPB 3478, UFPB 3479. **Colombia:** IAvH-P 11929, male, 366 mm DW, IAvH-P 11937, male, 280 mm DW. **Peru:** IAvH-P 11927, male, 408 mm DW, IIAP uncatalogued, 3, 1 female and 2 males, 194–208 mm DW, MUSM 0002, male, 328 mm DW, MUSM 1389, 2, 1 female and 1 male, 204 – 207 mm DW, MUSM 7352, female, MUSM 9423, male, 428 mm DW, MUSM 47105, male, 214 mm DW, MZUSP 14772, female, 221 mm DW, MZUSP 14773, female, 236 mm DW, MZUSP 117831, female, 200 mm DW, USNM 264005, male, 184 mm DW.

DISCUSSION

The present revision of *Paratrygon* from the Orinoco basin revealed two new species described herein and indicated that the type species of the genus, *P. aiereba*, is geographically restricted to the Amazon basin (Fig. 59). The main morphometric differences between these species, specially among both new sympatric species of

Orinoco basin, are shown in Tab. 7. Furthermore, the available literature did not provide any morphological evidence that *P. aiereba* occurs in rivers of the Orinoco basin.

Recent molecular analyses of potamotrygonids from Colombian and Venezuelan river basins indicated that specimens of *Paratrygon* from the Orinoco and Amazon possess significant differences in three mitochondrial markers: ATPase 6, COI and *Cytb* (see García-Villamil *et al.*, 2013; García-Villamil *et al.*, 2016). Possibly, all specimens of *Paratrygon* from the Orinoco basin analyzed in these studies were of *P. orinocensis*, and the molecular differences pointed out by these authors, therefore, served only to separate this new species from *P. aiereba*. However, Garcia *et al.* (2016, p. 4486) mentioned a *Heliotrygon* specimen clustered and grouped together in their analysis with genus *Paratrygon*, and which “could be an organism that belongs to the new *Paratrygon* species from the Orinoco river”; maybe this specimen could be a *P. parvaspina* one, due to some characters of this species of *Paratrygon* that resembles some of genus *Heliotrygon*, such as the reduction of the following characters: spiracular process, concavity on anterior margin of disc, and caudal sting.

Possibly the first mention of *Paratrygon orinocensis* was made by Fernández-Yépez (1949) as an occurrence of *Disceus thayeri* in Caño Orupe mouth, an affluent of the Orinoco River (at mid basin), near the mouth of the Bitá River. He briefly described an adult female, and the description of its coloration is very similar to the color pattern observed in the specimens analyzed here. Almost 50 years later, Lasso *et al.* (1996) collected about 40 specimens of this new species in the Caño Guaritico sub basin region (an affluent of the Apure River) and identified them as *P. aiereba*. Barbarino, Lasso (2005; 2009) analyzed about 70 specimens captured by fishermen in the lower part of the Apure River, and also possibly Arauca and Payara rivers (both rivers drain in the Orinoco River very close to the Apure River mouth; see Fig. 2 in Barbarino, Lasso, 2005); they also identified these specimens as *P. aiereba*. Specimens of *P. aiereba* described from the delta of the Orinoco River by Lasso *et al.* (2009) possibly were specimens of *P. orinocensis*; indeed Lasso *et al.* (2011) described the occurrence of this species (as *P. aiereba*) in the delta region, and some specimens analyzed (USNM 233944) and here identified as *P. orinocensis* were collected there. Lasso, Sánchez-Duarte (2012) described the occurrence of this species (as *P. aiereba*) in the Arauca, Inírida, Meta and Tomo rivers, all tributaries of the middle

TABLE 7 | Main morphometric differences in proportions of disc width (%DW) between the three species of genus *Paratrygon*; (N) corresponds to the number of specimens analyzed.

	<i>Paratrygon aiereba</i>			<i>Paratrygon orinocensis</i>			<i>Paratrygon parvaspina</i>		
	Mean	Range	N	Mean	Range	N	Mean	Range	N
Spiracle length	6.0	4.4 – 11.6	45	5.6	4.5 – 7.9	26	5.2	4.9 – 5.8	5
Preorbital length	31.2	25.3 – 35.0	45	29.9	26.3 – 32.1	25	32.2	28.8 – 36.2	5
Prenasal length	29.5	27.0 – 32.4	45	27.5	24.7 – 30.3	26	31.5	29.8 – 33.0	5
Preoral length	33.0	30.2 – 36.3	45	30.9	28.1 – 34.0	26	35.0	33.8 – 36.8	5
Distance between cloaca and tail tip	87.8	19.5 – 183.0	42	100.7	26.2 – 189.3	26	50.4	25.1 – 82.5	5
Distance between cloaca and caudal sting	23.5	17.5 – 31.3	41	23.5	17.2 – 36.0	26	21.1	17.3 – 23.1	4
Caudal sting length	11.3	3.0 – 17.9	38	12.0	6.7 – 15.3	22	6.2	5.6 – 7.1	4

portion of the Orinoco River. Muñoz-Osorio, Mejía-Falla (2013) described a pregnant female specimen of *P. aiereba*, which aborted a female embryo, as the first occurrence in the Bitá River (*P. orinocensis*). According to Lasso *et al.* (2013) this species could also occur in the Capanaparo, Caroní, Caura, Cinaruco and Ventuari rivers (Orinoco basin); these authors observed some morphological differences between Orinoco and Amazon basin populations of *P. aiereba* that they analyzed (however, they identified all specimens as *P. aiereba*). García *et al.* (2016) in their molecular analyses of potamotrygonid relationships, sampled some specimens of *Paratrygon* from the Caura River (Guiana Shield; Venezuela); these were identified as *P. aiereba*, but they could possibly be specimens of *P. orinocensis*. Therefore, all authors cited above indicated the occurrence of *P. orinocensis* practically in the same localities of the specimens examined, with just some authors adding tributaries of middle and lower portion of the Orinoco River to the distribution of this new species (Lasso, Sánchez-Duarte, 2012; Lasso *et al.*, 2013).

Biological aspects of *P. orinocensis* were provided by Lasso *et al.* (1996; 2013; 2016), Barbarino, Lasso (2005; 2009), Lasso, Sánchez-Duarte (2012) and Muñoz-Osorio, Mejía-Falla (2013). This new species is one of the largest species of potamotrygonids. Mean disc width of specimens analyzed is 299.8 mm, with the greatest specimen, an adult male (IAvH-P 12449, holotype), reaching 573 mm (Tab. 1); however, Lasso *et al.* (1996) and Barbarino, Lasso (2005) report female specimens with 780 and 1570 mm of disc width. Indeed, these authors show that females reach larger sizes and weights than males (Lasso *et al.*, 1996, Figs. 4–5; Barbarino, Lasso, 2005, Figs. 8–9). *Paratrygon orinocensis* is an essentially piscivorous potamotrygonid, with its diet composed mainly of fishes of the orders Characiformes and Siluriformes, along with shrimps of the genus *Macrobrachium* (Lasso *et al.*, 1996; 2013; Barbarino, Lasso, 2005). Specimens observed in these studies were collected mainly in the main channels of streams and rivers, and also in the temporary beaches that form in the rainy seasons, indicating these areas as regular habitats used by this species (Lasso *et al.*, 1996; 2013; Barbarino, Lasso, 2005; Lasso, Sánchez-Duarte, 2012). Maturity possibly occurs at 450 mm DW for males and at 400 mm DW for females as indicated by our observations and by Lasso *et al.* (1996) and Barbarino, Lasso (2005). Females generally give birth to one or two neonates with approximately 200 mm DW (Lasso *et al.*, 1996; 2013; Muñoz-Osorio, Mejía-Falla, 2013); however, Barbarino, Lasso (2005, Tab. 2) reported on female specimens that aborted four to eight fetuses.

Finally, the molecular studies of García-Villamil *et al.* (2013) and García-Villamil *et al.* (2016) corroborate our morphological observations (also previously cited by Lasso *et al.*, 2013) on the recognition of distinct species of *Paratrygon* in the Orinoco basin. Little or almost nothing is known about the biology, habits, behavior, and further occurrence of *Paratrygon parvaspina*, which doubtlessly is the least known species of *Paratrygon*. The few literature references on this new species are local checklists of freshwater fishes of Colombia that cited specimen IAvH-P 4684 (Maldonado-Ocampo *et al.*, 2006; 2008; Mejía-Falla *et al.*, 2007; Lasso, Sánchez-Duarte, 2012). Specimens of *P. parvaspina* are very rare in fish collections that contain potamotrygonids (TSL, pers. obs.), and supposedly this new species can be difficult to be captured in the field which could explain the gap of biological information in the literature and paucity of specimens in collections. Despite being easily distinguishable from the other two species of *Paratrygon* (see diagnosis), further information about its biology (habitat, reproduction, feeding

behavior) is necessary to evaluate its conservation status. It is important to note that the conservation status of *P. aiereba* should also be revised due to the change in its geographic occurrence with the description of the two new species in the Orinoco basin.

The first authors who mentioned the possible loss of the original type specimen of *Paratrygon aiereba* were Castex, Castello (1969, p. 16): “*The type specimen which founded the systematical valid description of Trygon aiereba has not yet been found; [...] currently the collection of Müller y Henle has been distributed in different european Museums after the Second World War.*”. Rosa (1985a; 1991) revised the taxonomic history of *P. aiereba* and concluded that the holotype, originally deposited in the Zoologische Staatssammlung München (ZSM, Bavarian State Collection of Zoology), was lost, probably destroyed in Munich during World War II. Rosa (1985a; 1991) and Carvalho *et al.* (2003) also analyzed the type-specimens of *Trygon stroglyopterus* Jardine, 1843 (ZMB 4632) and *Disceus thayeri* Garman, 1913 (MCZ 297-S and MCZ 563-S) and concluded that *P. aiereba* was the senior synonym of *T. stroglyopterus* and *D. thayeri* (through comparison of the type-specimens of these species with the original description of *P. aiereba* made by Müller, Henle, 1841).

Carvalho *et al.* (2003) maintained the taxonomic resolution of Rosa (1985a; 1991) and also included MCZ 606-S as a type-specimen of *D. thayeri*. Neumann (2006; 2011), who revised the catalog of type specimens of fishes from the ZSM collection, did not mention any information about the deposition of the type-specimen of *P. aiereba* described by Müller, Henle (1841). During the personal visits of the first and last authors (TSL, MRC) to the collections in Berlin (Museum für Naturkunde) and Munich (ZSM) in 1996 and 2014, no documents were found regarding the deposition of the original type-specimen of *P. aiereba* (Loboda, 2016), agreeing with the observations made by the previous authors.

In the absence of an existing type specimen, the main diagnostic characters of *P. aiereba* have to be understood from the original account of Müller, Henle (1841), who provided the following diagnostic characters based on the holotype: disc oval, without lateral and anterior angulations, tail long (two times the disc length) and slender with a caudal sting at its anterior one-fifth, mouth wide without oral papillae, relatively great distance between head and anterior margin of disc, eyes very small, teeth flat and distributed in few rows, knob-shaped spiracular process developed and present in posterior portion of spiracles, dermal denticles over the disc, brown dorsal disc coloration, and whitish ventral coloration with dark margins (Müller, Henle, 1841, p.196). Although some of these characters can be attributed to the genus *Paratrygon*, two characters can be interpreted as diagnostic to *P. aiereba*: the brown dorsal coloration, and the knob-shaped developed spiracular processes. *Paratrygon orinocensis* and *P. parvaspina* have, respectively, gray and beige-yellowish predominant dorsal colorations, and both of these new species do not possess spiracular processes as developed and knob-shaped as in *P. aiereba* (especially *P. parvaspina* whose process is very reduced). Besides the characters of the holotype, one very important information provided in the original description was the type locality: Brazil. *Paratrygon orinocensis* and *P. parvaspina* do not occur in Brazil being restricted to the Orinoco basin. Information provided in previous studies of *Paratrygon* populations (Garcia *et al.*, 2016; Loboda, 2016) corroborate that *P. aiereba* is restricted to the Amazon basin, and that *P. orinocensis* (“*Paratrygon* sp.” of Garcia *et al.*, 2016 and “*Paratrygon* sp.1” of Loboda, 2016) and *P. parvaspina* (“*Paratrygon* sp.2” of Loboda, 2016) are restricted to

the Orinoco basin. The extremely long tail described from the holotype indicates that it was a small juvenile specimen with an intact tail. According to Rosa (1991, p. 434, Tab. 1) the disc width of the type specimen described by Müller, Henle (1841) was 196 mm (converting 1 German Zoll, used by the authors, to 26.15 mm).

There is a high probability that the original type-specimen of *P. aiereba* described by Müller, Henle (1841) had been collected by the naturalists Johann Spix and Carl von Martius during their four-year journey in Brazil (1817–1820) (L. F. Silveira, 2016, MZUSP, pers. comm.), wherein thousands of specimens of animals and plants were collected and sent directly to Munich. Müller, Henle (1841) described *P. aiereba* from just one specimen deposited in the Zoological Museum of Munich (“*Ein Exemplar im zoologischen Museum zu München*”) and did not mention the collectors or a specific collection date of this specimen. In their foreword, the authors cited that they visited Munich in the autumn of 1840, when J. Spix was already dead. While still alive, J. Spix published volumes on his zoological collections made in his journey with von Martius in Brazil, but these volumes were mainly about new species of birds and reptiles. When he passed away in 1826, he had not finalized his work on fishes, but Louis Agassiz published this work, “*Selecta genera et species piscium Brasiliensium*”, in two fascicles in 1829 and 1831 with a post-mortem authorship dedicated to Spix written by von Martius (Kottelat, 1988). These volumes have just one mention of “*Aiereba*”, and that is in the foreword written by von Martius where he references (by their native names) the diversity of some marine stingrays found in the Brazilian coast: “*etiam Rajarum species plures (Nari-Nari, Aiereba, Jabubira, Jabebireté etc.) occurrunt.*” (Very many species of rays also [Nari-Nari, Aiereba, Jabubira, Jabebireté etc.] occur.) (Spix, Agassiz, 1829–1831, p. II). However, these species are not present in the catalog.

The absence of “*Aiereba*” in Spix and Agassiz’s book on Brazilian fishes does not necessarily indicate that the specimen described by Müller, Henle (1841) was not collected during Spix and von Martius’ expedition. Von Martius also cited in the foreword of Spix, Agassiz (1829–1831, p. VIII): “*nec ex Rajis desunt species nonnullae, aquas Brasiliae dulces inhabitantes, quae atroci aculeo minentur, praesertim sub Aequatore et in provinciis Rio Negro et Matto Grosso dictis.*” (but there are some species of ray too, inhabiting the fresh waters of Brazil, which are dangerous enough to pose a threat with their savage stings, especially at the equator and in the provinces named Rio Negro and Mato Grosso). Kottelat (1988) cited that Agassiz “*added [a] few other species [of fishes] selected from many not illustrated but present in Spix’s collections*”, and showed a document (AEN 115/2–5; Kottelat, 1988, Fig. 4) “*which is a list of the fishes in the zoological collection in München, hand-written by Agassiz on 22 August 1829*”, which shows some ray specimens labeled as “*spec. nov. bras.*”. Four of these specimens of rays were written by Agassiz as three new species of the genus *Raja* (Kottelat, 1988, Fig. 4), a nominal genus frequently used at the time for many different batoids. Thus, in 1829, there were at least three species of rays unidentified in the Munich collection that were most likely collected by Spix and von Martius during their four-year journey in Brazil, and possibly one of these specimens could be the type-species of *P. aiereba* analyzed and described by Müller, Henle (1841) as *Trygon aiereba*.

Additionally, von Martius also mentions freshwater stingrays, without further details or description, in just two specific parts of the third volume of Spix, Martius’ travel diaries (published in three volumes; Spix, von Martius, 1981). Both are in the second

chapter of the eighth book named “Excursions around Belém do Pará and arrangements to travel to the countryside along the Amazonas river”. One on page 52, where they mention: “Many people in the house occupy themselves almost continually by fishing; among the fishes of the river, they boast especially about the stingrays”. And on page 58: “Sharks frequently occur upstream, and with the stingrays, so abundant, it is very unsafe to bathe in the river. Especially because these fishes have the custom of hiding their flat bodies in the shallow waters and move violently their tail armed with a strong sharp sting against their enemies” (Spix, von Martius, 1981). Furthermore, the areas visited by Spix and von Martius correspond with the distribution solely of *P. aiereba* among *Paratrygon* species, as seen in the map of their travels in the Amazon basin (see Figs. 59–60; also Loboda, 2016).

However, despite all evidence that allow us to attribute the capture of the holotype of *P. aiereba* (described by Müller, Henle, 1841) to Spix and von Martius, the fact is that the holotype was lost: no indication of the type-specimen of *P. aiereba* was found by Rosa (1985a; 1991) and Neumann (2006; 2011) in ZSM archives and collection (also H.-J. Paepke, 2020, pers. comm.). Close to half of Spix’s collection was purchased by the Neuchatel museum, but no stingrays are present there (Kottelat, 1988). And finally, as exposed by Rosa (1991) the remaining collection of Spix’s fishes was destroyed by a British bombing raid during WWII (the collection of fishes, about to be moved, caught fire and was incinerated; Terofal, 1983).

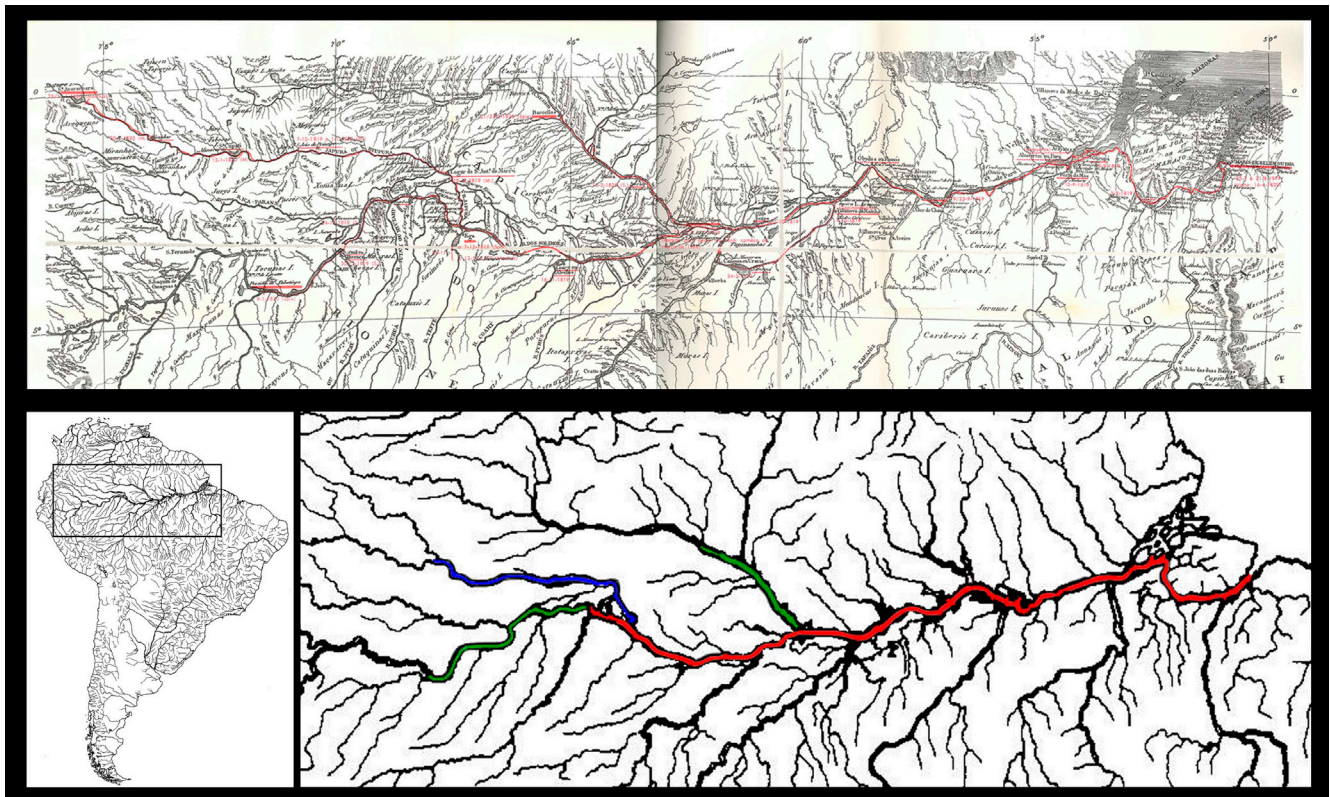


FIGURE 60 | Maps showing the journey of J. Spix and C. von Martius in the Amazon basin (1819–1820). Above, map modified from the original (from Spix, Martius, 1981). Below, a draft map of South America highlighting the routes of both naturalists. Red = route where both naturalists made together. Green = route made by J. Spix. Blue = route made by C. von Martius.

Therefore, with the holotype lost and the evidence mentioned about the original location where Spix and von Martius collected it (Spix, von Martius, 1981, “*Excursions around Belém do Pará*”), here we designate a neotype for *P. aiereba* in accordance to Article 75 of the International Code of Zoological Nomenclature (ICZN, 1999): specimen MZUSP 117155, an adult male (603 mm DW; Fig. 33) collected in the Colares municipality, Pará state, near the capital Belém (Fig. 59). The qualifying conditions (Article 75.3) of this designation are in agreement with those laid out in the code. In relation to paragraphs 75.3.1, and 75.3.6 (for the “*purpose of clarifying the taxonomic status or the type-locality*” and “*evidence that the neotype came as nearby as practicable from the original type-locality*”, as mentioned above, Spix and von Martius probably collected the holotype of *P. aiereba* near Belém, being the Guamá Bay of that area perhaps the location itself or at least very plausibly close to where the holotype was collected; the neotype (MZUSP 117155) was collected in the municipality of Colares which is exactly from the Guamá Bay, a few kilometers north of Belém (Figs. 59–60). In relation to paragraphs 75.3.2 and 75.3.5 (“*a statement of characters [...] [or] a bibliographic reference to such a statement*”, and “*evidence that the neotype is consistent with the former name-bearing type*”, characters cited in the original description (Müller, Henle, 1841, p. 196) such as the knob-shaped spiracular process and the brown dorsal tone are consistent with differences between the neotype of *P. aiereba* and the two new species of the Orinoco basin. Furthermore, in relation to paragraph 75.3.3 (“*data and description sufficient to ensure recognition of the specimen designated*”, the neotype has the following characters attributed to *P. aiereba*, spiracles great and quadrangular with large knob-shaped processes, an evident pair of large, dark spots on the preorbital region of the disc, and two or three high and broad based dorsal thorn rows on tail. Concerning paragraph 75.3.4 (“*reasons for believing the name-bearing type-specimen were lost or destroyed*”), all of the reasons exposed by Castex, Castello (1969) and Rosa (1991), and complemented by Terofal (1983), Kottelat (1988), and Neumann (2006, 2011), about the bombing raid during WWII, and by our own observations during visits to the relevant collections of Munich and Berlin, corroborate that the holotype has indeed been destroyed.

The exclusion of *Trygon stroglyopterus* Jardine, 1843 from the synonym list of *P. aiereba* is due to the conclusions of Loboda (2016), who analyzed the type specimen, ZMB 4632, and found some morphological similarities between it and a group of specimens (“*Paratrygon* sp. 3” of Loboda, 2016) collected in Uraricoera river, Roraima state, Brazil (the region of the type-locality of ZMB 4632). These specimens present differences in some morphological characters (dorsal coloration, dermal denticles and some skeletal components) with *P. aiereba*, *P. orinocensis* and *P. parvaspina* (Loboda, 2016), and a more detailed study is being concluded (TSL, work in progress).

ACKNOWLEDGMENTS

We are grateful to Carlos Montaña and Claudia Alejandra Medina Uribe (IAvH), Jose Ivan Mojica (UNC), Aléssio Datovo, Mário de Pinna, Osvaldo Oyakawa and Michel Gianeti (MZUSP), Fernando Marques (IBUSP), Jeff Williams, Jeffrey Clayton, Kris Murphy and Sandra Raredon (Smithsonian Institute), Karsten Hartel (MCZ-Harvard University), H.-J. Paepke and Peter Bartsch (ZMB), and Dirk Neumann (ZSM) for

assistance and help during the visits of TSL and MRC to their respective institutions. Mónica A. Morales-Betancourt (IAvH), Rodamir Unda, Fernando Trujillo, Beiker Castañeda, Lilia Java and Aldo Curico (Fundación Omacha) for the assistance and help during the field work of C. A. Lasso. Alejandra Goynechea (Defenders of Wildlife), F. Trujillo (Fundación OMacha) and the Instituto Alexander von Humboldt for financial support to C. A. Lasso. Special thanks to Sandra Raredon (Smithsonian Institute), Hugo Idalgo and Reginaldo Barboza Silva (Hospital Veterinário - FMVZ-USP) for their contributions making the digital X-Ray images of some specimens, and also Ênio Mattos and Phillip Lenktaitis in generating SEM images of dermal denticles. We are very grateful to Paulo Presti (MZUSP) for the illustrations of the skeletal components of *P. aiereba*. For taxonomic discussions and contributions we are also grateful to Luis Fabio Silveira (MZUSP) and João Paulo Capretz Batista da Silva (UFPB). We also thank the considerations made by the reviewers and editors. Finally, this work was only possible due to the financial support provided by FAPESP (Fundação de Amparo à Pesquisa do Estado de São Paulo) through grants 2011/23420-0 and 2014/03277-6 to TSL, and the research fellowship from CNPq (Conselho Nacional de Ciencia e Tecnologia) 305271/2015-6 to MRC.

REFERENCES

- **Araújo MLG.** Dinâmica de População e Conservação de *Paratrygon aiereba* (Chondrichthyes-Potamotrygonidae) no Médio Rio Negro, Amazonas. [PhD Thesis]. Manaus: Universidade Federal do Amazonas; 2011.
- **Bailey RM.** Comment on the proposed suppression of *Elipesurus spinicauda* Schomburgk (Pisces). Z.N.(S.) 1825. Bull Zool Nomencl. 1969; 25:133-34.
- **Barbarino A, Lasso CA.** Pesquería y aspectos biológicos de la raya manta *Paratrygon aiereba* (Müller y Henle, 1841) (Myliobatiformes: Potamotrygonidae), en el río Apure (Venezuela). Mem Soc Cienc La Salle. 2005; 163:93-108.
- **Barbarino A, Lasso CA.** La pesca comercial de la raya manta *Paratrygon aiereba* (Müller & Henle, 1841) (Myliobatiformes, Potamotrygonidae), en el Río Apure (Venezuela). Acta Apuroquia. 2009; 1(1):24-31.
- **Bigelow HB, Schroeder WC.** Fishes of the western North Atlantic, part two: Sawfishes, Guitarfishes, Skates and Rays. New Haven: Memoirs Seals Foundation for Marine Research; 1953.
- **Carvalho MR.** *Potamotrygon rex*, a new species of Neotropical freshwater stingray (Chondrichthyes: Potamotrygonidae) from the middle and upper Rio Tocantins, Brazil, closely allied to *Potamotrygon henlei* (Castelnau, 1855). Zootaxa. 2016a; 4150(5):537-65. <https://doi.org/10.11646/zootaxa.4150.5.2>
- **Carvalho MR.** Description of two extraordinary new species of freshwater stingrays of the genus *Potamotrygon* endemic to the Rio Tapajós basin, Brazil (Chondrichthyes: Potamotrygonidae), with notes on other Tapajós stingrays. Zootaxa. 2016b; 4167(1):1-63. <https://doi.org/10.11646/zootaxa.4167.1.1>
- **Carvalho MR.** Neotropical stingrays: Family Potamotrygonidae. In: Last PR, White WT, Carvalho MR, Séret B, Stehmann MFW, Naylor GJP, editors. Rays of the World. Ithaca: Cornell University Press; 2016c. p.619-55.
- **Carvalho MR, Lovejoy NR.** Morphology and phylogenetic relationships of a remarkable new genus and two new species of Neotropical freshwater stingrays from the Amazon basin (Chondrichthyes: Potamotrygonidae). Zootaxa. 2011; 2776:13-48.

- **Carvalho MR, Ragno MP.** An unusual, dwarf new species of Neotropical freshwater stingray, *Plesiotrygon nana* sp. nov., from the upper and mid Amazon Basin: the second species of *Plesiotrygon* (Chondrichthyes: Potamotrygonidae). *Pap Avulsos Zool.* 2011; 51(7):101-38. <http://dx.doi.org/10.1590/S0031-10492011000700001>
- **Carvalho MR, Lovejoy NR, Rosa RS.** Family Potamotrygonidae (river stingrays). In: Reis RE, Kullander SO, Ferraris C, Jr., editors. Checklist of the Freshwater Fishes of South and Central America. Porto Alegre: Edipucrs; 2003. p.22-29.
- **Carvalho MR, Maisey JG, Grande L.** Freshwater stingrays of the Green River Formation of Wyoming (Early Eocene), with the description of a new genus and species and an analysis of its phylogenetic relationships (Chondrichthyes: Myliobatiformes). *Bull Am Mus Nat Hist.* 2004; 284:1-136. [https://doi.org/10.1206/0003-0090\(2004\)284%3C0001:F SOTGR%3E2.0.CO;2](https://doi.org/10.1206/0003-0090(2004)284%3C0001:F SOTGR%3E2.0.CO;2)
- **Carvalho MR, Sabaj-Perez MH, Lovejoy NR.** *Potamotrygon tigrina*, a new species of freshwater stingray from the upper Amazon Basin, closely related to *Potamotrygon schroederi* Fernández-Yepéz, 1958 (Chondrichthyes: Potamotrygonidae). *Zootaxa.* 2011; 2827:1-30.
- **Carvalho MR, Loboda TS, Silva JPCB.** A new subfamily, Styraacuninae and new genus, *Styraacura*, for *Himantura schmardae* (Werner, 1904) and *Himantura pacifica* (Beebe & Tee-Van, 1941) (Chondrichthyes: Myliobatiformes). *Zootaxa.* 2016; 4175:201-21. <http://doi.org/10.11646/zootaxa.4175.3.1>
- **Castex MN, Castello HP.** Nuevas sinonimias para el género monotípico *Disceus* Garman 1877 (Potamotrygonidae) y observaciones sistemáticas a la familia Paratrygonidae Fowler 1948 (dubit.). *Acta Sci Inst Latinoamer Fisiol Reprod.* 1969; 7:1-43.
- **Castex MN, Castello HP.** Nuevas sinonimias para el género monotípico *Disceus* Garman, 1877 (Potamotrygonidae) y observaciones sistemáticas a la familia Paratrygonidae Fowler, 1948 (dubit.). *Acta Sci. Inst. Latinoamer. Fisiol. Reprod.* 1969; 7:1-43.
- **Compagno LJV.** Phyletic relationships of living sharks and rays. *Am Zool.* 1977; 17(2):303-22. <https://doi.org/10.1093/icb/17.2.303>
- **Compagno LJV.** Endoskeleton. In: Hamlett WC, editor. *Sharks, Skates and Rays: The Biology of Elasmobranch Fishes.* Baltimore: The John Hopkins University Press; 1999. p.69-92.
- **Compagno LJV, Cook SF.** The exploitation and conservation of freshwater elasmobranchs: status of taxa and prospects for the future. *J Aquaricult Aquat Sci.* 1995; 7:62-90.
- **Deynat PP, Séret B.** Le revêtement cutané des raies (Chondrichthyes, Elasmobranchii, Batoidea). I - Morphologie et arrangement des denticules cutanés. *Ann Sci Nat, Zool Biol Anim.* 1996; 17:65-83.
- **Dingerkus GJ, Uhler LD.** Enzymes clearing of alcian blue stained whole small vertebrae for demonstration of cartilage. *Stain Technol.* 1977; 52(4):229-32. <https://doi.org/10.3109/10520297709116780>
- **Duméril AHA.** Histoire naturelle des poissons ou ichthyologie générale. Tome Premier. I. Elasmobranchés. Plagiostomes et Holocéphales ou Chimères. Paris: Librairie Encyclopédique de Roret; 1865.
- **Eigenmann CH.** The freshwater fishes of British Guiana, including a study of the ecological grouping of species and the relation of the fauna of the plateau to that of the lowlands. *Mem Carnegie Mus.* 1912; 5(1):1-578. <https://doi.org/10.5962/bhl.part.14515>
- **Fernández-Yépez A.** *Disceus thayeri* Garman en Venezuela. *Ibidem.* 1949; 7:1-2.
- **Ferrão C, Soares JPM.** *Theatrum rerum naturalium brasiliae, Brasil-Holandês, Dutch-Brazil.* Rio de Janeiro: Editora Index; 1993.
- **Fontenelle JP, Carvalho MR.** Systematic implications of brain morphology in Potamotrygonidae (Chondrichthyes: Myliobatiformes). *J Morphol.* 2016; 277(2):252-63. <https://doi.org/10.1002/jmor.20493>
- **Fontenelle JP, Carvalho MR.** Systematic revision of the *Potamotrygon scobina* Garman, 1913 species-complex (Chondrichthyes: Myliobatiformes: Potamotrygonidae), with the description of three new freshwater stingrays species from Brazil and comments of their distribution and biogeography. *Zootaxa.* 2017; 4310(1):1-63. <https://doi.org/10.11646/zootaxa.4310.1.1>

- **Fontenelle JP, Silva JPCB, Carvalho MR.** *Potamotrygon limai*, sp. nov., a new species of freshwater stingray from the upper Madeira River system, Amazon Basin (Chondrichthyes: Potamotrygonidae). *Zootaxa*. 2014; 3765(3):249-68. <http://dx.doi.org/10.11646/zootaxa.3765.3.2>
- **Fowler HW.** Os peixes de água doce do Brasil. Vol I. Arq Zool, São Paulo. 1951; 6(I-XII):405-625.
- **Frederico RG, Farias IP, Araújo MLG, Charvet-Almeida P, Alves-Gomes JA.** Phylogeography and conservation genetics of the Amazonian freshwater stingray *Paratrygon aiereba* Müller & Henle, 1841 (Chondrichthyes: Potamotrygonidae). *Neotrop Ichthyol*. 2012; 10(1):71-80. <https://doi.org/10.1590/S1679-62252012000100007>
- **García DA, Lasso CA, Morales M, Caballero SJ.** Molecular systematics of the freshwater stingrays (Myliobatiformes: Potamotrygonidae) of the Amazon, Orinoco, Magdalena, Esequibo, Caribbean, and Maracaibo basins (Colombia - Venezuela): evidence of three mitochondrial genes. *Mitochondrial DNA Part A*. 2016; 27(6):4479-91. <http://dx.doi.org/10.3109/19401736.2015.1101536>
- **García-Villamil DA, Lasso CA, Caballero SJ.** Aproximación a la filogenia molecular de la familia Potamotrygonidae en Colombia y Venezuela: aplicaciones en sistemática y conservación. In: Lasso CA, Rosa RS, Sánchez-Duarte P, Morales-Betancourt MA, Agudelo-Córdoba E, editors. IX Rayas de agua dulce (Potamotrygonidae) de Suramérica, Parte I. Colombia, Venezuela, Ecuador, Perú, Brasil, Guyana, Surinam y Guayana Francesa: diversidad, bioecología, uso y conservación. Bogotá: Serie Editorial Recursos Hidrobiológicos y Pesqueros Continentales de Colombia, Instituto de Investigación de Recursos Biológicos Alexander von Humboldt (IAvH); 2013. p.283-95.
- **Garman S.** On the pelvis and external sexual organs of selachians, with special references to the new genera *Potamotrygon* and *Disceus* (with descriptions). *Proc Bos Soc Nat Hist*. 1877; 19:197-215.
- **Garman S.** On the lateral canal system of the Selachia and Holocephala. *Bull Mus Comp Zool*. 1888; 6(11):167-72.
- **Garman S.** The Plagiostoma. *Memoirs of the Museum of Comparative Zoology*. Cambridge: Harvard College; 1913.
- **Günther A.** Catalogue of the fishes in the British museum. London: Printed by order of the trustees; 1870.
- **International Commission on Zoological Nomenclature (ICZN).** International code of zoological nomenclature. 4th ed. London: International trust for zoological nomenclature Natural History Museum [Internet]. London; 1999. Available from: <https://www.iczn.org/the-code/the-international-code-of-zoological-nomenclature/>
- **Jordan DS.** A preliminary list of fishes of West Indies. *Proc US Natl Mus*. 1887; 9:554-608.
- **Kottelat M.** Authorship, dates of publication, status and types of Spix and Agassiz's Brazilian fishes. *Spixana*. 1988; 11(1):69-93.
- **Lasso CA, Agudelo Córdoba E, Jiménez-Segura LF, Ramírez-Gil H, Morales-Betancourt M, Ajiaco-Martínez RE et al.** Catálogo de los recursos pesqueros continentales de Colombia. Bogotá: Serie Editorial Recursos Hidrobiológicos y Pesqueros Continentales de Colombia, Insitudo de Investigación de Recursos Biológicos Alexander von Humboldt; 2011.
- **Lasso CA, Morales-Betancourt MA, Castañeda B, Ortíz-A L, Sierra-Quintero MT.** Aspectos sobre la historia natural de las rayas de agua dulce (Potamotrygonidae) en el área de influencia de los municipios de Puerto Carreño (Vichada) e Inírica (Guainía), Orinoquia colombiana. In: Lasso CA, Rosa R, Morales-Betancourt MA, Garrone-Neto D, Carvalho M, editors. XV. Rayas de agua dulce de Suramérica, Parte II. Colombia, Brasil, Perú, Bolivia, Paraguay, Uruguay y Argentina. Bogotá: Serie Editorial Recursos Hidrobiológicos y Pesqueros Continentales de Colombia, Insitudo de Investigación de Recursos Biológicos Alexander von Humboldt; 2016. p.325-60.
- **Lasso CA, Rial AB, Lasso-Alcalá O.** Notes on the biology of the freshwater stingrays *Paratrygon aiereba* (Müller & Henle, 1841) and *Potamotrygon orbigny* (Castelnau, 1855) (Chondrichthyes: Potamotrygonidae) in the Venezuelan llanos. *Aqua*. 1996; 2(3):39-52.

- **Lasso CA, Rosa R, Morales-Betancourt MA, Garrone-Neto D, Carvalho MR, editors.** XV. Rayas de água dulce de Suramérica. Parte II. Colombia, Brasil, Perú, Bolivia, Paraguay, Uruguay y Argentina. Bogotá: Serie Editorial Recursos Hidrobiológicos y Pesqueros Continentales de Colombia, Instituto de Investigación de Recursos Biológicos Alexander von Humboldt; 2016.
- **Lasso CA, Rosa RS, Sánchez-Duarte P, Morales-Betancourt MA, Agudelo-Córdoba E, editors.** IX Rayas de água dulce de Suramérica, Parte I, Colombia, Venezuela, Ecuador, Perú, Brasil, Guyana, Surinam y Guayana Francesa: diversidad, bioecología, uso y conservación. Bogotá: Serie Editorial Recursos Hidrobiológicos y Pesqueros Continentales de Colombia, Instituto de Investigación de Recursos Biológicos Alexander von Humboldt; 2013.
- **Lasso CA, Sánchez-Duarte P.** *Paratrygon aiereba*. In: Mojica JI, Usma JS, Álvarez-León R, Lasso CA, editors. Libro rojo de peces dulciacuícolas de Colombia. Bogotá: Instituto de Investigación de Recursos Biológicos Alexander von Humboldt; 2012. p.132–34.
- **Lasso CA, Sánchez-Duarte P, Lasso-Alcalá OM, Martín R, Samudio H, González-Oropeza K et al.** Lista de los peces del delta del río Orinoco, Venezuela. *Biota Colomb.* 2009; 10(1-2):123–48.
- **Loboda TS.** Revisão taxonômica e morfológica do gênero *Paratrygon* Duméril, 1865 (Chondrichthyes: Myliobatiformes: Potamotrygonidae). [PhD Thesis]. São Paulo: Universidade de São Paulo; 2016.
- **Loboda TS, Carvalho MR.** Systematic revision of the *Potamotrygon motoro* (Müller & Henle, 1841) species complex in the Paraná-Paraguay basin, with description of two new ocellated species (Chondrichthyes: Myliobatiformes: Potamotrygonidae). *Neotrop Ichthyol.* 2013; 11(4):693–737. <https://doi.org/10.1590/S1679-62252013000400001>
- **Lovejoy NR.** Systematics of myliobatoid elasmobranchs: with emphasis on the phylogeny and historical biogeography of neotropical freshwater stingrays (Potamotrygonidae: Rajiformes). *Zool J Linn Soc.* 1996; 117(3):207–57. <https://doi.org/10.1111/j.1096-3642.1996.tb02189.x>
- **Maldonado-Ocampo JA, Lugo M, Bogotá-Gregory JD, Lasso CA, Vásquez L, Usma JS et al.** Peces del río Tomo, cuenca del Orinoco, Colombia. *Biota Colomb.* 2006; 7(1):113–28.
- **Maldonado-Ocampo JA, Vari R, Usma JS.** Checklist of Freshwater Fishes of Colombia. *Biota Colomb.* 2008; 9(2):143–237.
- **Marcgrav G.** *Historiae Rerum Naturalium Brasiliae.* Livro VI. Leiden: Elsevier; 1648.
- **Mejía-Falla PA, Navia AF, Mejía-Ladino LM, Acero PA, Rubio EA.** Tiburones y rayas de Colombia (Pisces Elasmobranchii): lista actualizada, revisada y comentada. *Bol Invest Mar Cost.* 2007; 36:111–49. <https://doi.org/10.25268/bimc.invemar.2007.36.0.203>
- **Miranda Ribeiro A.** Fauna Brasiliense, Peixes 2 (Desmobrânquios). *Archos Mus Nac Rio de Janeiro.* 1907; 14:129–217.
- **Mojica JI, Usma JS, Álvarez-León R, Lasso CA, editors.** Libro Rojo de peces dulceacuícolas de Colombia. Bogotá: Instituto de Investigación de Recursos Biológicos Alexander von Humboldt, Instituto de las Ciencias Naturales de la Universidad Nacional de Colombia, WWF Colombia, Universidad de Manizales; 2012.
- **Moreira RA, Loboda TS, Carvalho MR.** Comparative anatomy of the clasper of the subfamily Potamotrygoninae (Chondrichthyes: Myliobatiformes). *J Morphol.* 2018; 279(5):598–608. <https://doi.org/10.1002/jmor.20795>
- **Müller J, Henle FGJ.** *Systematische Beschreibung der Plagiostomen.* Berlin: Verlag von Veit und Comp; 1841.
- **Muñoz-Ososrio LA, Mejía-Falla PA.** Primer registro de la raya manzana, *Paratrygon aiereba* (Müller & Henle, 1841) (Batoidea: Potamotrygonidae) para el río Bitá, Orinoquia, Colombia. *Lat Am J Aquat Res.* 2013; 41(1):189–93.
- **Navarro EA, Suassuna A.** Dicionário tupi antigo: a língua indígena clássica do Brasil: vocabulário português-tupi e dicionário tupi-português, tupinismos no português do Brasil, etimologias de topônimos e antropônimos de origem tupi. São Paulo: Global Editora; 2013.
- **Neumann D.** Type catalogue of the Ichthyological Collection of the Zoologische Staatssammlung München. Part I: Historie type material from the “Old Collection”, destroyed in the night 24/25 April 1944. *Spixiana.* 2006; 29(3):259–85.

- **Neumann D.** Type catalogue of the Ichthyological Collection of the Zoologische Staatssammlung München. Part II: Fish types inventoried after 25 April 1944. *Spixiana*. 2011; 34(2):231–86.
- **Nishida K.** Phylogeny of the suborder Myliobatoidei. *Mem Fac Fish Sci Hokkaido Univ.* 1990; 37(1/2):1–108.
- **Rosa RS.** A systematic revision of the South American freshwater stingrays (Chondrichthyes: Potamotrygonidae). [PhD Thesis]. Williamsburg: College of William and Mary; 1985a.
- **Rosa RS.** Further comment on the nomenclature of the freshwater stingray *Elipesus spinicauda* Schomburgk, 1843 (Chondrichthyes, Potamotrygonidae). *Rev Bras Zool.* 1985b; 3(1):27–31. <http://dx.doi.org/10.1590/S0101-81751985000100003>
- **Rosa RS.** *Paratrygon aiereba* (Müller & Henle, 1841): the senior synonym of the freshwater stingray *Disceus thayeri* Garman, 1913 (Chondrichthyes: Potamotrygonidae). *Rev Bras Zool.* 1991; 7(4): 425–37. <http://dx.doi.org/10.1590/S0101-81751990000400001>
- **Rosa RS, Castelo H, Thorson TB.** *Plesiopygion iwamae*, a new genus and species of neotropical freshwater stingray. *Copeia*. 1987; 1987(2):447–58.
- **Rosa RS, Charvet-Almeida P, Quijada CCD.** Biology of the South American potamotrygonid stingrays. In: Carrier JC, Musick JA, Heithaus MR, editors. *Sharks and their relatives II: biodiversity, adaptive physiology and conservation*. New York: CRC Press; 2010. p.241–81.
- **Sánchez-Duarte P, Lasso CA, Acosta-Santos A, Morales-Betancourt MA, Agudelo-Córdoba E, Bonilla-Castillo CA et al.** *Paratrygon aiereba*. *Cuenca del Amazonas*. En: Lasso CA, Rosa RS, Sánchez-Duarte P, Morales-Betancourt MA, Agudelo-Córdoba E, editors. *IX Rayas de água dulce de Suramérica, Parte I, Colombia, Venezuela, Ecuador, Perú, Brasil, Guyana, Surinam y Guayana Francesa: diversidad, bioecología, uso y conservación*. Bogotá: Serie Editorial Recursos Hidrobiológicos y Pesqueros Continentales de Colombia, Instituto de Investigación de Recursos Biológicos Alexander von Humboldt; 2016. p.151–56.
- **Santos GM, De Mérona B, Juras AA, Jégu M.** Peixes do baixo Rio Tocantins: 20 anos depois da Usina Hidrelétrica de Tucuruí. Brasília: Eletronorte; 2004.
- **Shibuya A, Zuanon J, Araujo MLG, Tanaka S.** Morphology of lateral line canals in Neotropical freshwater stingrays (Chondrichthyes: Potamotrygonidae) from Negro River, Brazilian Amazon. *Neotrop Ichthyol.* 2010; 8(4):867–76. <https://doi.org/10.1590/S1679-62252010000400017>
- **Silva JPCB.** Phylogeny of the major groups of Chondrichthyes based on the comparative anatomy of the skeleton of the paired fins and girdles. [PhD Thesis]. São Paulo: Universidade de São Paulo; 2014.
- **Silva JPCB, Carvalho MR.** A new species of Neotropical freshwater stingray of the genus *Potamotrygon* Garman, 1877 from the Río Madre de Dios, Peru (Chondrichthyes: Potamotrygonidae). *Pap Avulsos Zoo.* 2011; 51(8):139–54. <https://doi.org/10.1590/S0031-10492011000800001>
- **Silva JPCB, Loboda TS.** *Potamotrygon marquesi*, a new species of neotropical freshwater stingray (Potamotrygonidae) from the Brazilian Amazon Basin. *J Fish Biol.* 2019; 95(2):594–612. <https://doi.org/10.1111/jfb.14050>
- **Spix JB, von Martius CP.** Viagem pelo Brasil: 1817–1820. São Paulo: Edusp; 1981.
- **Spix JB, Agassiz L.** *Selecta genera et species piscium quos in itinere per Brasiliam annis MDCCCXVII - MDCCCXX.* Monaco: Typis C. Wolf; 1829–1831.
- **Stehmann MFW.** Batoid Fishes. In: Fischer W, editor. *FAO species Identification Sheets for Fisheries Purposes, Western Central Atlantic, fishing area*. Rome: FAO, United Nations; 1978.
- **Taniuchi T, Ishihara H.** Anatomical comparison of clasper of freshwater stingrays (Dasyatidae and Potamotrygonidae). *Gyoruigaku Zasshi.* 1990; 37(1):10–16. <https://doi.org/10.11369/jji1950.37.10>
- **Terofal F.** *Fischausbeute der Brasilien-Expedition 1817–1820 von J. B. v. Spix und C. F. Ph. v. Martius.* *Spixiana.* 1983; 9:313–17.
- **Thorson TB, Woorton RM, Georgi TA.** Rectal gland of freshwater stingrays, *Potamotrygon* spp. (Chondrichthyes: Potamotrygonidae). *Biol Bull.* 1978; 154(3):508–16. <https://doi.org/10.2307/1541076>

AUTHOR'S CONTRIBUTION 

Thiago Silva Loboda: Conceptualization, Data curation, Formal analysis, Funding acquisition, Investigation, Methodology, Project administration, Resources, Software, Supervision, Validation, Visualization, Writing–original draft, Writing–review and editing.

Carlos Andrés Lasso: Conceptualization, Data curation, Formal analysis, Funding acquisition, Investigation, Methodology, Project administration, Resources, Software, Supervision, Validation, Visualization, Writing–original draft, Writing–review and editing.

Ricardo de Souza Rosa: Conceptualization, Data curation, Formal analysis, Funding acquisition, Investigation, Methodology, Project administration, Resources, Software, Supervision, Validation, Visualization, Writing–original draft, Writing–review and editing.

Marcelo Rodrigues de Carvalho: Conceptualization, Data curation, Formal analysis, Funding acquisition, Investigation, Methodology, Project administration, Software, Supervision, Validation, Visualization, Writing–original draft, Writing–review and editing.

Neotropical **Ichthyology**OPEN  ACCESS

This is an open access article under the terms of the Creative Commons Attribution License, which permits use, distribution and reproduction in any medium, provided the original work is properly cited.

Distributed under
Creative Commons **CC-BY 4.0**

© 2021 The Authors.
Diversity and Distributions Published by SBI



Official Journal of the
Sociedade Brasileira de Ictiologia

ETHICAL STATEMENT

Not applicable.

COMPETING INTERESTS

The authors declare no competing interests.

HOW TO CITE THIS ARTICLE

- **Loboda TS, Lasso CA, Rosa RS, Carvalho MR.** Two new species of freshwater stingrays of the genus *Paratrygon* (Chondrichthyes: Potamotrygonidae) from the Orinoco basin, with comments on the taxonomy of *Paratrygon aiereba*. Neotrop Ichthyol. 2021; 19(2):e200083. <https://doi.org/10.1590/1982-0224-2020-0083>